NTNU
Norwegian University of
Science and Technology

Nanoparticle Mobility in Pig Small Intestine Mucus (PSIM)

Optimization of Methods used to study
Diffusion of Nanoparticles through PSIM, and
the Effect of G-block

Ingrid Wien

Biotechnology (5 year)
Submission date: December 2015
Supervisor: Kurt Ingar Draget, IBT
Co-supervisor: Catherine Taylor Nordgård, IBT

Norwegian University of Science and Technology
Department of Biotechnology

Preface

This master thesis was conducted at the Norwegian University of Science and Technology, Institute of Biotechnology from January 2015 to December 2015. The thesis was written in collaboration with a research group led by Professor Kurt Ingar Draget, which is part of the EU-project COMPACT. Through the work with this thesis I have met many challenges and made new experiences. I have learned much about practical laboratory work and about scientific writing. This year has made me more independent both when it comes to planning my own experiments and trusting my own research. I feel I have obtained a lot of knowledge about research, although I know I still have much to learn. I would like to thank my supervisors Prof. Kurt Ingar Draget and Dr. Catherine Taylor Nordgård for giving me the opportunity to work with them, and for all possible guidance and support throughout this period. The interest they have shown in my work has helped and motivated me through this year. I would also like to thank Morten Johnsen Dille for help in the laboratory, Astrid Bjørkøy for education on the confocal microscope and Signe Moe for helping with Matlab coding.

To all my friends; thank you for supporting me, cheering me on and distracting me when I need distracting. To my family and especially my parents; thank you for always supporting me, and letting me choose my own ways. You always know the right things to say, and I find so much comfort in your guidance. My dearest husband Glenn, thank you for being there for me night and day, for listening to me when I need it, for supporting me, and for telling me to take a break when I become too obsessed. You kept me from losing myself in this process. In the end I would like to thank my fantastic dog Diva for listening without understanding, and for always being ready to take a walk with me, when I need some air.

Trondheim, December 2015

Ingrid Skjærvik Wien

Abstract

Mucus is found almost everywhere in nature in a variety of animal species. For many animals like humans mucus is necessary for life to be obtained as it is needed to breathe, eat and reproduce. In addition it functions as a barrier, protecting the body from foreign materials by covering them in mucus before they are removed. This efficient way of removing foreign materials also provides a large obstacle for drug delivery. Oral drug delivery is by far the preferred route because of its simplicity and because the large absorptive surface in the gastro intestine (GI). Delivery of small molecular drugs by this route is possible, but larger molecules are trapped in mucus located in the GI tract, and removed from the body before reaching its site of action. There have been performed studies showing that the alginate G-block polymers can alter the physical properties of mucus, and increase the pore size of the mucin network. By increasing the pore size, the G-block could be used in drug delivery as it increases the transport over the mucosal barrier.

In this thesis, methods for studying diffusion of nanoparticles through pig small intestine mucus (PSIM) were to be studied and optimized. The nanoparticles used were different types of FluoSpheres® and also rhodamine labelled SNEDDS. The project was part of the work package 4 in the Collaboration on the Optimization of Macromolecular Pharmaceutical Access to Cellular Targets (COMPACT) project. By using the optimized methods diffusion through PSIM was observed both with and without the use of G-block together with the nanoparticles to study the effect of G-block on the diffusion. Both fluorometer and confocal microscopy was used to study the diffusion.

The optimization of methods demonstrated that some methods were more functional than others. The Transwell system and µ-slides were the most successful methods, which generated similar results which could be compared to each other. From the results gathered from these studies there would seem to be indications that G-block does in fact have an effect on the diffusion of nanoparticles through PSIM. The effect was not always very prominent, and several tests with independent replicates should be conducted. Still, the G-block demonstrated an increase in diffusion through PSIM when it was present.

Sammendrag

Mucus finnes nesten overalt i naturen, i mange ulike dyrearter. For mange dyr, slik som mennesker, er mucus nødvendig for livets opprettholdelse da det trengs for å kunne puste, spise eller reprodusere seg. I tillegg virker det som en barriere, og beskytter kroppen vår ved å pakke fremmedlegemer inn i et slimlag før de fjernes. Denne effektive metoden for å fjerne fremmedlegemer virker også som et hinder for levering av medisiner. Oral levering av medisiner er den mest populære ruten på grunn av sin enkelhet og fordi mage-tarm systemet har en stor absorberende flate. Levering av små molekylære medisiner via denne ruten er ikke et problem, men store molekyler blir fanget i slimet i mage-tarm systemet, og fjernet fra kroppen før de når sitt mål. Flere studier har blitt gjennomført som viser at G-blokk polymerer kan endre de fysiske egenskapene til mucus og øke porestørrelsen i mucin nettverket. Ved å øke porestørrelsen kunne G-blokk brukes i medisinlevering, da det øker transporten over slimbarrieren.

I denne oppgaven skulle metoder for å studere diffusjon av nanopartikler gjennom tynntarmslim fra gris studeres og optimaliseres. Nanopartiklene som ble brukt var ulike typer FluoSpheres® i tillegg til rhodamine-merkede SNEDDS. Prosjektet var en del av arbeidspakke 4 i Collaboration on the Optimization of Macromolecular Pharmaceutical Access to Cellular Targets (COMPACT) prosjektet. Ved å bruke de optimaliserte metodene ble diffusjon gjennom tynntarmslim fra gris observert, både med og uten G-blokk sammen med nanopartiklene for å studere effekten av G-blokk på diffusjonen. Både fluorometer og konfokalmikroskop ble brukt for å studere diffusjonen.

Optimaliseringen av metoder viste at noen metoder var mer funksjonelle enn andre. Transwell systemet og µ-slides viste seg å være de mest suksessfulle metodene, da de genererte liknende resultater som kunne sammenlignes med hverandre. Fra resultatene samlet fra disse studiene virker det som det er indikasjoner på at G-blokk har en effekt på diffusjon av nanopartikler gjennom tynntarmslim fra gris. Effekten var ikke alltid veldig framtredende, og flere tester med uavhengige paralleller burde nok gjennomføres. Likevel demonstreres en økning i diffusjon gjennom tynntarmslim fra gris når G-blokk var til stede.

Table of contents

1 Introduction and theory

1.1 Scientific introduction

1.1.1 Mucus

Although somewhat unappreciated, mucus is an important component to life as we know it and one of nature's great success stories. The human body for example is dependent on mucus to help maintain normal function as it is necessary for breathing, eating and reproducing amongst others. The organs that are exposed to the external environment, such as for example the eyes, gastrointestinal (GI) tract, reproductive tract and the respiratory tract; protect their epithelia cell layer by producing mucus to cover the cells. But the mucous layer does not just offer protection from the external environment, it also have other functions. In the cervical for example, it regulates the sperm transport, water balance and has anti-microbial properties. It also helps with lubrication in the mouth and the GI tract, as well as having functions in ion transport and regulation in the respiratory tract (Khanvilkar et al., 2001).

Mucus protects the epithelial surfaces in our body by lining the wall of various body cavities. It functions as a semipermeable barrier by efficiently trapping foreign particles and pathogens and clearing them from the body, while at the same time enabling exchange of nutrients, water, hormones and other vital components (Ensign et al., 2012, Cone, 2009). In the GI tract mucus is composed of two layers, with one firmly adherent layer in contact with the epithelial cells, and a loosely adherent layer on top of that (figure 1.1). The turnover time of mucus depends on the physical location in the body (Boegh and Nielsen, 2014). The tear film is cleansed and replaced approximately every 10 seconds, while the nasal mucus has a turnover time of 10 minutes. In the stomach of rats on the other hand, the turnover time can be as long as four to six hours. It is the cilia on the epithelial surfaces of the respiratory tract which sweep the mucus from the sinuses, nose, middle ears and lungs and to the pharynx. The mucus is then swallowed and the virus, bacteria or other unwanted substance within it are rapidly inactivated by the stomach acid. Mucus is constantly renewed and it is this renewal that prevents the stomach from digesting itself (Boegh and Nielsen, 2014, Cone, 2005).

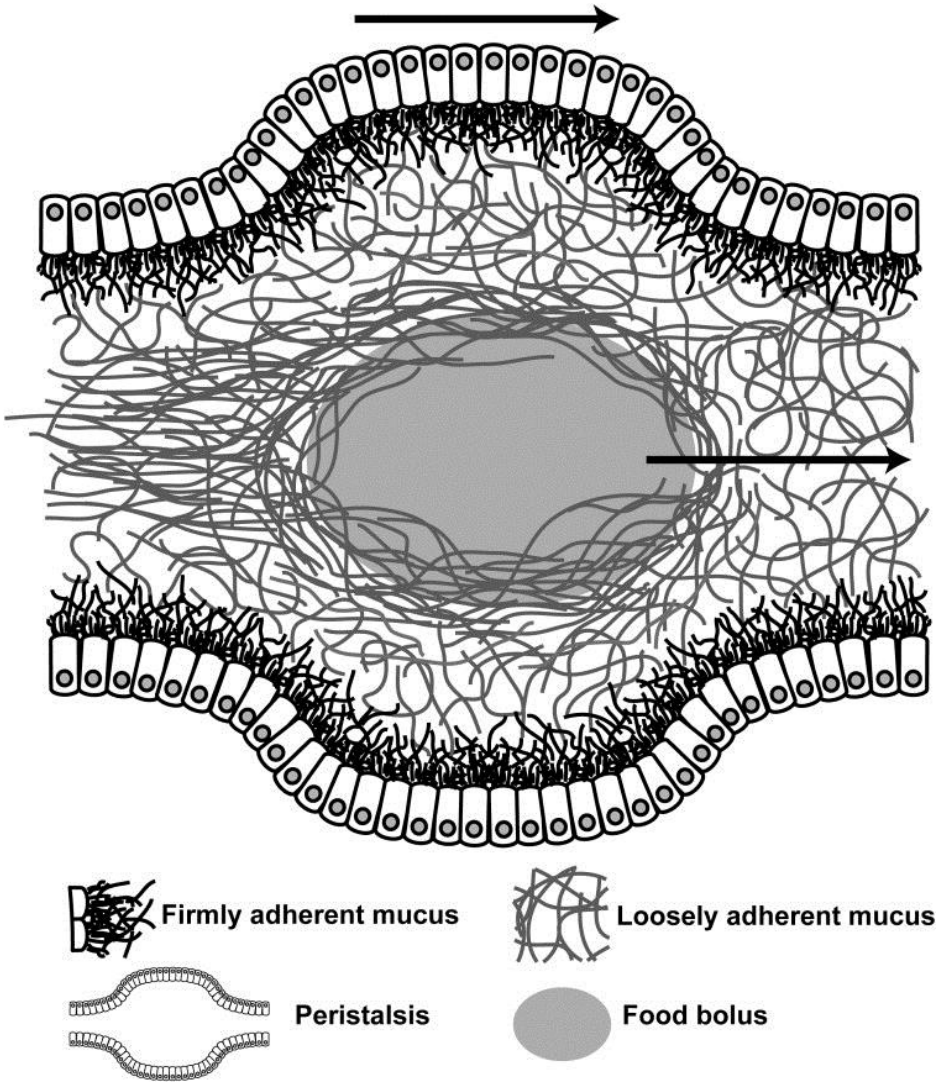

Figure 1.1: *Schematic illustration of how digested food is removed from the GI tract. The firmly adherent layer is attached to the epithelial cells while the loosely adherent layer is moving on top of that. Mucus from the loosely adherent layer wraps itself around the food and the peristaltic contractions push the food through the GI tract. Nutrients are extracted from the food by enzymes and emulsifying lipids that are able to penetrate the mucus "blanket" (Ensign et al., 2012).*

Mucus contains several components and the exact composition may vary depending on the site of secretion, the physical or mechanical role of the mucus and if there is any disease to consider. The overall content in mucus is water (~95 %), glycoproteins and lipids (0,5 – 5 %) mineral salts (0,5 – 1 %), and free proteins (1%). The main protein component of mucus is mucins, which comprise 2-5 % of mucus gels wet weight. These can either be secreted from cells or membrane-bound. The secreted mucins link together by disulfide bonds to form large

molecules, which entangle and crosslink to form dynamic viscoelastic gels (Ensign et al., 2012). The mucins are long, flexible chains with glycosylated regions which are highly hydrophilic. These regions are separated by "naked", hydrophobic areas of the protein. This alternating between hydrophobic and hydrophilic regions on the mucin makes it capable of sticking to any surface with which it can form multiple low-affinity hydrophobic/hydrophilic bonds. These bonds are formed in addition to the bonds that form between specific glycans on mucins and bacteria. Although the low-affinity bonds have short half-lives and break very easily, if the number of bonds are high enough there will always be one or more low-affinity bond linking foreign materials like for example particles to the mucin fibres (Cone, 2005). In figure 1.2 an illustration of the biochemical structure of mucin is presented.

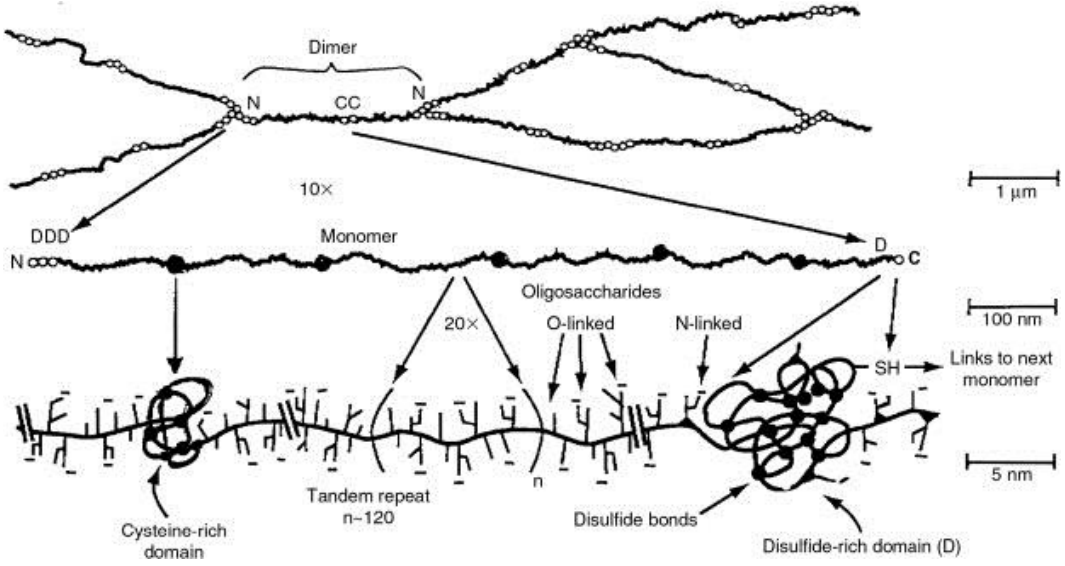

Figure 1.2: *Model of the major biochemical features of mucin at three different magnifications (Cone, 2009).*

The viscoelasticity of mucus is essential for the transportation of pathogens and particles out of the respiratory tract. If mucus in the respiratory system becomes to runny, gravity will overcome the ciliary transport and mucus runs down into the lungs or out the nose. If it is too firm on the other hand, it becomes too viscous to be transported by cilia, as in the case of cystic fibrosis (Cone, 2005).

The thickness of the mucus layer also differs between the locations in the body. In the GI tract, the mucus is thickest in the stomach and the colon, and the small intestine has the

thinnest layer. The thickness of the mucus layer in the small intestine also varies greatly. This depends on the digestive activity, where a very fibrous diet will wipe away more of the loosely adherent layer of mucus (Boegh and Nielsen, 2014, Cone, 2005). In pig the mucus layer in the small intestine have been observed to be 53.8 – 22.1 µm (Varum et al., 2012). Mucus will wrap itself around particles so they do not come in contact with the epithelial cells, and the particle wrapped in mucus is removed from the body as seen in figure 1.1. (Boegh and Nielsen, 2014, Cone, 2005).

1.1.2 Drug delivery and biopharmaceuticals

Ever since humans first started experimenting with herbal remedies we have tried to learn more about the connection between biology and technology. From the time of the first humans and up to today's modern society a lot has happened in the understanding and evolution of drugs and their methods of delivery (Rosen and Abribat, 2005). In the beginning there was little understanding of the interaction between biology and technology, and the concept of advanced drug delivery systems was not greatly understood (Rosen and Abribat, 2005, Hoffman, 2008).

The field of controlled drug delivery began in the 1960's, and has evolved ever since that (Hoffman, 2008). General administration of drugs to targets can be performed in several ways. When rapid absorption is essential the parenteral route is normally preferred. This is drug injection through hollow needles into the muscles (intramuscular), the veins (intravenous) or under the skin (subcutaneous). Many dislike this route of delivery because it is painful and inconvenient, so there is much focus on needle-free drug delivery. Drugs can also be delivered through the respiratory route by inhalation. This is seen in direct treatment of asthmatic problems. Other delivery routes focus more on the treatment from outside the body, such as the topical route. This route is best for local treatment as the drug is applied to the skin (Aulton and Taylor, 2007).

Today the most common route of drug delivery is oral delivery. This is the drug administration that is most accepted by patients, and since the human intestinal epithelium is highly absorptive with a absorptive surface area in the GI of 300-400 m^2 (Ensign et al., 2012), it should have advantages over other delivery forms, since there is no need for needles, inhalers or medical personnel to help deliver it.

Oral delivery is an easy way to administrate medicines to patients and it is well suited for small molecule drugs like the pain killer ibuprofen due to the high absorptive capacity of the GI tract. However, this route also has some disadvantages. The onset of action is very slow, the absorption is irregular and enzymes and gastric juices destroy certain drugs. Many large molecule drugs like insulin are not as well suited for oral delivery due to poor solubility, stability and/or bioavailability. Drugs made of proteins and/or nucleic acids are referred to as

biopharmaceuticals and will be discussed further in the next section (Ensign et al., 2012, Guiochon and Beaver, 2011).

1.1.2.1 Biopharmaceuticals

There is always a drive to find new pharmaceuticals and treatments for different diseases. Over the last years the field of biotechnology and the pharmaceutical industry in general has gained a higher interest in pharmaceuticals, and particularly biopharmaceuticals (Staub et al., 2011). Biopharmaceuticals have a biological origin and are consisting of proteins and/or nucleic acids. The biopharmaceuticals are large, high weight molecules made form heterogeneous mixtures derived from cells, plants or animals, and they differ from traditional low molecular weight drugs in several ways, and most obviously in size, as they are much larger than conventional small molecule drugs like aspirin (molecular weight 180 Da) (Guiochon and Beaver, 2011, Sekhon, 2010, Crommelin et al., 2003). The importance of these large weight molecules are acknowledge and more research are focused around the future of biopharmaceuticals (Strohl and Knight, 2009). Biopharmaceuticals have advantages in the sense that they potentially could cure diseases rather than just treat the symptoms. They are highly specific in their site of action which gives fewer side effects. At the same time there is an uncertainty connected to the long-term safety of these drugs, and they also have problems with low solubility and poor stability (Sekhon, 2010, D'Haens, 2007, Ensign et al., 2012).

The improvements in recombinant DNA technology these last decades have made it possible to develop many new therapeutic proteins to meet medical needs. There is a growing number of biopharmaceuticals on the marked, and there is expected that half of all new drugs in the near future will be biomolecules. One of the first known biopharmaceutical was purified insulin from pig and cow in 1923, for use in treating patients with type 1 diabetes mellitus. In 1982 the first synthetic insulin was released to the marked, a recombinant human insulin called Humulin® (Staub et al., 2011, Strohl and Knight, 2009). Since Humulin was first marketed, more than 165 new therapeutic proteins have been released to the marked (Strohl and Knight, 2009).

Insulin, being a good representative for biopharmaceuticals, illustrates one of the great obstacles in drug delivery of biopharmaceuticals. Persons suffering from type 1 diabetes mellitus need to take as many as 60 000 injection of insulin during their lifetime. The biopharmaceuticals must in most cases be delivered by injections due to their low absorption, gastrointestinal degradation, and first-pass metabolism by the liver. These injections are both painful and inconvenient, and thus an oral delivery of biopharmaceuticals would be preferable (Kwon et al., 2013, Orive et al., 2004).

1.1.2.2 Nanoparticles in drug delivery

As mentioned before, there are several difficulties in oral delivery of drugs, and especially biopharmaceuticals. Delivery to the site of action is dependent on the drugs ability to overcome the obstacles in its way. The primary challenge to oral delivery is the environment in the gastrointestinal tract, with its low pH and the presence of digestive enzymes. The site of drug absorption is in the small intestine which is covered with a layer of mucus that must be penetrated by the drug. By using nanoparticle drug carriers, these problems might be overcome (Boegh and Nielsen, 2014, Ensign et al., 2012).

Nanomaterials are generally in the size range of 1 – 100 nm (Zhang et al., 2008). Medicinal use of nanoparticles has become more common over the last decades, and the particles normally range from 10 nm to 1000 nm when used in medicine (Rosen and Abribat, 2005). Many drugs are not suitable for oral delivery due to poor stability, low solubility and bioavailability. These drugs might overcome some of their problems by encapsulating them in nanoparticles which at the same time can allow for targeted drug delivery (Ensign et al., 2012). For biopharmaceutics such as insulin, which would normally not survive the gastric environment, the encapsulation in nanoparticles may mean that they have a chance of being delivered by the oral route instead of intravenously (Damgé et al., 1990).

The advantages by encapsulating drugs in nanoscale structures can be many. The nanoparticle surface characteristics can be changed in many ways to increase mucoadhesion, cell targeting or cellular uptake, and at the same time protect the drug from the environment of the GI tract. By specializing the nanoparticles in such a manner many advantages is seen, efficiency is improved, toxicity is lowered and systemic side effects are minimized (Ensign et al., 2012,

Damgé et al., 1990, Zhang et al., 2008). It has also been debated that nanoparticles may interact with the mucus network to make larger pores in the network structure (McGill and Smyth, 2010, Wang et al., 2011).

To make nanoparticles with increased mucoadhesive nature might seem strange, since the mucus is something to avoid when drug delivery is regarded. The reason for this is the attempt to improve the residence time of nanoparticles in the GI tract, and so enhance the drug absorption. One way to do that is to simply give the nanoparticles a positive surface charge, which will make electrostatic interactions between the negatively charged mucins and the nanoparticles. However, a nanoparticle that can penetrate the mucus barrier will enhance the drug absorption even more by quickly penetrating the loosely adherent layer, which is cleared from the intestine quickly, and be retained longer in the firmly adherent layer (Ensign et al., 2012).

1.1.2.3 Self-nanoemulsifying drug delivery systems (SNEDDS)

One type of nanoscale drug delivery systems is self-nanoemulsifying drug delivery systems (SNEDDS). SNEDDS are fine oil-in-water emulsions consisting of a mixture of drug, oil, surfactant and co-surfactant. The formation of this nanoemulsion occurs when the components mentioned above are introduced into aqueous phases during gentile agitation (Date and Nagarsenker, 2007, Balakumar et al., 2013, Tran et al., 2014). When the SNEDDS come into the stomach it will rapidly disperse into droplets in the size range of 20 nm – 200 nm. Such nano-sized droplets may improve dissolution velocity as well as bioavailability, because of the large surface area of the formed nanoemulsions. (Balakumar et al., 2013, Sakloetsakun et al., 2013, Wang et al., 2009, Friedl et al., 2013).

Selecting the right components for SNEDDS is very important, as the successful formulation of SNEDDS depend on it. The physicochemical and biological properties of the components used in the fabrication of SNEDDS influence the self-nanoemulsification, and factors like pH and temperature of the aqueous phase, ratio of the components and physicochemical properties of the drug must be considered (Date et al., 2010). Selecting the right oil, surfactant

and co-surfactant is critical in the improvement of solubility and payload in SNEDDS formulation (Tran et al., 2014).

Unlike many other thermodynamically unstable dispersion systems, such as emulsions and suspensions, SNEDDS are thermodynamically stable and have a high solubilizing capacity for lipophilic drugs (Tran et al., 2014, Sakloetsakun et al., 2013). The SNEDDS are shown to result in a higher drug uptake as a consequence of their ability to prolong residence time on mucosal membrane and ability to reach greater mucosal surface areas (Sakloetsakun et al., 2013).

SNEDDS have been shown to enhance the absorption of lipophilic drugs, such as ibuprofen (figure 1.3) (Jyothi and Sreelakshmi, 2011, Wang et al., 2009). Ibuprofen is a drug used in pain treatment and thus it is important that the onset of action is fast. Already the bioavailability of ibuprofen is close to 100 % due to high absorption, but the drug have low solubility in aqueous acidic media and so the onset of absorption depends on the administrated formulation. By incorporating ibuprofen into SNEDDS more than 95 % of the encapsulated ibuprofen was released within 30 minutes, which is a large improvement compared to the traditional tablet formulation (Wang et al., 2009). SNEDDS can hence reduce the limitation due to slow and incomplete dissolution of drugs with poor water soluble properties (Sakloetsakun et al., 2013).

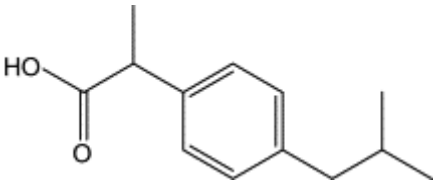

Figure 1.3: *Molecular structure of ibuprofen (Wang et al., 2009).*

Most therapeutic peptides such as insulin are difficult to deliver through the oral route due to their extreme hydrophilic nature. They have poor permeability and low stability in the GI environment, and this make them unsuited for oral delivery. It is thought that SNEDDS may be a solution to this problem, as the insulin could be capsuled into the SNEDDS (Date et al., 2010, Sakloetsakun et al., 2013).

As described there are many advantages by using SNEDDS to deliver drugs through the oral route. Due to the anhydrous nature of SNEDDS they can be filled into hard gelatin capsules for increased commercial viability and patient compliance (Date and Nagarsenker, 2007, Tran et al., 2014). It generates a quick onset of action, which is very important in many drugs. The drug dose can be reduced for many drugs since the SNEDDS improve bioavailability or therapeutic effect for hydrophobic drugs, and with the lower drug dose it will also be a reduction in dose-related side effects (Date et al., 2010).

In this thesis SNEDDS consisting of 10 % ethanol, 30 % (w/w) soybean oil, 30 % Maisine™ 35-1 and 30% Cremophor RH 40 was used in some of the experiments. These SNEDDS are close to neutral in charge as the Cremophor RH 40 is non-ionic (Nielsen et al., 2007). The fluorophore Rhodamine-6G was dissolved in the ethanol, and would provide the SNEDDS with fluorescence to make them easier to detect. These SNEDDS have a particle size of 60 nm and were obtained from Bioneer: FARMA.

1.1.3 Alginate and G-block

Alginates can be found both as the structural substance in marine brown alga (*Phaeophyceae*) as well as protective capsular polysaccharide made by some bacteria like for example the *Azotobacter vinelandii* and some *Pseudomonas*-species. These bacteria also use the alginate for adhesion to surfaces. The alginate is a linear copolymer made of (1→4)-linked β-D-mannuronic acid (M) and α-L-guluronic acid (G) residues (Smidsrød and Moe, 2008, Draget and Taylor, 2011). The chemical composition and sequence of the two uronic acids is complex and varies in proportion. The β-D-mannuronic acid (M) and α-L-guluronic acid (G) residues vary little in chemical structure but they do adapt different conformation. The M and G are C-5 epimers of each other meaning that there will be a switch-over in the monomeric chair conformation with M in the $^4C_1$-conformation and G in the $^1C_4$-conformation. The reason for this change in conformation is the need for the bulky carboxyl group to be in the equatorial position, which gives the molecule much more stability (Draget et al., 1997, Kashima and Imai, 2012, Smidsrød and Moe, 2008). See figure 1.4 for illustration.

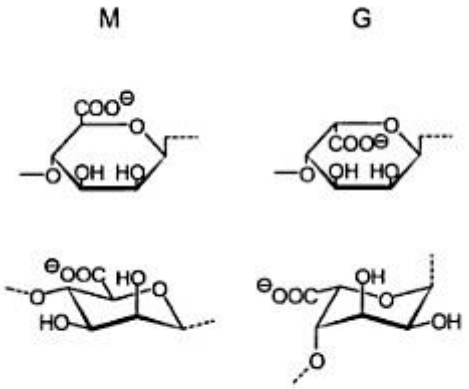

Figure 1.4: *The monomers of alginate. To the left are the β-D-mannuronic acid (M) in $^4C_1$-conformation, and to the right the α-L-guluronic acid (G) in $^1C_4$-conformation. Figure from the book "Biopolymer chemistry" by Smidsrød and Moe (Smidsrød and Moe, 2008).*

Alginate can be described as a block polymer, containing three different types of blocks. There are M-blocks, G-blocks and MG-blocks, with alternating M and G structure and no consistency in the amount or length of the blocks (Smidsrød and Moe, 2008, Draget, 2011, Draget and Taylor, 2011). How the M and G components of alginates are distributed in

alginates also depends on the type of organism which produces it. Differences in the bacteria the alga or even different parts of the alga may give rise to different alginates (Smidsrød and Moe, 2008). With the G in the $^1C_4$-conformation, the linkages in the G-blocks are diaxial leading to the hindrance of rotation around the glycosidic bond, which alongside the polyelectrolytic nature of the molecule may be causing the stiff and extended nature of the alginate molecule (Draget, 2011, Draget and Taylor, 2011). Figure 1.5 gives an illustration of alginate.

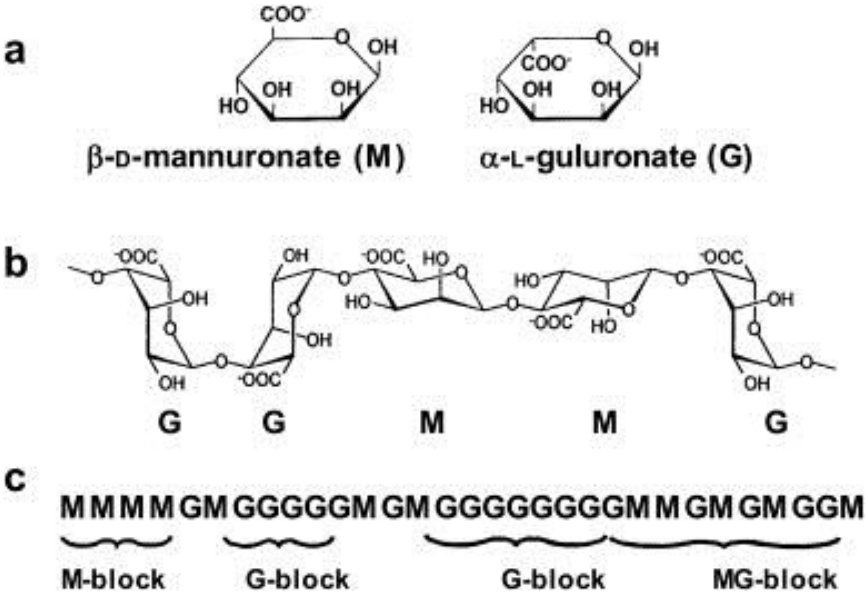

Figure 1.5: *Illustration of alginate from Draget and Taylor, with alginate monomers (a), chain conformation (b) and block distribution (c) (Draget and Taylor, 2011).*

Due to a polyelectrolyte nature the alginates are able to selectively bind cations, which gives the basis for the alginates gel-formation (Draget and Taylor, 2011). The binding of cations (most commonly calcium (Ca^{2+})) largely depend on the number of G-units in the alginate molecule, that is the length of the G-block. When two or more alginate chains align there will be a cavity between the g-blocks which will function as a binding site for the calcium. Long G-block will give a stronger gel than short G-blocks do (Draget et al., 1997, Smidsrød and Moe, 2008). The formation of these junctions in the gel-network is often referred to as the "egg-box model" due to its appearance, as shown in figure 1.6 (Grant et al., 1973).

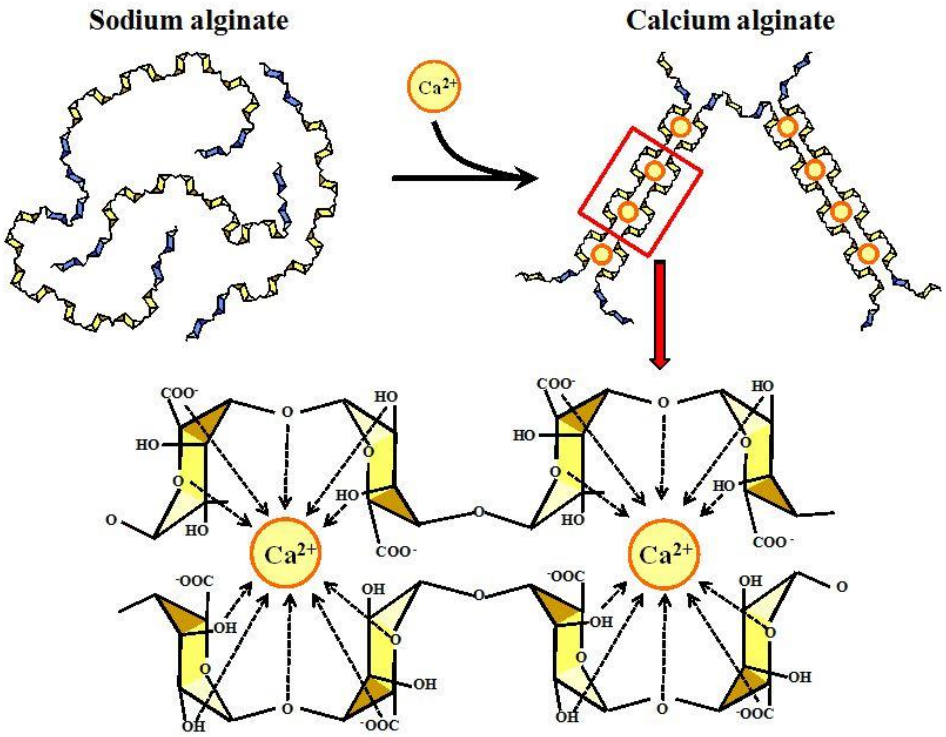

Figure 1.6: *Illustration of the egg-box model showing how the alginate binds calcium in gel-formation. Obtained from (Kashima and Imai, 2012).*

Alginates have a large area of use industrially because of their gelling, viscosifying and stabilizing properties. They are used commercially for a variety of purposes as for example food stabilizers, thickening agents and as gelling agents. There is also an increasing interest in alginates in biomedical industries. The alginates ability to gel under very mild conditions almost independent of temperature, alongside its very well understood molecular composition both as liquid and gel makes it suitable for biomedical and pharmaceutical uses. It is for example already been used in wound dressing, as material for dental impression and in drug delivery, and it is highly suitable for immobilization of biocatalysts such as living cells (Rehm and Valla, 1997, Draget et al., 1997, Draget and Taylor, 2011, Taylor Nordgård and Draget, 2011).

The alginate G-block samples are obtained by acid hydrolysis of high molecular weight alginates with a high content of guluronic acid residues (Nordgård et al., 2014). Tests have been performed and are still being performed as to whether the G-blocks can disrupt the cross-links in the network of mucous substrates (Taylor Nordgård and Draget, 2011). By results obtained from such experiments there is suggested that G-block have the ability to

change the network in mucus in such a way that the barrier functions are reduced, and there for improving nanoparticle mobility in mucus (figure1.7). The basis of mucin-mucin interaction includes electrostatic interactions, hydrophobic interactions, hydrogen bonding, and van der Waals forces. Interfering with any of these interactions can alter the barrier properties This is important in the field of mucosal drug delivery as it may help in the delivery of nanomedicine, which is largely hindered by the mucosal barrier (Nordgård et al., 2014).

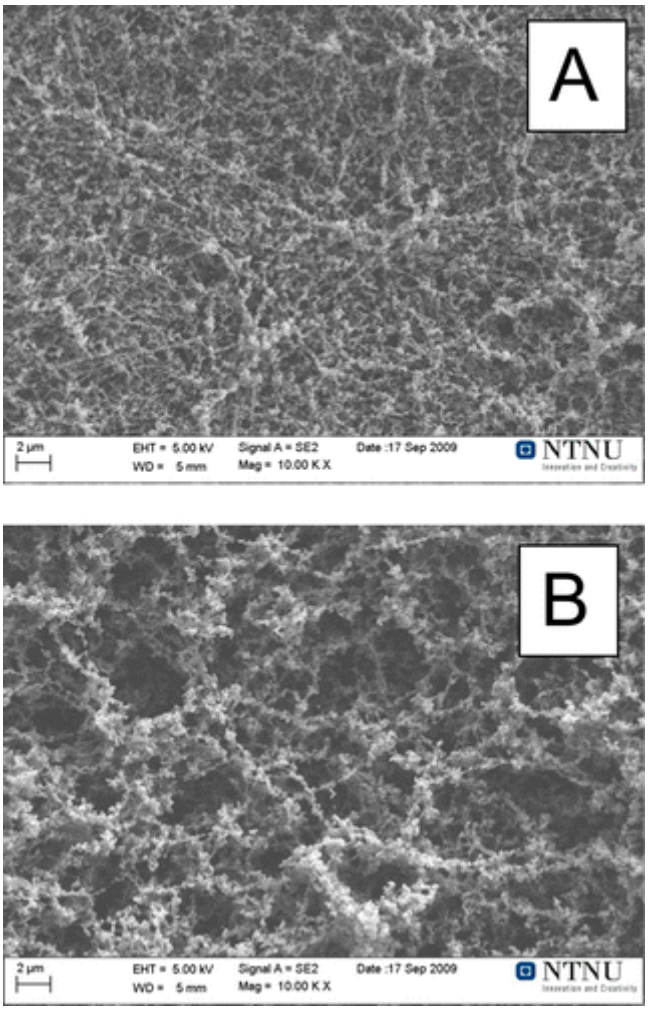

Figure 1.7: *Scanning electron microscopy of 20 mg/ml purified pig gastric mucus without (A) and with (B) 4.8 mg/ml guluronate oligomers added. It would appear that the mucus sample containing G-block have larger pore size than the one without G-block. From (Nordgård et al., 2014).*

There is suggested that one reason for the G-blocks ability to alter the network of the mucus is the polyelectrolyte nature of the G-block. This interferes with the electrostatic interactions in mucus by competitive inhibition, leading to reduction in network cross-links and a weakening in the mucus gel. The alterations in barrier properties could also come as a result of inhibition of the interactions between the matrix mucins and the mobile components (Nordgård et al., 2014, Taylor Nordgård and Draget, 2011).

1.1.6 COMPACT

Collaboration on the Optimization of Macromolecular Pharmaceutical Access to Cellular Targets (COMPACT) is an EU-project which has as objective to "*reduce delivery and targeting bottlenecks for developing novel innovative biopharmaceutical based medicines*" (COMPACT, 2015). My master project will be connected to COMPACT and the work package 4 (wp4), which focuses on oral delivery. During my project I will be working with ex vivo mucus from the small intestine (SI) of pigs, to study the diffusion of nanoparticles through mucus.

1.2 My aim for the thesis

The aim of this thesis is to develop and optimize robust methods for studying nanoparticle diffusion in mucus. I will also run tests with and without G-block to see if the presence of G-block will affect the diffusion in any way. The particles I work with are fluorescent particles of different size and types. The fluorescence of the particles is important for me to be able to detect the particle diffusion in a simple way. See the material and method for more information on the different elements used during this work.

1.3 Motivation for this thesis

Drug delivery through the GI-tract is well known and favored for small molecular drugs, but it may also be the future of drug delivery for larger molecular drugs like biopharmaceuticals, as it is highly user friendly and practical (Ensign et al., 2012, Guiochon and Beaver, 2011). Through this work the diffusion of nanoparticles through PSIM was studied, and the optimization of the methods used where studied. The studies would also be performed with and without G-block, since there has been debated that G-block may affect the diffusion of nanoparticles through mucus, by altering the barrier properties of mucus (Nordgård et al., 2014).

In this thesis the work has been focused on diffusion methods like Transwell and different µ-slides. There are many methods to study diffusion of drugs and particles through mucus, like multiple particle tracking (MPT), side-by-side systems, side-on-three compartment diffusion, fluorescence recovery after photobleaching (FRAP) and many more including Transwell systems (Groo and Lagarce, 2014).

FRAP is a method which uses a high-intensity laser to bleach a spot on a uniformly fluorescent field. The spot bleached by the laser will not be fluorescent and the time it takes to recover the fluorescence is measured. The fluorescence is recovered when fluorescent particles form areas around the spot has moved into it and replaced the bleached particles (Saltzman et al., 1994, Groo and Lagarce, 2014). The technique of FRAP shows advantages in form of speed of experiment and resolution both spatial (µm) and in time (µs) (Meyvis et al., 1999). Another method vastly used in studies of particle diffusion is MPT. Multiple particle tracking is a method where the movement of tens of particles can be tracked simultaneously in real-time by microscope video. This makes it possible to study both individual and ensemble particles (Suh et al., 2005, Crater and Carrier, 2010, Dawson et al., 2004). The particles are mixed into the mucus and then studied as they move in the mucus. The mobility is studied in a short time scale and at relatively small distances of a couple of µm (Suh et al., 2005, Wang et al., 2011). As mentioned the particles are mixed into the mucus when studying particle movement using MPT. This stirring of the mucus may affect the local movement of the particles, due to the making of larger pores in the mucus. It could be that the particle movement is observed as relatively large, while the particles in fact only moves in a confined

space, without actually diffusing through the mucus. When using other methods this might not be a problem. And therefor there will always be a need for several methods.

Although these are established methods, there is still a need to optimize new methods for study of particle diffusion. Mucus is a complex material and more methods are needed to be able to study it further. There is not possible to detect all the answers from one method. In this thesis both the time scale and the distance gave limitations to the methods. Many methods focus on diffusion and movement over short distances as in the case of MPT (Suh et al., 2005, Wang et al., 2011). When the mucus located in the small intestine is to be penetrated, the particles must move tens of µm before reaching the epithelium (Varum et al., 2012). This calls for optimization of a method to study diffusion over a longer distance, as is the ambition of this thesis.

1.4 Technical introduction

For the last two decades there has been an increase in the use of fluorescence in science, and there is a constant development of instrumentation and technology related to detecting fluorescence. Although there is a continuous development of techniques and instruments, the principles of basic fluorescence are the same as always, and it is important that these principles are understood by the practitioners (Lakowicz, 2013).

Luminescence is the emission of light from any substance. It is common to divide into two types of luminescence; fluorescence and phosphorescence, which are separated by differences in their excitation state. When light is absorbed by a molecule, the photons in the light will give energy to excite electrons to a higher state. The absorption of light and excitation of electrons takes place in 10^{-15} second. The electron cannot stay in this excited state since it is an unstable state, and it quickly returns to the stable ground state. When returning to this ground state, the electron emits energy in the form of a photon, which is detected as luminescence (figure 1.8) (Lakowicz, 2013, So and Dong, 2002).

Fluorescence has a shorter emission time than phosphorescence, and the two can be separated by this. While phosphorescence lifetime normally spans from milliseconds to seconds, and sometimes even longer, the lifetime of fluorescence typically lies near 10 nanoseconds. Since some of the energy from the absorption is lost in the short time before emission, the fluorescent energy is emitted at longer wavelength than the energy that was absorbed. Fluorescence are normally emitted by aromatic molecules where the part of the molecule responsible for the fluorescence is called a fluorophore (Lakowicz, 2013, Guilbault, 1990).

Fluorescence is a good way to detect nanoparticles, and by making the particles fluorescent they can be detected using different tools, like a fluorometer or a confocal laser scanning microscope.

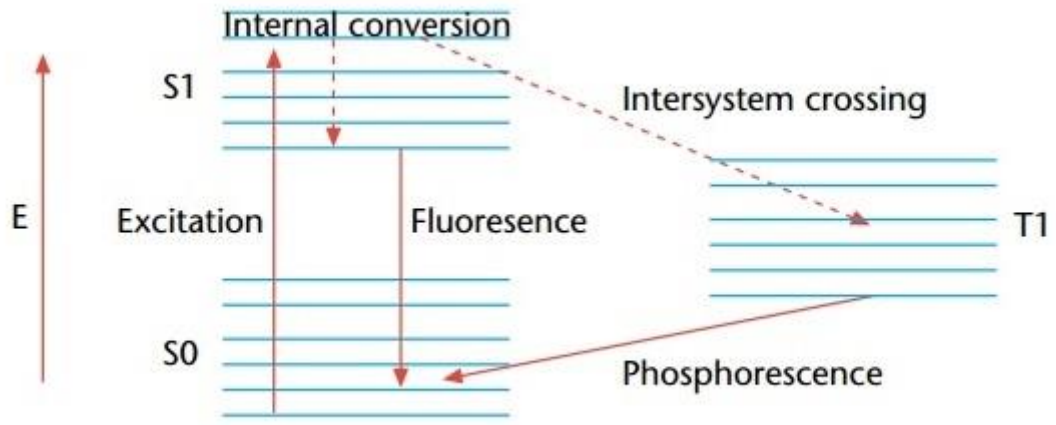

Figure 1.8: *The theory of fluorescence is explained by a simplified Jablonski energy diagram. An electron gains energy (E) from absorbing photons. As this happens the electron is excited and moves from the ground singlet electronic state (S0) to a higher singlet electronic state (S1). As the electron descend to the ground state, some energy is lost to heat or radiation. The rest is released as fluorescence. T1 is the lowest energy triplet state, and by intersystem crossings to T1, the energy is emitted as phosphorescence. Figure modified from (So and Dong, 2002).*

1.4.1 Fluorometer

Different techniques can be uses to detect fluorescence, and one of them is the use of fluorescence spectroscopy or fluorometer. A fluorometer is able to measure low concentrations of substances with high reliability. The instrumental design of the fluorometer is straight forward and figure 1.9 shows a schematic illustration of the instrument (Guilbault, 1990, So and Dong, 2002).

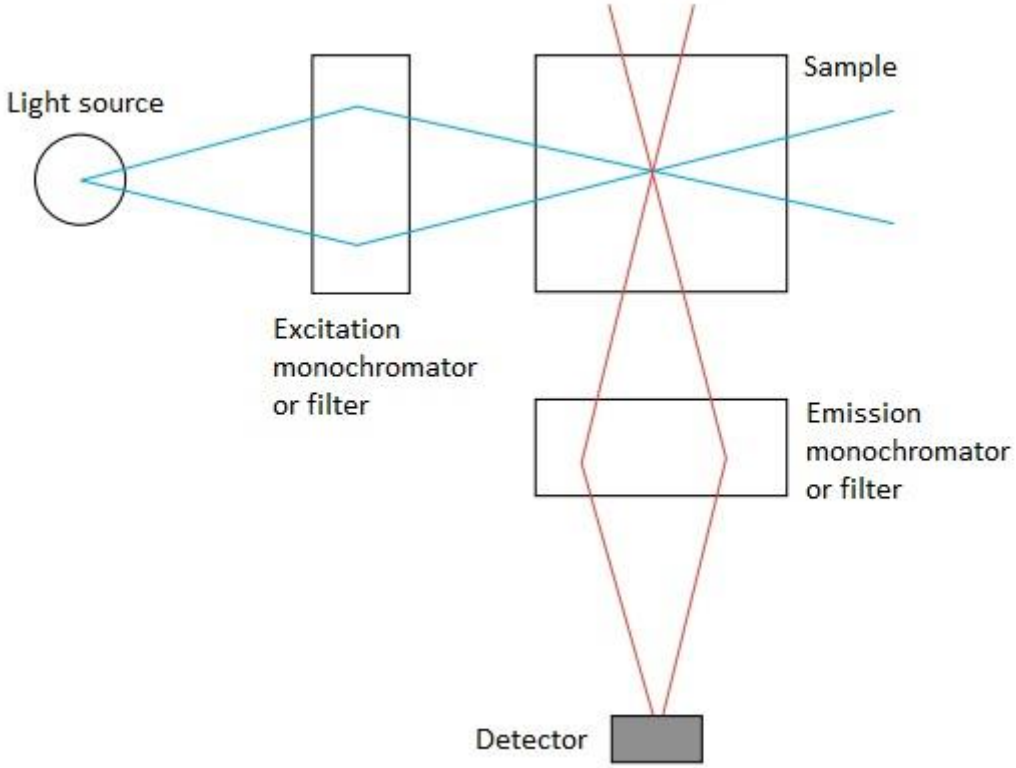

Figure 1.9: *Basic fluorometer design. Light from a light source travels through a monochromator or filter before reaching the sample, where some of the wavelengths from the light is absorbed. The emitted fluorescence from the sample is sent in a 90° angle from the light source, through another filter before reaching the detector. Modified from (So and Dong, 2002).*

A light source sends light through a monochrometer or a filter and in to a sample chamber, where a cuvette containing the sample is placed. Some wavelengths of the light are absorbed by the molecules in the sample, causing electron excitement and emission of fluorescence from the sample. The sample chamber has an integrated optical component which sends the emitted fluorescence out in a 90° angle from the light source, and then through another filter before it reaches a highly sensitive detector. The detector is placed in a 90° angle to eliminate the background caused by the light source (So and Dong, 2002, Guilbault, 1990).

1.4.2 Confocal

The confocal laser scanning microscope (CLSM), often referred to only as a confocal microscope, is an important tool in series imaging of cell structure or fluorescent samples. In a traditional light microscope the entire depth of the sample is illuminated simultaneously causing an out-of-focus blur from the parts of the sample that are above or below the focus point. The background fluorescence results in a blurry image, making it difficult to see details in the specimen. A confocal microscope in contrast, has eliminated this background fluorescence by several alterations. The illumination is concentrated to one small point, and the specimen is scanned point-by-point, and at the same time the background fluorescence from above or below the focal plane is removed by using a spatial filter, like a pinhole or a slit (Paddock, 1999, Wright and Wright, 2002). A pinhole is placed on the excitation side to illuminate only a small spot on the specimen, but since there is often a laser used in the microscope the pinhole is not always needed, as the laser can create a tightly focused beam. By scanning the sample point-by-point in this manner, you get optical sections which can be put together to create a sharp digital image with fluorescence details of the complete sample. Only information in the focal plane of interest will reach the photodetector, and placing a second pinhole in front of the photodetector secures that a minimal amount of out-of-focus light reaches it. Since the confocal works best when the out-of-focus light is dense, there is no need for very thin samples (Drazba, 2006, Paddock, 1999). The confocal microscope is presented schematically in figure 1.10.

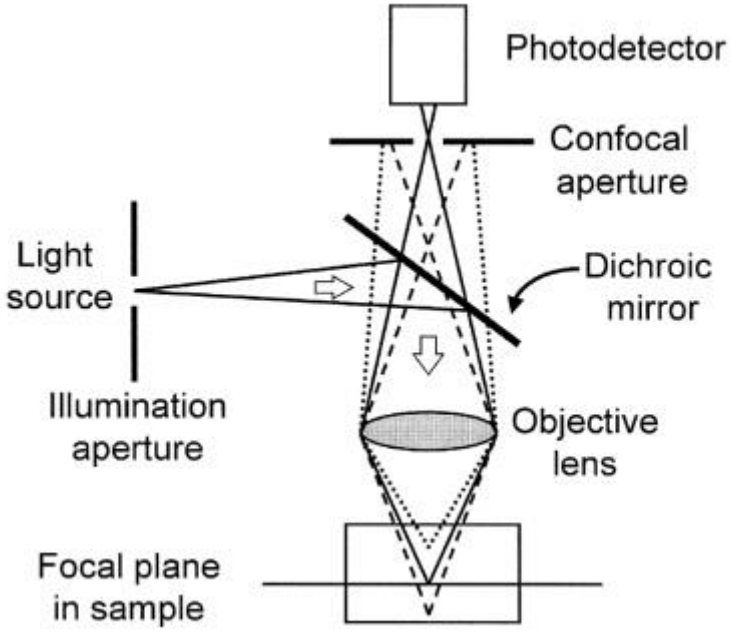

Figure 1.10: *Basic illustration of a confocal microscope where the light is first sent through a pin hole (illumination aperture) and then reflected by a mirror and focused on the sample by an objective lens. Light from the focal plane is reflected through the second pinhole (confocal aperture) and is detected by a photodetector. Light from above and below the focal plane is stopped by the confocal aperture and does not reach the photodetector. Figure from (Wright and Wright, 2002).*

2 Materials and method

2.1 Materials

2.1.1 Saline solution

A physiological saline solution (0.9 %) was prepared for use in the different experiments by dissolving sodium chloride (NaCl, 9 g) (Merck KGaA, Sodium Chloride Ph Eur, for analysis) in Milli-Q water (1 l).

2.1.2 Red 100 nm FluoSpheres® carboxylate microspheres

Red FluoSpheres® carboxylate microspheres in a 2% aqueous suspension from Invitrogen (0.1 µm red fluorescent (580/605), F8801, Lot: 483011) was diluted in physiological saline to a total concentration of 0.025%

2.1.3 Yellow-green 100 nm FluoSpheres® carboxylate microspheres

Yellow-green FluoSpheres® carboxylate microspheres in a 2% aqueous suspension from Invitrogen (0.1 µm yellow-green fluorescent (505/515) F8801, Lot: 1173467) was diluted in physiological saline to a total concentration of 0.025%

2.1.4 Yellow-green 40 nm FluoSpheres® carboxylate microspheres

Yellow-green FluoSpheres® carboxylate microspheres in a 2% aqueous suspension from Life (0.04 µm yellow-green fluorescent (505/515) F8795, Lot: 1571781) was diluted in physiological saline to a total concentration of 0.025%

2.1.4 Pig small intestine mucus

Pig small intestine mucus (PSIM) was portioned and frozen. When thawed it was kept cold, except during experiments.

2.1.5 Biosimilar mucus

The biosimilar mucus was obtained from another master student. The protocol for making biosimilar mucus is in appendix E.

2.1.6 Agar

For use in the diffusion experiment with the chemotaxis slide, 1% agar was made by dissolving 1 g agar powder (Pharmagar plus from B&V, ISO 9001:2008, 230/15) per litre physiological saline (NaCl 0.9 %). The mixture was heated to over 94 °C for several minutes with stirring to obtain an even solution.

2.1.7 Rhodamine – 6G

The rhodamine – 6G was from Sigma, supplied by Bioneer Pharma for use with SNEDDS.

2.1.8 Rhodamine loaded SNEDDS

The SNEDDS pre-concentrate and Rhodamine-6G was obtained from Mathias Fanø at Bioneer:FARMA (P13). Full protocol for preparing the SNEDDS is presented in appendix F.

SNEDDS was prepared by dissolving SNEDDS pre-concentrate in ethanol (100%). The pre-concentrate consist of 30 % (w/w) soybean oil, 30 % Maisine™ 35-1 and 30% Cremophor RH 40. The fluorophore Rhodamine-6G was dissolved in the ethanol, and would provide the SNEDDS with fluorescence to make them easier to detect. The solution was then diluted 100 times in Milli-Q water. Before using the SNEDDS in experiments they were diluted in saline that was 10 times more concentrated than physiological saline, so that we have SNEDDS in physiological saline rather than in MQ-water. The size and the stability of the SNEDDS were measured on a Malvern Zetasizer.

2.1.9 G-block

Alginate G-block prepared by Camilla Reehorst was used for the G-block experiments in this thesis. The number-average degree of polymerisation (DPn) for the G-block was 12. A G-block stock solution (50 mg/ml) was made by dissolving G-block in MQ-water and mixing it to a homogeneous solution. It was further diluted by using physiological saline as solvent.

2.2 Method

2.2.1. PSIM diffusion studies using Transwell

2.2.1.1. Experimental design

The overall goal in this experiment is to see if nanoparticles are able to diffuse through mucus. The experiment was performed by using Transwell® Permeable Supports well plates from Corning. Figure 2.1 shows the basic function of the Transwell experiment. The insert with the donor chamber is placed in a well containing physiological saline. The membrane at the bottom of the insert is covered in PSIM mixed with the fluorescent carboxylate nanoparticles FluoSpheres® or other nanoparticles. By using fluorescent particles the detection of diffused particles can easily be measured on a fluorometer. After a given time a sample of the saline in the acceptor chamber is transferred to a cuvette and replaced by new physiological saline. Physiological saline is also added in the cuvette to increase the volume. This must be done because the fluorometer cannot measure fluorescence in the sample if the volume is too small. By measuring the fluorescence with a fluorometer over time it is possible to make a graph showing the diffusion of the fluorescent nanoparticle through the mucus layer.

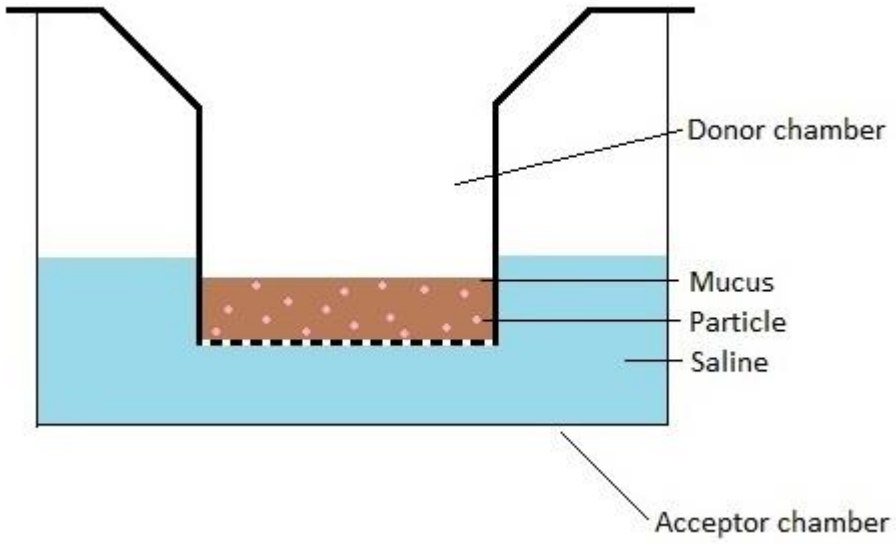

Figure 2.1: *Illustration of the experimental setup of the Transwell with mucus and fluorescent nanoparticles.*

There are different types of well plates and inserts depending on the experiment. In the diffusion experiments performed in this thesis, 24-well plates with 12 insert was used to begin with. After some time the 12-well plate with 6 inserts was tested and the 6-well plate was used in later experiments. See table 2.1 for more details about the dimensions of the wells.

Table 2.1: *Table showing Transwell information about growth area, pore size and type of membrane for the inserts used in this project. Information is collected from the Corning instruction manual.*

Number of wells on the plate	Insert membrane growth area (cm^2)	Pore size of insert membrane (µm)	Membrane material
24	0.33	0.4	Polyester (PET)
12	1.12	3.0	PET
6	4.2	3.0	PET

2.2.1.2 Optimization of the Transwell diffusion method

With background in the experiments by Friedl et al. (Friedl et al., 2013) the diffusion study was performed using red 100 nm carboxylate FluoSpheres® on a 24-well Transwell. A

standard curve for the red 100 nm carboxylate FluoSpheres® was made by measuring a known concentration of the FluoSpheres® suspension on the fluorometer at excitation of 580 and emission of 605. The next sample contained 1 ml of the last sample and 1 ml saline, so that the concentration was half of the last concentration. This was done several times to give more measurements, and thus a standard curve. The final standard curve is presented in figure 2.2. For the other types of FluoSpheres® and for the SNEDDS, standard curves were made in the same way, only they were measured at the excitations and emissions that correspond to those specific fluorescent nanoparticles. The other standard curves are presented in appendix A2 and appendix A3.

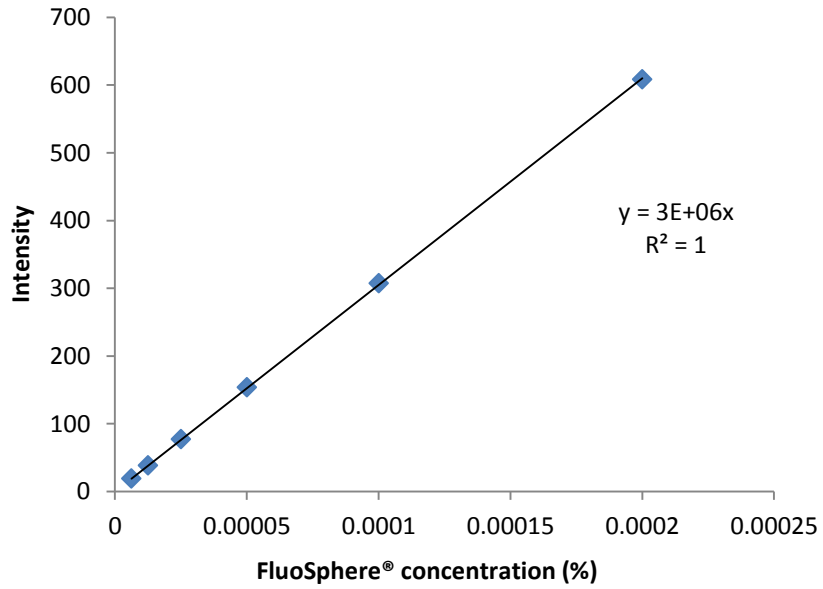

Figure 2.2: *Standard curve for red carboxylate FluoSpheres®. Intensity plotted against concentration. Measurements were conducted on a fluorometer at excitation 580 and emission 605.*

2.2.1.2.1 PSIM diffusion studies using 24-well Transwell

By using a protocol made by former master student Stine Wøien, it was decided to start with an amount of 600 µl saline in the acceptor chamber. To determine the needed volume in the donor chamber it was tested how much PSIM was needed to cover the entire area of the filter. Frozen PSIM was thawed in the cold room overnight and after some tests it was decided to use 90 µl PSIM and 10 µl FluoSpheres® (0.025%) in the donor chamber. The FluoSpheres® was mixed into the PSIM. Samples of 300 µl were collected from the acceptor chamber after

0 hours, 1 hour, 2 hours, 4 hours and 24 hours and placed in cuvettes for measurrements on a fluorometer. When removing 300 µl from the acceptor chamber for samples, the extracted volume was to be replaced by 300 µl physiological saline to maintain a total volume of 600 µl in the acceptor chamber. 1700 µl of physiological saline was added to the cuvettes with the collected samples to make the total volume in the cuvette large enough to be measured by the fluorometer. This was done for several independent replicates in different wells.

In addition to these diffusion measurements, controls containing PSIM and physiological saline were measured on the fluorometer every hour for four hours, and controls containing FluoSpheres® and physiological saline were measured on the fluorometer every half hour for four hours. In the PSIM controls it was 90 µl PSIM and 10 µl physiological saline. The FluoSpheres® controls contained 90 µl physiological saline and 10 µl FluoSpheres®.

All fluorescence measurements for red 100 nm carboxylate FluoSpheres® were performed at excitation of 580 and emission of 605.

2.2.1.2.2 PSIM diffusion studies using 12-well Transwell

Due to varying results in the 24-well system I wanted to test diffusion in a 12-well system with larger area and larger pore size (see table 2.1). To determine the volume needed in the chambers the guidelines in the corning manual was used.

At first a control containing the red 100 nm carboxylate FluoSpheres® and physiological saline were tested to see if the results would be different from the results on the 24-well system. 50 µl FluoSpheres® (0.025%) and 450 µl physiological saline was added to the donor chamber and 1500 µl physiological saline was added to the acceptor chamber. Samples of 750 µl was removed from the acceptor chamber every half hour for four hours and one at 24 hours to see if the curve would flatten out. The removed sample was added to a cuvette along with 1250 µl physiological saline to be measured on the fluorometer. In the acceptor chamber the extracted 750 µl was replaced by physiological saline.

Diffusion studies were then preformed with the 100 nm red carboxylate FluoSpheres® and PSIM. The PSIM was thawed in the cold room overnight, and 450 µl was administrated into the donor chamber of the Transwell. On top of the PSIM 50 µl of red FluoSpheres® was

added, and carefully stirred into the PSIM. Under the insert with the donor chamber, 1500 µl physiological saline was added to the acceptor chamber. After 30 minutes, 1 hour, 2 hours, 4 hours, 6 hours and 24 hours samples of 750 µl was taken from the acceptor chamber and measured on the fluorometer in the same manner as for the FluoSpheres® controls. In addition a control containing 450 µl PSIM and 50 µl physiological saline was measured in the same way.

2.2.1.2.3 PSIM diffusion studies using 6-well Transwell

On the 6-well Transwell, diffusion studies with red 100 nm carboxylate FluoSpheres® (0.025%) in PSIM was performed to see if the size of the area would affect the diffusion, if the pore size remained the same. In addition to this, diffusion studies with yellow-green 40 nm carboxylate FluoSpheres® (0.025%) and rhodamine loaded SNEDDS (0.45%) was performed both with and without G-block (5 mg/ml) in the nanoparticle suspension. The 40 nm FluoSpheres® was used because they have a size that is closer to the size of the SNEDDS. The volume needed in the wells was calculated so that the thickness of PSIM would be the same as for the 12-well system (see appendix B6 for calculations).

In the donor chamber 1700 µl PSIM and 190 µl red 100 nm carboxylate FluoSpheres® were carefully mixed together. In the acceptor chamber there was 2800 µl physiological saline. 1400 µl was pipetted out and into a cuvette. It was replaced by adding 1400 µl physiological saline in the acceptor chamber. 600 µl of physiological saline was added to the cuvette to make a total volume of 2000 µl. The cuvette was then placed into the fluorometer which measured the intensity at excitation of 580 and emission of 605.

For the measurements of effect of G-block on diffusion through PSIM the nanoparticle suspensions was made with and without G-block in them. The diffusion studies was performed in the exact same way as before only the intensity by which the measurements was made were different. For the yellow-green 40 nm carboxylate FluoSpheres® the excitation was 505 and the emission 515. For the SNEDDS the excitation was 526 and the emission 555.

Controls was performed for both the yellow-green 40 nm carboxylate FluoSpheres® and the SNEDDS by adding 1700 µl physiological saline and 190 µl nanoparticle suspension with and without G-block to the donor chambers. Controls with PSIM were also measured at the intensities for the two nanoparticle suspensions. The PSIM controls contained 1700 µl PSIM and 190 µl physiological saline instead of nanoparticle.

2.2.2 PSIM diffusion studies using µ-Slides Chemotaxis 3D

2.2.2.1 Experimental design

These slides are originally designed for use in observing cells and their chemotactical response to chemical gradients. The slide is designed with two large-volume chambers connected by a small gap. Each of the two chambers has two ports for filling. The gap between them also has two ports. By having two entrances to the chambers and the gap, they can be filled without any air bubbles, since the air is pushed out the other port while filling from one of them. Figure 2.3 shows the slide and the chambers.

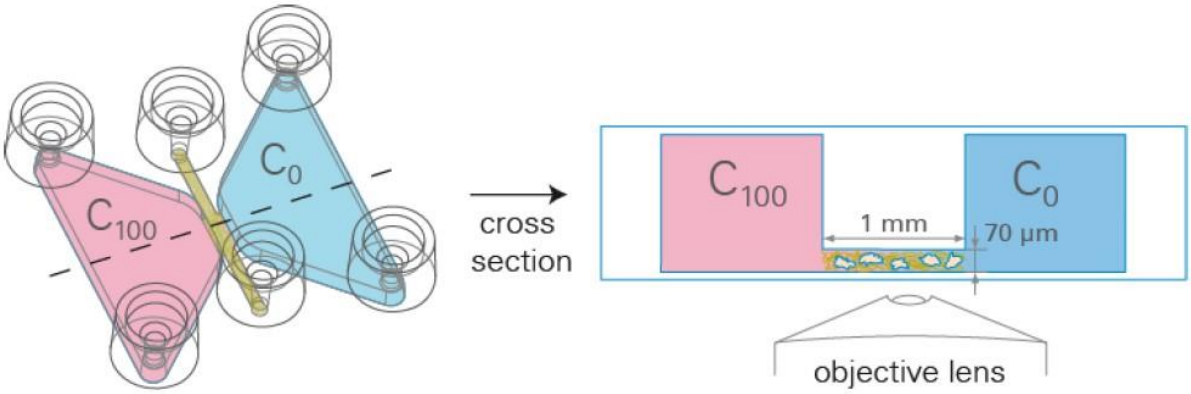

Figure 2.3: *Illustration that shows an overview and cross section of the µ-slide chemotaxis. To the left is one of the main chambers (pink) and to the right is the other main chamber (blue). Between the chambers there is a small gap (brown). The picture is from the Ibidi instruction manual.*

The gap between the two chambers does in itself function as a channel. So in this experiment the application for the slides is changed from chemotaxis study to a diffusion study through PSIM. The gap is considerably smaller than the chambers, with a height of 70 µm and a width of 1mm. Therefor the substance filled into the gap will remain in the gap due to the surface tension, unless the application force is too great and pushes it out to the cambers. The idea is to fill the gap with a 1% agar gel. This will set and make a good way to keep the mucus in place, while getting a clear front to the mucus. Then one chamber will be filled with PSIM, and the other with the fluorescent particle. The particle will then diffuse through the agar gel,

and into the PSIM. Then a confocal microscope can be used to study the diffusion of particles into the PSIM.

2.2.2.2 Optimizing the method

First a 1% agar solution was made as described in section 2.1.6. The µ-slide chemotaxis was then placed on a small metal plate in a heat cabinet. Due to the poor heat capacity in the plastic of the µ-slide, it was placed on a metal-plate to keep it warm for some time after removing it from the heat cabinet. When the plate and the slide were warm, and the agar melted, the agar was inserted into the gap on the µ-slide. To do this a special pipet tip, which is rounded in the end, was used. This was to prevent it from getting stuck in the entrance to the gap. When the agar had filled the inside of the gap it was allowed to set into a gel by cooling down to room temperature.

When the agar gel was cooled down, one of the chambers were filled with PSIM using the same type of pipet tip. In the other chamber a few drops of physiological saline were added. This was to prevent the gel from drying out. The entrances to the gap and the chamber with mucus were then closed using parafilm. Before studying it on the confocal microscope, the last chamber was filled with yellow-green 40 nm FluoSpheres®. The slide could then be studied as the particles diffused through the agar and into the PSIM.

Several studies were performed to test the ability of yellow-green 100 nm carboxylate FluoSpheres® to diffuse through the agar. First the diffusion was tested on a 12-well Transwell system. The PSIM was exchanged with agar gel. Two different tests were conducted in addition to FluoSpheres® control and agar (1%) control, and they are presented in table 2.2. The tests were conducted in several wells and each had 450 µl agar gel in the donor chamber and 50 µl FluoSpheres® on top of the agar. Some of the wells also had 200 µl physiological saline on top of the agar before adding the FluoSpheres®. This was to see if the physiological saline could increase the diffusion by eliminating any crust formation on the agar gel due to it drying out. For all the replicates there was 1500 µl physiological saline in the acceptor chamber. After 24 hours the samples of 750 µl was collected and transferred to a cuvette along with 1250 µl physiological saline for measurements in the fluorometer at excitation of 505 and emission of 515.

Table 2.2: *Different replicates containing yellow-green carboxylate 100 nm FluoSpheres® and agar tested in 12-well Transwell.*

Samples	Content
Control	Agar gel (1%) Physiological saline
Control	FluoSpheres® (0.025%) Physiological saline
1	Agar gel (1%) FluoSpheres® (0.025%)
2	Agar gel (1%) FluoSpheres® (0.025%) Physiological saline

To make sure the filter of the Transwell does not affect the measurements test were also performed without the Transwell. In these tests the FluoSpheres® were mixed into the agar gel. Trays containing wells without filters were then places vertically and 500 µl of the agar gel was placed along the side of the well. When the gel was setting the tray was laid down again and the wells were filled with 1500 µl physiological saline, covering the agar gel. After 24 hours 750 µl was pipetted out of each well and measured on the fluorometer. Table 2.3 provides an overview of the content in the wells.

Table 2.3: *Content of wells in diffusion studies with yellow-green FluoSpheres® and agar (1%) tested without filter. Several replicates were tested for each sample.*

Sample	Content
Control	Agar gel (1%)
1	Agar gel (1%) FluoSpheres® (0.025%)

2.2.3 PSIM diffusion studies using µ-Slides VI $^{0.4}$

2.2.3.1 Experimental design

Since the agar provided an obstacle for the diffusion of nanoparticles through the PSIM, the µ-slides chemotaxis was changed for other µ-slides. In this experiment µ-Slide VI$^{0.4}$ from Ibidi (lot: 150317/3) was used. The design of the µ-slides is rather simple with a channel and an opening in each end. The opening in the end of the channel rises up from the plate in the form of a well. Each slide has six channels which gives the opportunity to perform several assays at once. Information about the dimensions of the channels can be found in 2.4. In figure 2.4 two photos of the slide is presented.

Table 2.4: *Table showing the dimensions of the channels found in the µ-slide. Information collected from the Ibidi instructions sheet for µ-Slide VI$^{0.4}$, version 2014-05-13.*

	Dimensions
Channel volume	30 µl
Channel length	17 mm
Channel width	3.8 mm
Channel height	0.4 mm

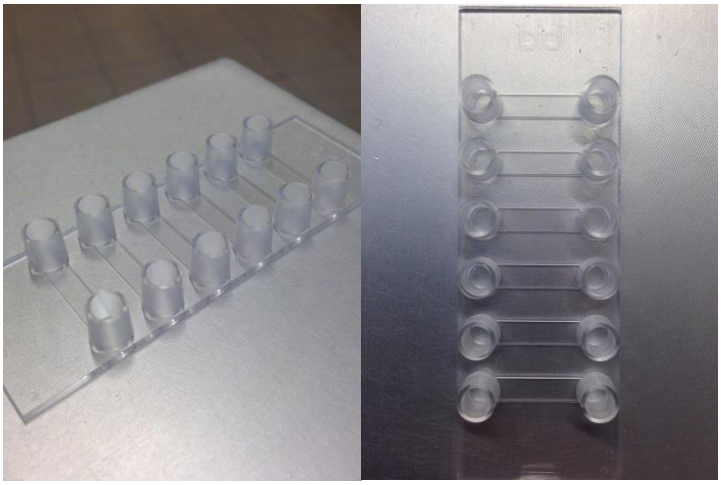

Figure 2.4: *two photos of the µ-slide from the side and from above. Each slide has six channels with two openings.*

The general idea of this experiment was to add mucus into the channel from one end while the fluorescent particle solution was added to the same channel from the other opening. The PSIM was supposed to be stopped in the areas of the channel where it was most easy to study it, like the centre of the canal. It would then be a clear front from which it would be possible to study the diffusion of particles through PSIM using a confocal microscope. In figure 2.5 a simple illustration of the experiment is shown. When optimizing the protocol, biosimilar mucus was used initially, to minimize the risk of using all the PSIM.

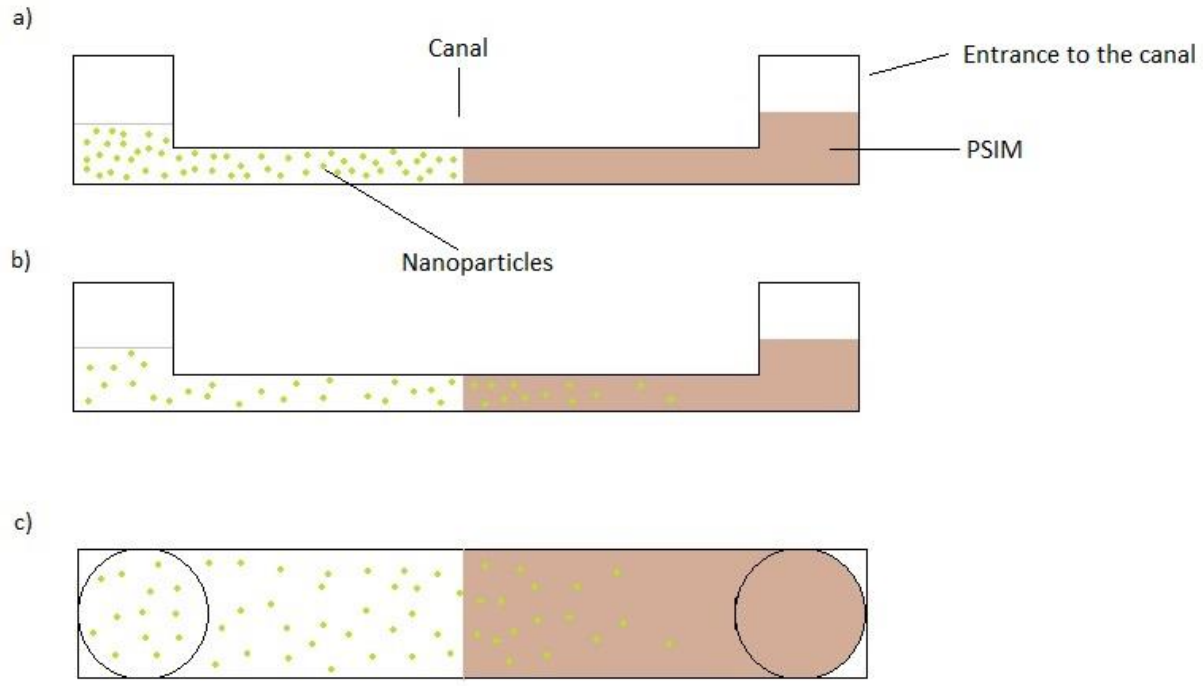

Figure 2.5: *Simple illustration of the µ-slides with a side view in a) and b), and seen from above in c). The idea is to fill the chamber with PSIM from one side and particle suspension from the other to create a front in the middle of the canal (a). After some time the particles will begin to diffuse into the PSIM (b). By using a confocal microscope there is possible to take images of the diffusing particles.*

2.2.3.2 Optimizing the method

First the biosimilar mucus was placed in the canal by inserting it from the opening and stopping the pressure when it reached the middle of the canal. From the other opening water was inserted by a syringe. The water was used during the beginning of this experiment to

prevent using nanoparticle suspension when PSIM was not used. By holding the µ-slide in an upright position while inserting the water and also making sure the water entered the canal along one of the sides, air bubbles between the water and the biosimilar mucus was prevented.

After mastering the insertion of the components in the canal the experiment was performed using PSIM. The PSIM showed signs of phase separation, probably due to excess water from the extraction of mucus from the small intestine, making the nanoparticle suspension fill the gaps and destroying the front. To prevent this it was attempted to wash the PSIM. The process of washing the PSIM is described in 2.2.1.2.2.

A syringe without tip was used to administrate the washed PSIM into the channels of the µ-slide. The PSIM was pushed into the channel until approximately halfway through the channel. Then the fluorescent nanoparticle was added to the channel by lifting the slide and thus the channel into an upright position and gently pipetting the particles into the channel. This was done using both yellow-green 40 nm FluoSpheres® and rhodamine loaded SNEDDS. The diffusion of the desired particle through mucus was studied using a confocal laser-scanning microscope (CLSM) Leica SP5 from Leica microsystems (Mannheim, Germany). The settings used on the confocal microscope are described in table 2.5.

Table 2.5: *The settings used on the confocal microscope when studying the diffusion of fluorescent nanoparticles into PSIM in the µ-slide.*

Samples	Laser	Laser power	Pinhole (µm)	Objective	Format	Detection in	Gain
Yellow-green 40 nm carboxylate FluoSpheres®	Argon	20%	111.33	63.0 x 1.20 water UV	512 x 512	PMT 1: Leica / FITC	PMT: 800 V
SNEDDS	Argon DPSS	20%	114	63.0 x 1,.20 water UV	512 x 512	HyD2	HyD: 200 %

2.2.3.3. Washing of PSIM

To prevent the PSIM from cracking up due to phase separation, it was washed. The protocol for washing of mucus was obtained from the article "Development and Evaluation of a Novel Mucus Diffusion Test System Approved by Self-Nanoemulsifying Drug Delivery Systems" by Friedl et al. (Friedl et al., 2013)

The SI mucus was thawed and measured on a scale. For 1 gram mucus it was added 5 ml physiological saline (0.9% NaCl), and it was agitated for 1 hour. This was done in the cold room to minimize the degradation of mucus. Then the mixture of mucus and physiological saline was centrifuged for 1 hour at 9000 rpm at 10°C.

The supernatant was thrown away, and the PSIM pellet was collected for further use.

3. Results and discussion

3.1 Diffusion studies of nanoparticles in PSIM using Transwell

Several steps were made in the development and optimization of methods for studying nanoparticle diffusion through PSIM. A standard curve for the 100 nm red carboxylate FluoSpheres® was created as described in methods 2.2.1.2. The red FluoSpheres® where used as a part of the diffusion studies with the Transwell system.

As described in section 2.2.1.1 under methods, the Transwell is a method where the nanoparticles, which in this case is FluoSpheres® and rhodamine loaded SNEDDS, are diffusing through the PSIM and a filter in the donor chamber and out to the acceptor chamber which contains physiological saline. Samples are taken from the acceptor chamber and the total fluorescence is measured on a fluorometer. Since the FluoSpheres® and the SNEDDS used in these experiments are made to be fluorescent, the fluorometer is an easy way of measuring the diffusion. Fluorescence from the particles is detected and the measured intensity gives an indication on how much of the particles have diffused through. For details around the methods used in these experiments see methods 2.2.1.2.

As mentioned in section 2.2.1.1 there are several different types of Transwell systems, with different volumes and pore sizes (table 2.1). When planning this first experiment it was based on the work by Friedl et al. in their study of diffusion of SNEDDS through pig gastric mucus (PGM) on 24 well Transwell plates (Friedl et al., 2013).

3.1.1 Diffusion studies through PSIM using a 24-well Transwell

Friedl et al. describes the use of a 24 well Transwell system to study diffusion of SNEDDS through PGM. They found this to be a method of many advantages, like its ability to test several replicates and different samples in the same setup, and the fact that it was easy to handle which means it is possible to reproduce the experiment (Friedl et al., 2013). This was found to be a good place to start the work and it was decided to test the diffusion of red 100 nm carboxylate FluoSpheres® through PSIM. As in the work by Friedl et al. the 24 well Transwell (design details in table 2.1) was used to test the diffusion, but in this work PSIM was used instead of PGM.

The FluoSpheres® was mixed into the PSIM in the donor chamber of the Transwell. This was done to make sure the different replicates have as similar conditions as possible. It would of course be more like the *in vivo* state to have the particles on top of the PSIM and then allow them to diffuse into and through the PSIM, but an *in vitro* experiment can never be exactly as the *in vivo* situation and in this case placing the particles on top of the PSIM could cause some problems. Due to the inhomogeneous nature of PSIM it may not fill the donor chamber in an even manner (Groo and Lagarce, 2014, Smart, 2005). The PSIM layer can be very thin some places, to the point where there is no PSIM at all, while other places may have very thick layers. If the particles were to be placed on top of the PSIM layer, the particles in some replicates would have a long way to diffuse to get through the PSIM and the filter, while others would be directly on the filter. This would give incorrect results and differences between the replicates. By mixing the particles into the PSIM it is not as critical to have an even PSIM layer in the donor chamber, and the conditions will be the same for all the samples. See figure 3.1 for an illustration.

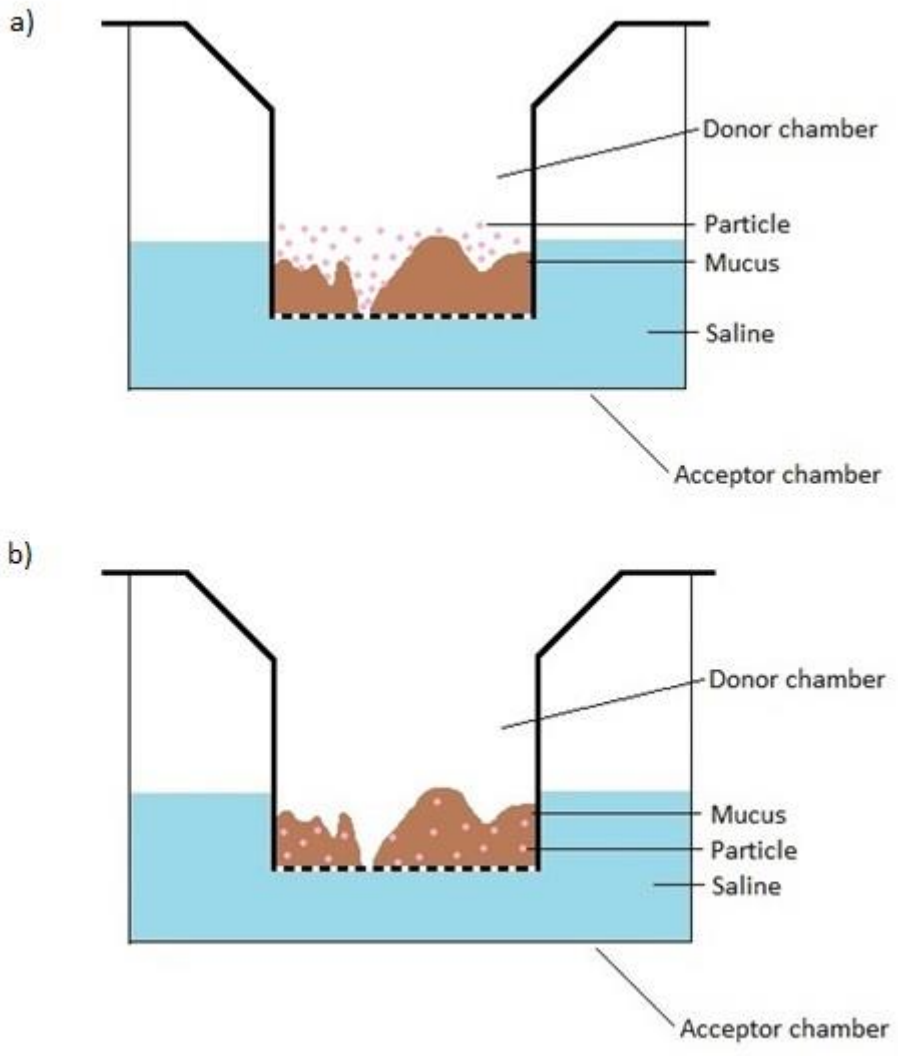

Figure 3.1: *Illustration of how PSIM can disperse itself in the donor chamber of the Transwell. By placing the nanoparticles on top of the PSIM they could potentially have very different diffusion lengths to reach the acceptor chamber (a). If the nanoparticles are mixed into the PSIM instead, the replicates will be more similar and the thickness of the PSIM would matter less (b).*

Ex vivo PSIM is not the easiest material to be working with and many choose to use other mucus models instead, like artificial mucus or mucins (Groo and Lagarce, 2014). There are several challenges working with PSIM, like its inhomogeneous nature which makes it difficult to work with, the extraction of it from the small intestines, and that the physical properties may differ between specimens because of individual variation (Groo and Lagarce, 2014). Never the less PSIM was used in these studies, as it was important to make it as similar to an *in vivo* situation as possible, and to see if the optimized methods would work with the PSIM.

There was no point in optimizing a method for an artificial mucus model, only to discover it would not work when the artificial mucus was replaced by PSIM.

For the diffusion study of nanoparticles through PSIM, red100 nm carboxylate FluoSpheres® (0.025%) were mixed into the PSIM and placed on the filter in the donor chamber. The test was conducted as described under methods 2.2.1.2.1 by filling 12 different wells with PSIM and FluoSpheres® in the donor chamber, and physiological saline in the acceptor chamber. Samples were collected from the acceptor chamber and the fluorescence was measured on a fluorometer. The results were then calculated and plotted as presented in figure 3.2. Raw data and calculations for all Transwell diffusion experiments are presented in appendix B.

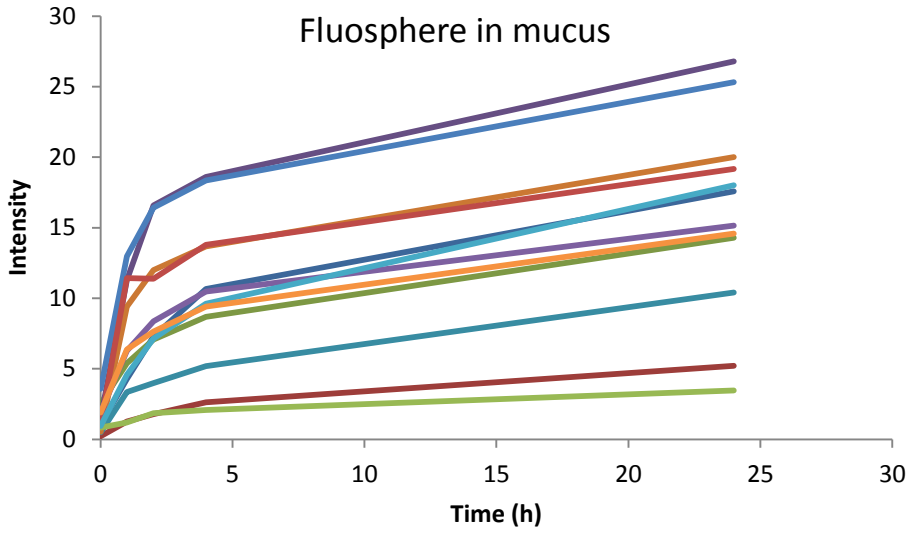

Figure 3.2: *Plot of the results from the first measurement of red carboxylate FluoSpheres® diffusion in mucus on the 24-well Transwell. Intensity of fluorescence is plotted over time measured in hours.*

From figure 3.2 it is clear that there are large variations in the results, and that the replicates are quite different from each other. Ideally all the results would be more similar if not exactly the same. They all seem to follow the same pattern, but at different levels of intensity.

Two control experiments were conducted with the FluoSpheres® and the PSIM separately. First a control containing PSIM and physiological saline was performed. The results are plotted in figure 3.3, and as seen there these results also varied from one another. PSIM is however not homogeneous (Groo and Lagarce, 2014, Smart, 2005), and the results were not

expected to be perfectly aligned. As a group of PSIM controls they are not that bad, and since they all have very low values, they can be considered similar for all practical purposes.

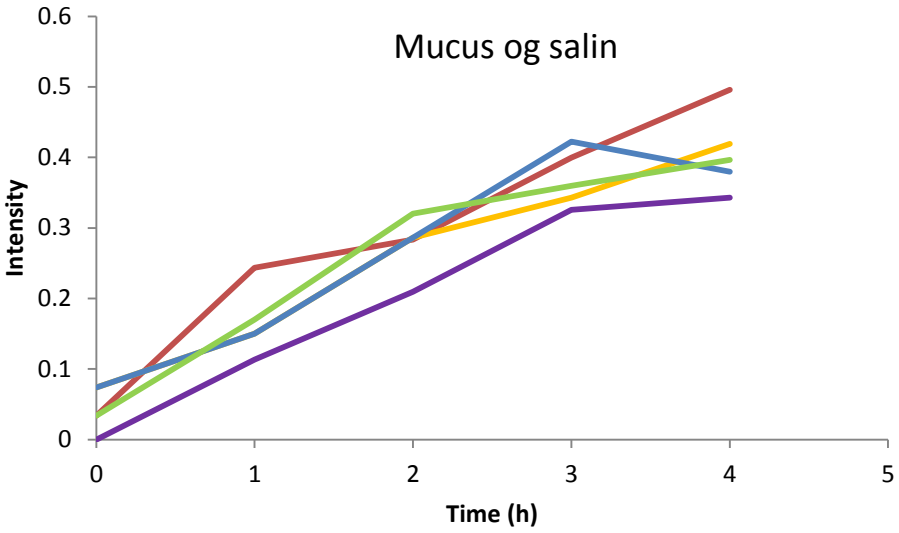

Figure 3.3: *Plot over the results of measuring the fluorescence from PSIM and physiological saline on the 24-well Transwell. Intensity of fluorescence is plotted over time measured in hours.*

In figure 3.4 the results of the other control-test is presented. This control contained the red FluoSpheres® (0.025%) and physiological saline instead of PSIM. There is a large variation in the results and there does not seem to be any direct pattern that the different replicates follow.

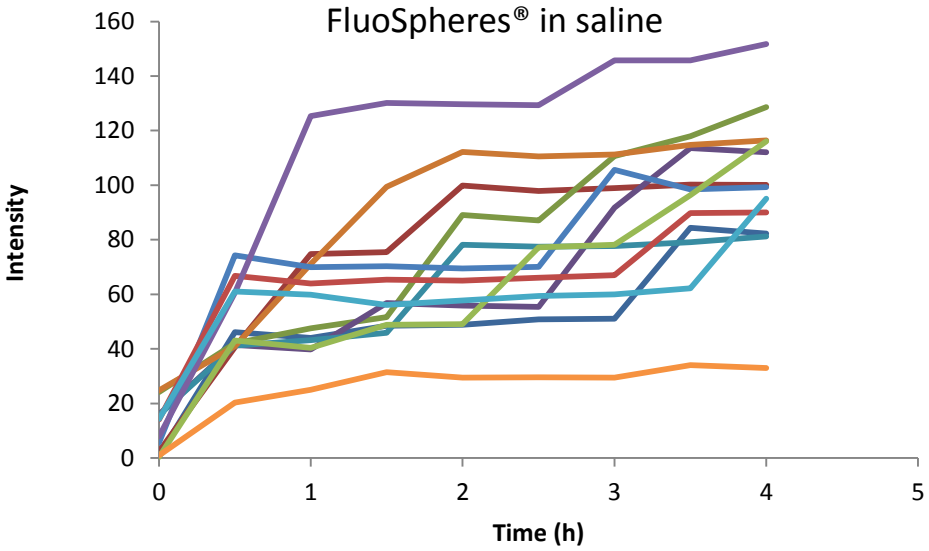

Figure 3.4: *Plot of FluoSpheres® in physiological saline on 24-well Transwell. Intensity of fluorescence is plotted over time measured in hours.*

There were generally large variations in the results presented in figures 3.2 – 3.4, which gave reason to believe that this was not the best method to measure the diffusion of nanoparticles through PSIM. One reason for these variations could be the relatively small size in the pores of the filter. The filter in the 24-well system have pores at 400 nm which in theory should be more than enough for the 100 nm FluoSpheres® to diffuse through. However, the results indicate that the diffusion of FluoSpheres® is somewhat sporadically, and they appear to be hindered by the filter in the Transwell. There have been claimed that nanoparticles and mucus may interact with one another to make larger holes in the mucin network (McGill and Smyth, 2010, Wang et al., 2011). Such interactions will also mean that the nanoparticles are attached to the mucus and that will make them unable to diffuse easily through the PSIM and the filter. It is also worth considering that the PSIM and the FluoSpheres® may cluster together to plug some of the pores in the filter. This would however not account for the large differences in the results from the controls containing FluoSpheres® and physiological saline, which are presented in figure 3.4. Therefore it is possible that the pore size of the filter might be the reason for the large variations of the results.

It was decided to do the measurements with 12 well Transwell systems with larger filter size and larger pores in the filter, instead of the 24 well. This was done to see if the variations in the results would be smaller. The results from the diffusion studies on the 24-well Transwell were very varying, indicating that something affected the diffusion of the nanoparticles. Most

likely the pore size of the filter is the reason for these varying results, as the pores might be too small. By changing to this 12-well system both the size of the pores and the size of the filter was increased (table 2.1). It would be possible to just alter the pore size and not the size of the well itself, but because of the small size of the 24-well it was desirable to change to a larger well. Most likely the change of well from a 24-well to a 12-well Transwell system will have an effect on the diffusion, and a higher diffusion due to larger pores and larger area is expected, but hopefully it will also be a more even diffusion.

3.1.2 Diffusion studies through PSIM using a 12-well Transwell

A control containing physiological saline and red 100 nm carboxylate FluoSpheres® (0.025%) was tested on the 12 well Transwell. The results were plotted as before and are presented in figure 3.5. It is clear that these results are much more even than the once presented in figure 3.4. Since the two factors that have changed are the pore size and the area of the filter, it is logical to assume that one of them is the reasons for the scattered results in figure 3.4. It would seem that the pore size of the filter was hindering the particles even though it in theory was enough space for the FluoSpheres® to diffuse through.

In the new results presented in figure 3.5 all the curves for the replicates have more or less the same shape indicating the results are similar for all replicates. The curves are leveling off at an intensity of about 580, which can be assumed to be the maximum diffusion. From the standard curve presented in figure 2.2 (section 2.2.1.2), and by calculations, it is observed that this will give an absolute weight of $9.5*10^{-5}$ mg for the red FluoSpheres® through the filter of the Transwell. Calculations can be found in appendix B4. When comparing this absolute weight of particle to the absolute weight of particle added to the donor chamber it would seem that the filter hinders some of the particles from diffusing through to the acceptor chamber. In the donor chamber there was an absolute weight of FluoSpheres® of 0.00125 mg. The absolute weight of FluoSpheres® in the acceptor chamber is thus 1/13 of the absolute weight of FluoSpheres® in the donor chamber, indicating that the filter hinders the diffusion of the FluoSpheres®. It is important to emphasize that these calculations are based on the theory of all the FluoSpheres® diffusing from the donor chamber to the acceptor chamber, and not on an even distribution of the particles. This will not be the case as there is not possible for all the FluoSpheres® to diffuse through as they seek to reach equilibrium. In other words it is not possible to reach 100 % diffusion. Still it is observed that much of the FluoSpheres® seem to be left in the donor chamber, which indicates something is hindering the diffusion. The physiological saline should not provide any obstacle for the diffusion, so it is natural to assume the filter is holding back some of the nanoparticles. Calculations presented in appendix B4.

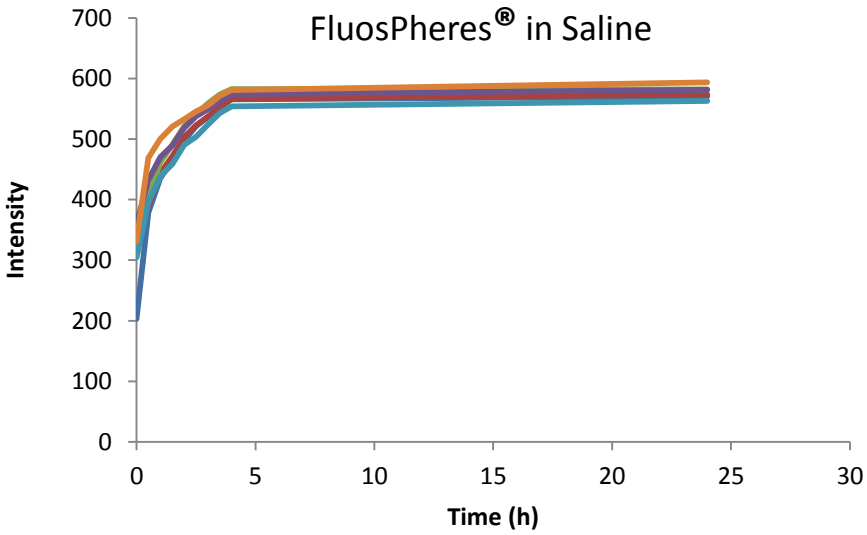

Figure 3.5: *Plot of FluoSpheres® in physiological saline on 12-well Transwell. Intensity of fluorescence is plotted over time measured in hours.*

Red FluoSpheres® diffusion in PSIM was tested on the 12 well Transwell and the intensity measured. The average of the results from independent wells is shown in figure 3.6 as the blue curve. At the same time a control experiment containing PSIM and physiological saline instead of FluoSpheres® was performed, and the average resulting intensity from these wells is shown as the red curve in figure 3.6.

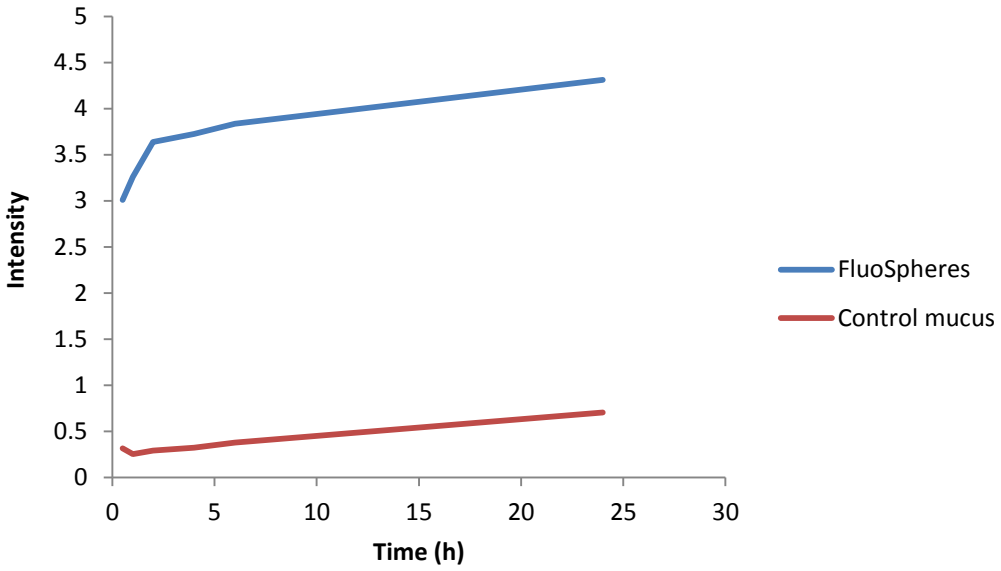

Figure 3.6: *Plot of the average results from FluoSpheres® in PSIM (blue) with average results from controls consisting of PSIM and physiological saline (red). Both are tested on the 12-well Transwell. Intensity of fluorescence is plotted over time measured in hours.*

From the plot in figure 3.5, the maximum intensity that comes out from the Transwell for the red carboxylate FluoSpheres® is at 580. This gives that the amount of FluoSpheres® that comes out through the PSIM and the filter in figure 3.6 is at approximately 0.62 % of maximum (See calculations in appendix B5). This is after correction for the background intensity created by PSIM. This is not very high amounts, but it demonstrates the barrier function of mucus in a good way. It does also show that the method of diffusion on Transwell systems seems to be working, since the results given in figure 3.6 indicates higher fluorescence for the samples containing FluoSpheres, than for the control samples of mucus without FluoSpheres®. This most likely means that some of the FluoSpheres® are able to diffuse through the PSIM and out into the acceptor chamber, giving a higher intensity of fluorescence.

Since the diffusion seemed to be more even after changing from the 24-well Transwell to the 12-well Transwell, it was reasonable to assume the increase of pore size in the filter gave a more uniform flow of FluoSpheres® through the filter leading to the acceptor chamber. It was however not certain if the increase of size of the filter itself did affect the diffusion. To test this, measurements was conducted using a 6-well Transwell system with larger area of the filter than the 12-well system, but with the same size of the pores in the filter.

3.1.3 Diffusion studies through PSIM using a 6-well Transwell

The diffusion of FluoSpheres® on the larger 6-wells would also be interesting to test to see if a change in area would affect the diffusion of nanoparticles through mucus. The pore size would remain the same as for the 12 well Transwell, but the area would increase by almost four times. This would also give an indication as to whether the improved results in figure 3.5 comes from increased pore size alone, or if the size of the area also affects the results. The expected results were that the size of the filter area would not affect the diffusion as much as the pore size of the filter. If the area of the large filter is twice the size of the smaller filter, one should in theory expect twice the amount to come through, but there would also be twice as much in the donor chamber of the Transwell, so the diffusion would in fact be the same. To test this theory, diffusion studies were performed using both the smaller 12-well Transwell and the larger 6-well Transwell.

When using the 6-well system it is important to consider the increase in used amount of PSIM to cover the filter in the donor chamber, and the increase in nanoparticle suspension used. To use more material is not financially favored, and should be avoided if possible. When considering this it would be more optimal to use the smaller 12-well Transwell but due to long delivery on the 12-well plates, the 6-well plates was used for further diffusion studies through PSIM.

In figure 3.7 the average intensity of FluoSpheres® in PSIM on the 12 well Transwell is marked as blue and the average intensity of FluoSpheres® in PSIM on the 6 well Transwell with the larger area is marked as green. The results are divided by their respected area so that they can be compared in the plot seen in figure 3.7.

The two plots are not identical, but when one sees the maximum percentage that comes out of the two, they do not differ that much. For the smaller area the amount that comes out when not calculating for background by the PSIM is 0.66 % and for the larger are it is 0.64 %. As a trend the larger area seems to have a smaller amount of FluoSpheres® coming through in the beginning of the experiment. However, after some time they seem to go toward the same result. All calculations and raw data for this experiment can be found in appendix B6. It is important to make a point of the fact that these experiments focusing on the area did not have

as many replicates as might be needed to make good results. But they provide an illustration of how the area affects the diffusion of nanoparticles through the PSIM, and these results were interpret in the way that the area eventually will not matter. In hindsight it is clear that the measurements should have been repeated with several replicates to increase the credibility of the experiments.

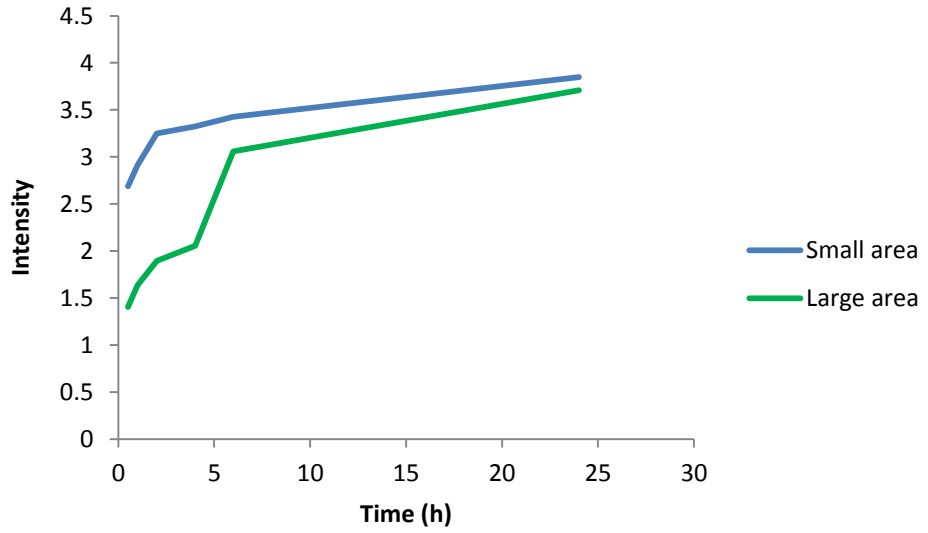

Figure 3.7: *Plot that shows the average results from diffusion of FluoSpheres® in PSIM on both the 12-well Transwell (blue) and the 6-well Transwell (green). Intensity of fluorescence is plotted over time measured in hours.*

Work by Nordgård et al. and Taylor Nordgård and Draget gives reasons to believe that the presence of G-block might increase the diffusion of nanoparticles in mucus (Taylor Nordgård and Draget, 2011, Nordgård et al., 2014). If this is the case it would be interesting to see if the Transwell method could be used to study such an effect. The 6-well Transwell was used in the further studies to test if an effect on diffusion caused by G-block could be detected using the Transwell method. This was tested with two types of nanoparticles, first with yellow-green 40 nm carboxylate FluoSpheres® and then with rhodamine loaded SNEDDS.

3.1.3.1 Diffusion studies on Transwell, with and without G-block added

The Transwell method was to be tested to see if it is suitable for use in measuring effect of G-block on diffusion of nanoparticles in PSIM. In the work by Nordgård et al. and Taylor Nordgård and Draget, it has been stated that G-block might be able to alter the nature of the

network found in mucus. It is argued that the G-block may change the barrier functions of the mucus by disrupting the cross-links in the mucus network due to the polyelectrolyte nature of G-block which makes it capable of competitive inhibition of the electrostatic interactions in mucus, and that G-block can inhibit of the interactions between the matrix mucins and the mobile components, which in this case would make the diffusion less difficult for the nanoparticles (Nordgård et al., 2014, Taylor Nordgård and Draget, 2011). This increase in pore size in the PSIM, or inhibition of interactions between the nanoparticles and the mucins would mean that the nanoparticles used in this study could diffuse through the PSIM and the filter more easily than if the PSIM network was intact. The Transwell method might be a good method for testing this theory further, as it is a relatively easily reproducible and low-cost method to use.

To test this method for studying the effect of G-block on diffusion of nanoparticles through PSIM, both yellow-green 40 nm carboxylate FluoSpheres® and rhodamine loaded SNEDDS were used on the 6 well Transwell, with and without G-block mixed into the particle dilution. The reason for changing the color of the FluoSpheres® from red FluoSpheres® to yellow-green FluoSpheres® comes from the change of size from 100 nm to 40 nm. The 40 nm FluoSpheres® are closer in size to the SNEDDS, which have a size of 60 nm. This makes them more easily compared. However, the 40 nm FluoSpheres® is not available in other colors than yellow-green and therefore it is changed, although this means changing the wavelength for measuring the fluorescence. Such a change in wavelength might affect the measurements, as there might be an increase in auto fluorescence from the PSIM.

In figure 3.8 the average of the results for the FluoSpheres® are presented as plots, while the average results for the SNEDDS are presented in figure 3.9 and 3.10. It is important to emphasize that the FluoSpheres® used in the Transwell tests in figure 3.8 are 40 nm in size and not 100 nm as the once used up till this point. Due to that, the intensity is higher than in the previous figures as more FluoSpheres® are able to diffuse through because of their small size. Measurements were performed with FluoSpheres® (0.025%) containing G-block and FluoSpheres® (0.025%) without G-block diffusing through PSIM on the 6-well Transwell. Control samples of the FluoSpheres® were also measured. They contained FluoSpheres® (0.025%) with and without G-block and physiological saline instead of PSIM. In addition a control containing PSIM and physiological saline was measured.

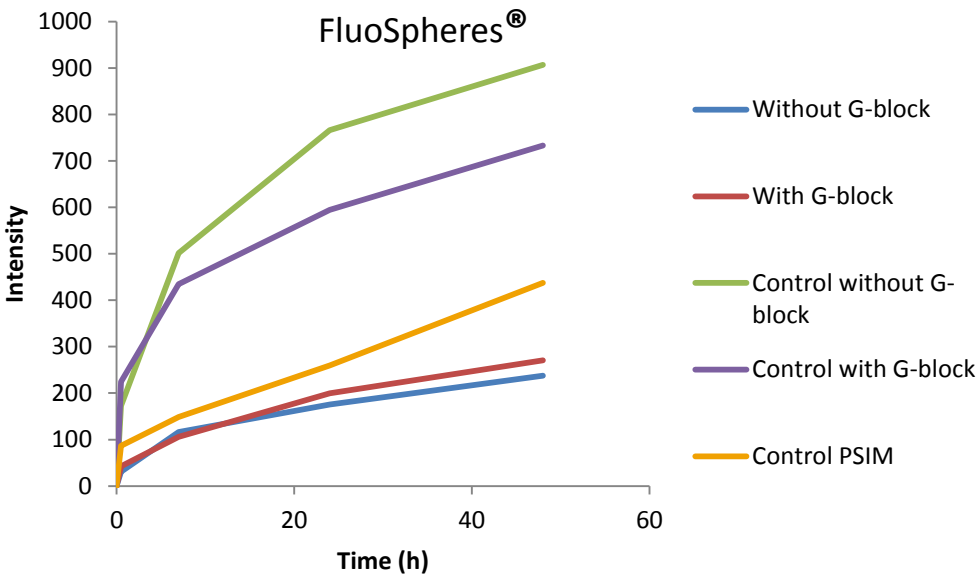

Figure 3.8: *Plot showing the average results of FluoSpheres® (0.025%) in PSIM, with and without G-block present (red and blue). The plot also shows average results from control samples containing FluoSpheres® (0.025%) with and without G-block (purple and green), where the PSIM is replaced by physiological saline. PSIM control is also measured (orange), where the FluoSpheres® are replaced by physiological saline. Intensity of fluorescence is plotted over time measured in hours.*

From figure 3.8 it is clear that both the FluoSpheres® control with and without G-block, where PSIM is replaced with physiological saline (purple and green) have a much higher intensity than the samples diffusing through PSIM (blue and red). This was as expected since the diffusion through PSIM hinders many of the nanoparticles. The two FluoSpheres® controls start out with very similar intensity, until the control without G-block rises steeply in intensity while the control with G-block rise less steeply giving a higher intensity for the control without G-block than the control with G-block. Due to relatively few independent replicates in this experiment it is not easy to draw conclusions from these results.

High intensity in the samples indicates more particles through the filter. Looking at the measurements for the samples of FluoSpheres® with and without G-block, it seems the samples with G-block present are at a slightly higher intensity than the samples without G-block (figure 3.8). These differences are not large, and again there is not easy to draw conclusions as to the effect of G-block from such few replicates. It might be a slight indication of an increasing diffusion when G-block is present, but this might simply be a

coincidence. These results are averages from several independent wells, and there is important to consider that the data have a wider range than is shown in such an average. By performing these experiments several times with several independent replicates the average would be more representative of the actual situation.

What was surprising is the large background from the PSIM control (orange). The background fluorescence from these samples is on average larger than both the FluoSpheres® with G-block and the FluoSpheres® without G-block. The PSIM have a much higher auto fluorescence at the ex/em of the yellow-green FluoSpheres® than it does for the red FluoSpheres®, which gives much more intensity on these measurements. This is unfortunate as the 40 nm FluoSpheres® does not come in the red color which is measured at a wavelength which gives much less auto fluorescence from the PSIM. A possible explanation for the low intensity of the FluoSpheres® samples with PSIM, which in fact is lower than the PSIM control without FluoSpheres®, may be interaction between the FluoSpheres® particles and the PSIM (Wang et al., 2011, McGill and Smyth, 2010), which again may hinder the particles further from passing through the filter. In addition such interactions would seem to make the PSIM less mobile and keeping it more in place in the donor chamber, thus giving results with intensity lower than for the PSIM control, since less of the PSIM is likely to diffuse through the filter.

For the SNEDDS the same trends were observed as for the FluoSpheres®. Measurements were performed with SNEDDS (0.45%) containing G-block and SNEDDS (0.45%) without G-block diffusing through PSIM on the 6-well Transwell. Control samples of the SNEDDS were also measured. They contained SNEDDS (0.45%) with and without G-block and physiological saline instead of PSIM. The SNEDDS are prepared with a higher concentration than the FluoSpheres®, which is done because the SNEDDS are less fluorescent than the FluoSpheres®. Controls containing PSIM and physiological saline were also measured. In figure 3.9 and 3.10 the averages of the results from several wells are presented. Due to difficult visualization of some of the samples in figure 3.9, these are presented alone in figure 3.10 so they can be separated more easily from one another.

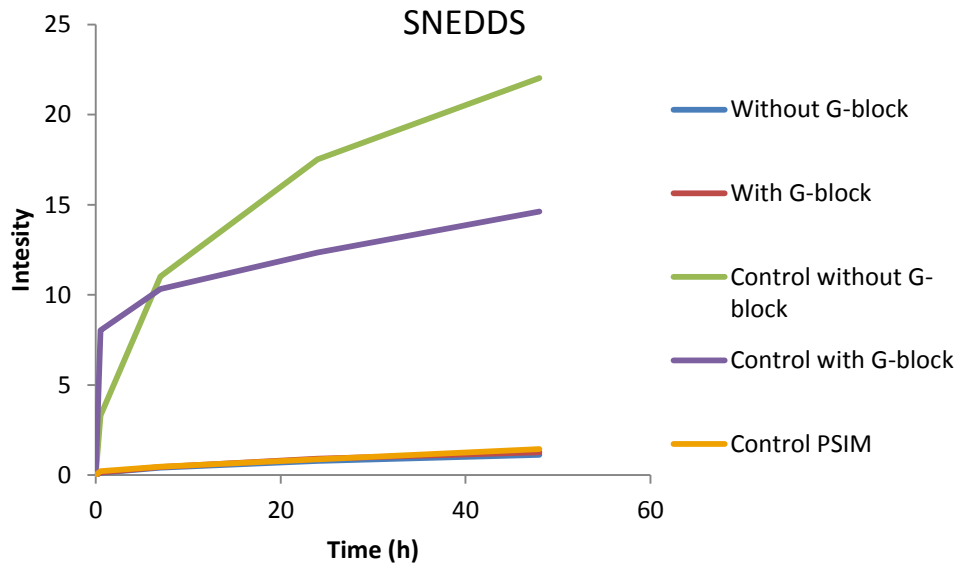

Figure 3.9: *Plot showing the average results of SNEDDS in PSIM with and without G-block present (red and blue). The plot also shows average results from control samples containing SNEDDS with and without G-block (purple and green), where the PSIM is replaced by physiological saline. A PSIM control is also measured (orange), containing PSIM and physiological saline instead of SNEDDS. Intensity of fluorescence is plotted over time measured in hours.*

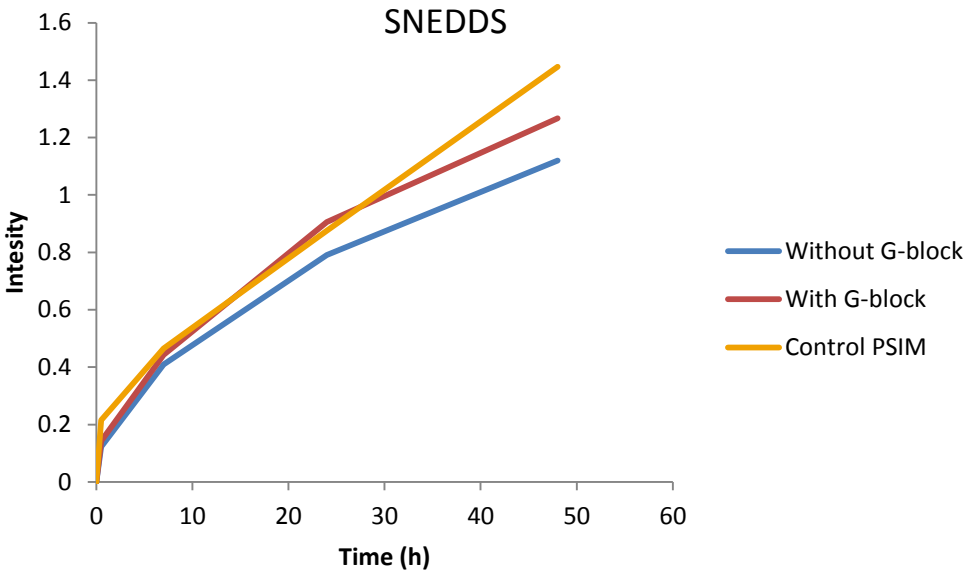

Figure 3.10: *Plot showing the average results of SNEDDS in PSIM, with and without G-block present (red and blue). The plot also shows average results from PSIM control samples with physiological saline instead of SNEDDS (orange). Intensity of fluorescence is plotted over time measured in hours.*

The SNEDDS controls (purple and green) are higher than both the tests with SNEDDS in PSIM (blue and red) and the PSIM control (orange). From figure 3.9 there is observed that the SNEDDS control without G-block has lower intensity than the SNEDDS control with G-block in the first hours, but then the intensity for the control with G-block flattens out, while the intensity without G-block continues to rise to be considerably higher. It is expected to see higher intensity in the control samples containing SNEDDS and physiological saline, since there is less hindrance when PSIM is not present. The intensity from the samples with SNEDDS is much lower than for the experiments with FluoSpheres®. This is due to less fluorescence in the SNEDDS, compared to the FluoSpheres®. In figure 3.10 the plot for the tested SNEDDS with and without G-block are presented again with the control for PSIM. The controls have so much higher intensity than these samples, so they are not easily distinguished in the plot with the SNEDDS controls. Since the values of the samples in figure 3.10 are so low and so similar to each other it is difficult to discuss much about the effect G-block might have on them. Again it is observed that the control containing PSIM and physiological saline have a high intensity compared to the SNEDDS samples with PSIM. This probably comes from auto fluorescence from the PSIM, as the fluorophore in these SNEDDS are measured at a wavelength between the once for the red FluoSpheres® and the yellow-green FluoSpheres®. To prevent this it would be possible to change the fluorophore in the SNEDDS in future experiments, to get as little auto fluorescence as possible from the PSIM.

When working with experiments to optimize methods, it will be useful to test the same theories using several methods, to see if they generate the same results. There might be so that one method gives a desirable result while another method gives different results. This is one of the reasons there is need for several methods to use during experiments and studies. If several methods and independent experiments generate the same results, there is much more plausible that the results are in fact close to the truth and perhaps can be regarded as conclusive. Because of this it was interesting to investigate the optimization of another method, to see if the results from the Transwell experiments would be supported or not. The µ-slide chemotaxis was interesting, as it had many qualities which were desirable in the diffusion studies of nanoparticles through mucus. These qualities included the use of an agent to hold the PSIM in place in a chamber, which would provide a clear front for the nanoparticles to diffuse into. Such a front could easily be studied using a confocal microscope.

3.2 Diffusion studies of nanoparticles through PSIM using µ-slides chemotaxis

The µ-slides chemotaxis are meant for use in study of cells chemotactical response to chemicals, but the design may also be very well suited for use in diffusion studies with nanoparticles through mucus. Figure 3.11 provides an illustration of the µ-slides chemotaxis. There are several reasons why these slides might be used in diffusions studies; they have a design that is made for use on a microscope and diffusion of nanoparticle can therefor easily be studied using a confocal microscope to detect and photograph the fluorescent particles. By using agar in the centre chamber or gap between the chambers the PSIM will stay in place in its chamber and there will be a clear interface between the mucus and the agar, giving a front that is very easily defined. This is an important feature because of mucus degradation. When working with PSIM or any other type of mucus *in vitro*, degradation of mucus will always occur, making it difficult to get a clear and stable front. Another advantage is the fact that the chambers have relatively small volumes making it possible to use small amounts of mucus. Because of the advantages of the design diffusion studies with the µ-slide chemotaxis were performed. It was also interesting to see if this method could verify some of the results from the diffusion studies on the Transwell.

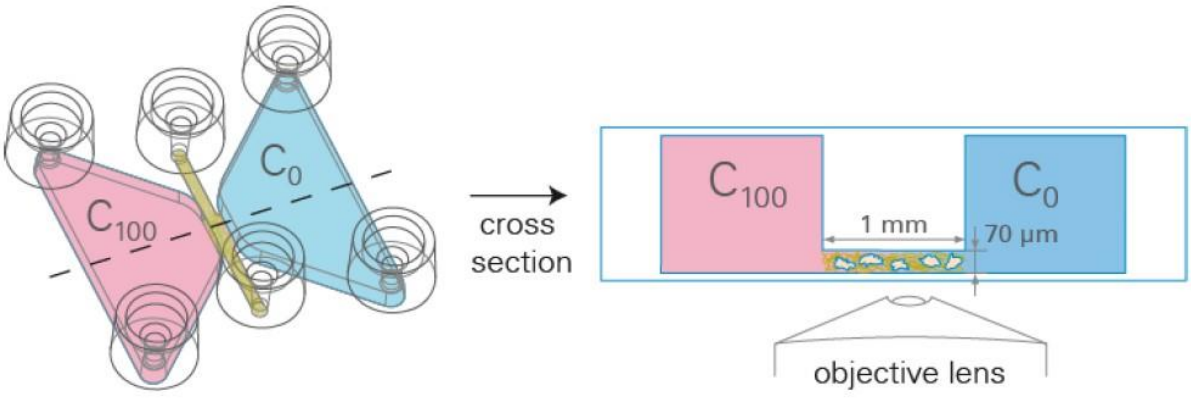

Figure 3.11: *Illustration that shows an overview and cross section of the µ-slide chemotaxis. To the left is one of the main chambers (pink) and to the right is the other main chamber (blue). Between the chambers there is a small gap (brown). The picture is from the Ibidi instruction manual.*

After inserting agar (1%) to the gap between the chambers and letting it set, PSIM was inserted to the first chamber using a rounded tip as described in methods 2.2.2.2. The yellow-green 100 nm carboxylate FluoSpheres® was then inserted to the second chamber and the µ-slide chemotaxis plate was studied on the confocal microscope. A photo of the plate is shown in figure 3.12.

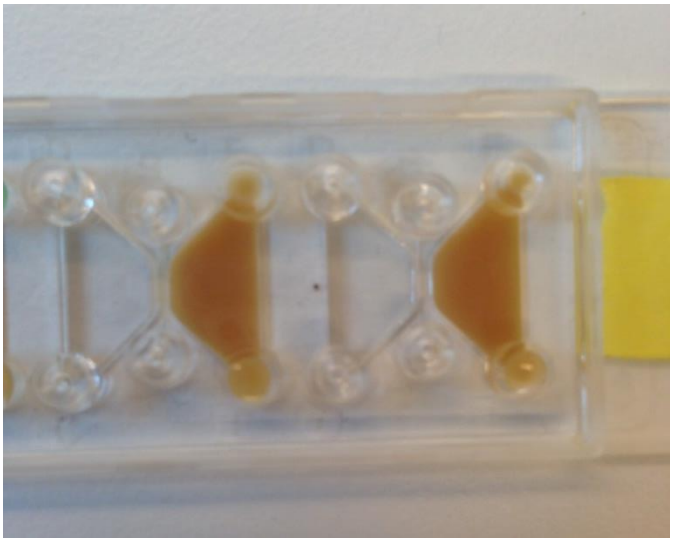

Figure 3.12: *Photo of the µ-slide chemotaxis plate with PSIM in the chambers on the right (brown) and FluoSpheres® suspension in the chambers on the left side. Between the two chambers is the gap containing agar (1%) gel.*

It was left for a period of 30 minutes while the microscope photographed it every minute. The result was somewhat unexpected. The expectation was that the FluoSpheres® would diffuse easily through the agar (1%) in a short period of time and then meet the PSIM and continue diffusing into it. What was observed was that the yellow-green 100 nm carboxylate FluoSpheres® did not seem to be able to diffuse into the agar (1%). There was little or no fluorescence to be detected there. In figure 3.13a a photo of the front between the FluoSpheres® and the agar (1%) taken by a confocal microscope at time t = 0 minutes is presented. Figure 3.13b presents a photo taken at the exact same place in the sample, at time t = 30 minutes. A plot profile was made of the two photos to compare them better. This is presented as figure 3.14.

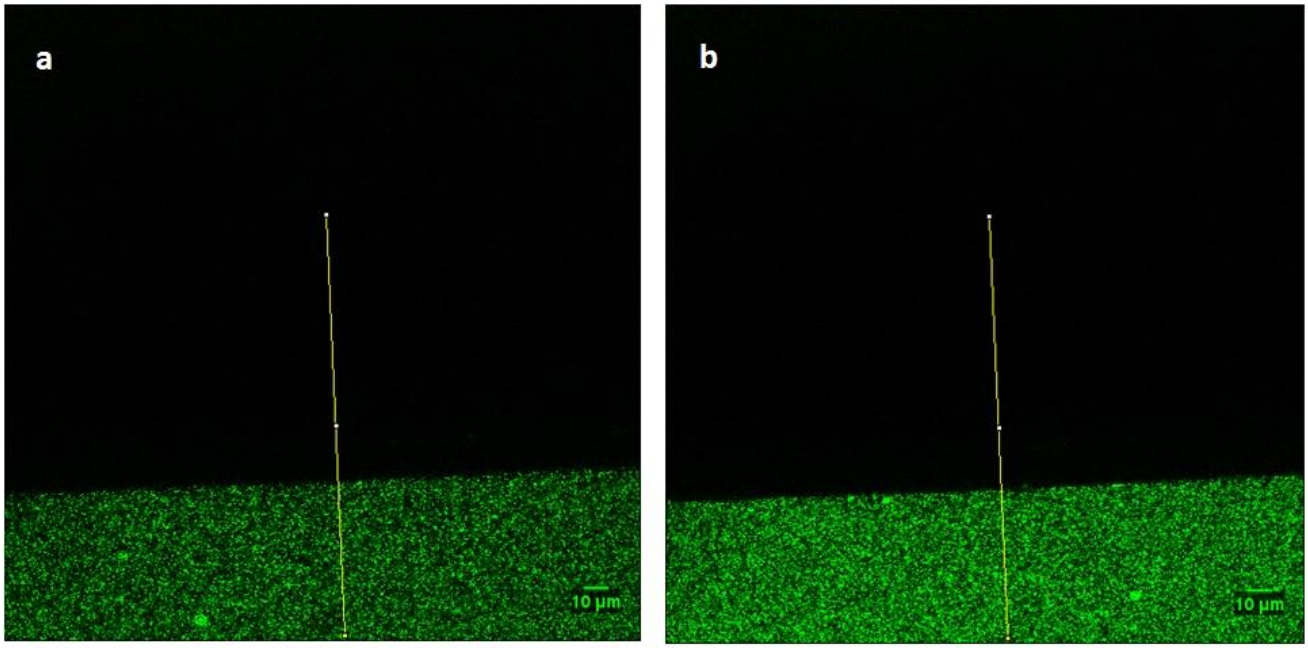

Figure 3.13: *Photo showing the fluorescence in the FluoSpheres® solution (lower side of the photo) and in the agar after time t = 0 minutes (a), and after time t = 30 minutes (b). The photo is taken using a confocal laser scanning microscope. The yellow line is the plane where the profile plot was measured from. On the lower right side there's scale bar.*

Note that there does not seem to be much difference between the two photos, except from the fact that there might be slightly more fluorescence in the FluoSpheres® side (lower side) of the picture in figure 3.13b. This might indicate that the FluoSpheres® are moving towards the agar (1%), but does not seem to be able to diffuse into it in the way that was expected.

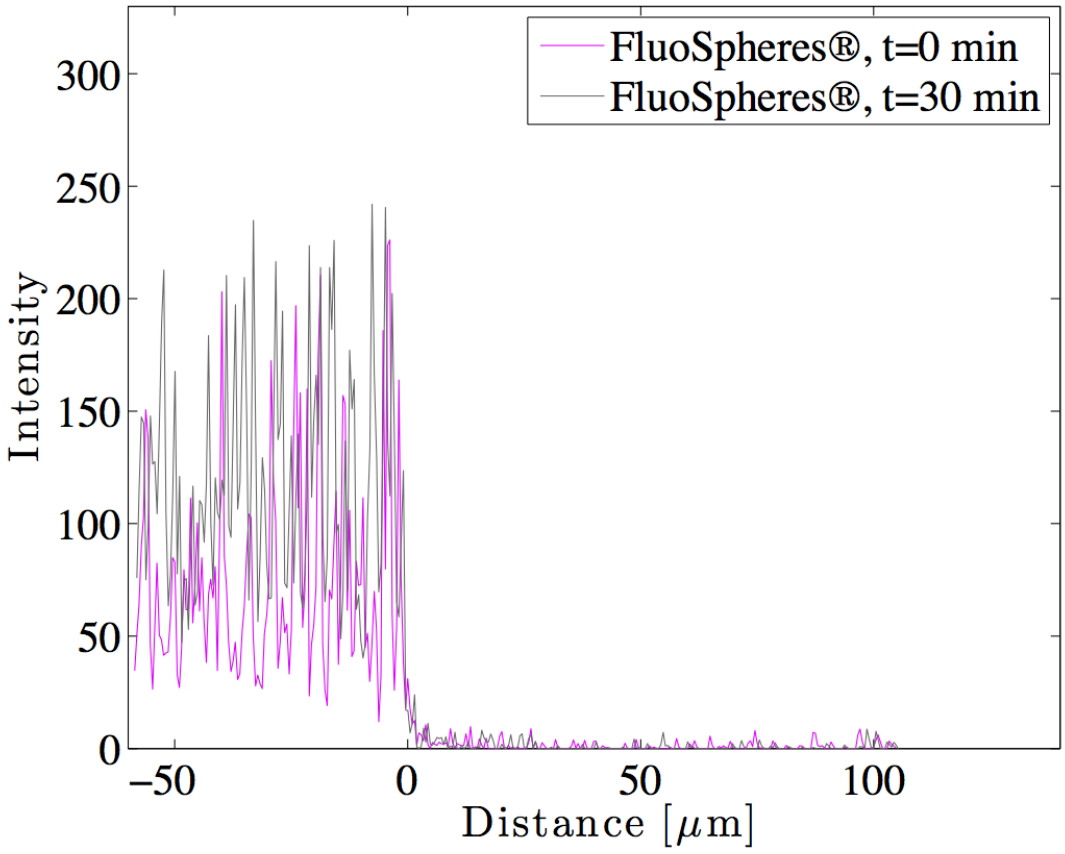

Figure 3.14: *Profile plot from photos shown in figure 3.12 and figure 3.13. The purple plot is for time t = 0 minutes and the black plot is for time t = 30 minutes. Intensity is plotted over distance measured in µm.*

From the profile plot in figure 3.14 it is possible to see that the fluorescence seem to be lower in the FluoSpheres® side after 0 minutes than after 30 minutes, while it does not seem to change in the agar side (right side) of the plot. A small amount of fluorescence is observed in the agar side as well, which might indicate that there is some diffusion into the agar (1%). Never the less this intensity is low and it seems clear that the agar does in fact inhibit the diffusion of the FluoSpheres®. It is also worth considering that the fluorescence observed in the agar is caused by auto fluorescence from the agar itself. Measures were made to avoid background, by calibrating the confocal microscope to not detect fluorescence from the agar gel.

Initially I would not expect agar (1%) to be an obstacle for the yellow-green 100 nm carboxylate FluoSpheres® because of its porous nature. In theory such a gel should not

provide much of an obstacle for the FluoSpheres® since it is uncharged and at such a low concentration of just 1 %. However, Smidsrød states that for alginate gels there is observed many pores, but most of them are small, and only a few of them are large (Smidsrød, 1973). This could very well be the case for agar gels as well, and if so it would be an obstacle for the FluoSpheres® to penetrate the agar gel.

To test if the yellow-green 100 nm carboxylate FluoSpheres® was in fact able to move through the agar (1%), the diffusion was tested on the Transwell system which had previously proved to be useful in diffusion studies through PSIM. In principle it would be the exact same procedure as with the PSIM on the 12-well Transwell only exchanging the PSIM with agar (1%). In addition the FluoSpheres® were placed on top of the agar, and not mixed into it like with the PSIM. In this way it is comparative to the situation in the µ-slide chemotaxis where the FluoSpheres® need to diffuse into and through the agar gel. For full procedure see methods 2.2.2.2.

It was important to find out if the agar was the component hindering the diffusion, for in that case it was not suited for this diffusion experiment after all. The agar was merely meant to function as an agent to hold the PSIM in place to create a clear front, not provide another obstacle for the FluoSpheres®. After the FluoSpheres® and the agar (1%) had been on the Transwell for 24 hours, samples from the acceptor chamber were measured using a fluorometer. Several different tests were performed, which are presented in table 3.1. The results presented in table 3.1 are average results from tests performed in different wells. The control with agar (1%) contained agar and physiological saline instead of FluoSpheres® in the donor chamber. This is to measure the background from the agar. The control for the FluoSpheres® contained yellow-green 100 nm carboxylate FluoSpheres® (0.025%) and physiological saline instead of the agar in the donor chamber. In addition two tests were performed with agar (1%) and yellow-green 100 nm carboxylate FluoSpheres® (0.025%), where one of the tests had 200 µl physiological saline on top of the agar before the FluoSpheres® were added. This was done to see if drying of the agar gel could be a factor to prevent the FluoSpheres® from diffusing into it. The raw data and calculations for table 3.1 can be found in appendix C1.

Table 3.1: *Showing results after diffusion study of FluoSpheres® (0.025%) on agar on a 12-well Transwell, after 24 hours.*

Test	Average results for intensity	Average after correction for background by agar (1%)	Percentage out of maximum diffusion (%)
Control Agar (1%)	17.99	-	-
Control FluoSpheres® (0.025%)	553.54	-	100
Agar (1%) and FluoSpheres® (0.025%)	25.08	7.10	1.3
Agar (1%) with 200 µl physiological saline on top and FluoSpheres® (0.025%)	45.71	27.73	5.0

Table 3.1 presents the different diffusion studies performed with agar on the 12-well Transwell. The calculated average results presented in the table 3.1 shows that only small amounts of FluoSpheres® diffuse through the agar and out to the acceptor chamber of the Transwell. The highest intensity was measured in the samples containing 1% agar with 200 µl physiological saline on top and FluoSpheres on top of that again. For this test 5 % of maximum diffusion from the FluoSpheres® control came out through the agar and the filter. This test contained the same amount and concentration of agar and FluoSpheres® as all the other samples but the physiological saline was added to the donor chamber prior to the FluoSpheres®. The added physiological saline might be the reason for what would appear to be a higher diffusion through this agar. If the agar gel quickly dries after setting it would be

expected it to create a thin film on top where it is exposed to the air. Such a dry crust would stop diffusion of FluoSpheres® into the agar gel. The physiological saline added to the top of the agar gel might be enough to keep it from drying out, thus it will not be a film and the FluoSpheres® can diffuse more easily through the agar.

A diffusion of 5% of maximum is not a very high percentage given that the original idea was that the agar would not provide a hinder for the FluoSpheres® at all. To be sure the agar was the component slowing the FluoSpheres® down and not the filter in the Transwell, tests were performed without the filter. The FluoSpheres® were mixed into the melted agar to create a 1% agar with FluoSpheres®.

The samples were measured on a fluorometer and the average of the results is presented in table 3.2. Raw data is found in appendix C2.

Table 3.2: *Showing results after diffusion study of FluoSpheres® (0.025%) mixed into agar (1%) without filter, after 24 hours.*

Test	Average results for intensity	Average after correction for background by agar (1%)	Percentage out of 100% (%)
Control Agar (1%)	20.01	-	-
Agar (1%) and FluoSpheres® (0.025%)	51.49	31.48	5.69

Again the percentage of diffused nanoparticle is very low, indicating that the agar may not be a suitable media to use in the µ-slide chemotaxis system to hold PSIM in place. If the FluoSpheres® cannot penetrate the agar (1%) and diffuse further into the PSIM, the agar is not suitable for these diffusion studies.

By further study of the theory behind agar gels it was discovered that several articles dismiss the theory that diffusion through agar gels is like free diffusion (Johnson et al., 1996, Ackers

and Steere, 1962). These tests had their basis in more concentrated agar gels, while the experiments performed in this thesis worked with relatively low concentrations since the agar was just needed to hold the PSIM in place. But even for low concentrations like 1% it is claimed that the diffusion is considerably lower than for free diffusion (Ackers and Steere, 1962). All though the agar is a porous gel when considering its two-dimensional structure, one also has to think about the steric hindrance that is present in the three-dimensional structure of the gel. In the unpublished work by Smidsrød (1973) the gel state of alginate gels are studied and it is claimed that though some pores are larger, most of them are small. If this can also be assumed to be the case for agar gels, it can explain why diffusion through the gel is difficult. In a section with a thickness of 40 nm he states that there are about 30 pores in the size range of 40 nm and only one or two in the size of 200 nm (Smidsrød, 1973).

One of the reasons for testing with agar (1%) in the first place was indications given by team members of the COMPACT in Denmark, who claimed to have performed successful diffusion studies with agar. This might however be for smaller molecules.

After testing the diffusion both on Transwell and without filter, this method was rejected, since other methods had proven more suitable, and since the agar was not very well suited for this work. It would also be possible to return to the µ-slide chemotaxis and attempt to find a different substance to fill the gap and keep the PSIM in place in the chamber. Such an agent would need to be of no hindrance to the diffusion of nanoparticles. Since the agar did not provide a good agent for keeping the PSIM in place, a new method was investigated. This was the µ-slide $VI^{0.4}$ ibiTreat which have canals which can be filled form both sides, and a relative small volume, so there is no need to use large amounts of PSIM. These µ-slides are also meant for use on a microscope and diffusion can therefor easily be studied using a confocal microscope. Photos of the µ-slide are presented in figure 3.15, with an illustration in figure 3.16.

3.3 PSIM diffusion studies using µ-slides

After abandoning the µ-slide chemotaxis ^{3D} another µ-slide (µ-slide VI$^{0.4}$ ibiTreat) was investigated for use in diffusion studies. This one has a different design from the µ-slide chemotaxis, and there is no space for agar between the nanoparticles and the PSIM. This is an advantage since the agar obviously was not a good component to be working with in this type of diffusion experiments, but at the same time it means that there will not be as easy to obtain a clear front between the PSIM and the nanoparticle suspension. Figure 3.15 shows two pictures of the µ-slide, and figure 3.16 show an illustration of the experimental setup in the µ-slide. To make this method functional there was a need for some optimization. The general idea, as described in section 2.2.3.1, was to introduce PSIM to the canal from one side and the nanoparticles from the other. In this way they would meet in the middle of the canal to provide a front that could be studied by confocal microscopy.

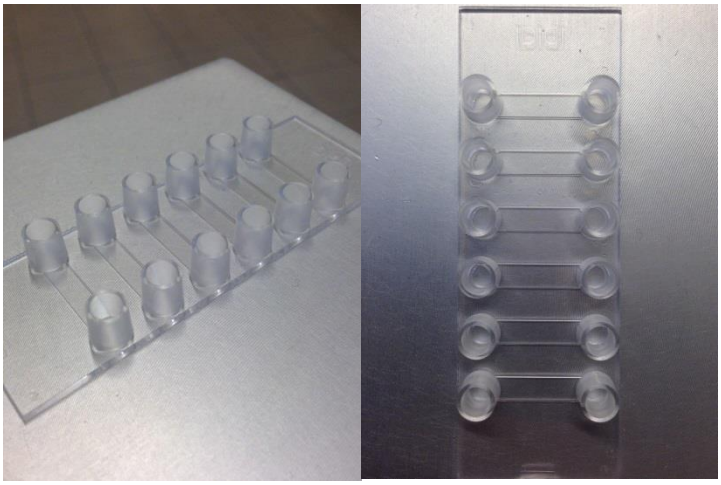

Figure 3.15: *Two photos of the µ-slide from the side and from above. Each slide has six channels with two openings.*

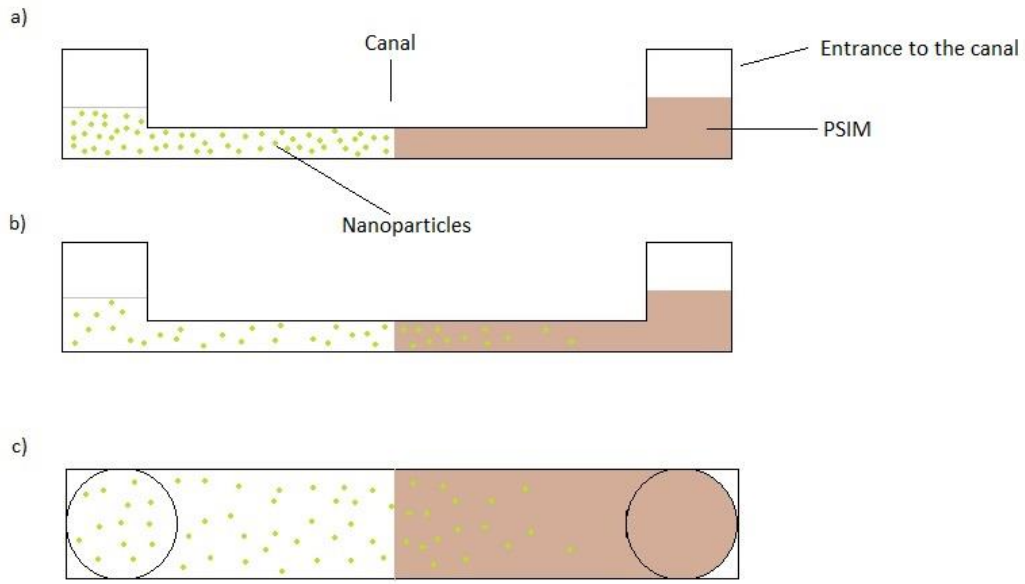

Figure 3.16: *Simple illustration of the µ-slides with a side view in a) and b), and seen from above in c). The idea is to fill the chamber with PSIM from one side and particle suspension from the other to create a front in the middle of the canal (a). After some time the particles will begin to diffuse into the PSIM (b). By using a confocal microscope there is possible to take images of the diffusing particles.*

A delicate touch was needed to be able to introduce the PSIM to the canal and stopping it in the middle. When pushing the piston on the syringe, it took very little force to press the PSIM all the way through the canal and up the opening on the other side. To avoid using all the PSIM on practicing the right pressure the work was initially done using biosimilar mucus. While working on this process of manipulating the biosimilar mucus to stop in the right position in the canal it was discovered that the front was slowly moving further through the canal by itself, probably due to capillary forces. Ideally this would not be a problem as the canal would be filled from the other side by a nanoparticle suspension. When testing that hypothesis using water instead of nanoparticles, it became clear that pushing liquid in from the other side of the canal would cause air to be trapped between the water and the biosimilar mucus. This would obviously be a problem as the two need to be in contact to be studied properly. By holding the µ-slide in an upright position while inserting the water and also making sure the water entered the canal along one of the sides, the air was pushed out by the water and the problem was solved. The next problem would in fact be the water itself. The

water was digging its way through the biosimilar mucus and out the other opening, and the biosimilar mucus would eventually mix completely with the water.

When working with PSIM in the µ-slides it very soon became clear that the PSIM was moving through the canal rapidly on its own after pressure was removed. This is most likely the result of capillary forces. By just filling the opening with PSIM it is drawn into the canal by the capillary forces. The problem was the lack of control of where the front was to end. In addition the PSIM seemed to develop canals and the water filled the canals making the front disappear. This could most likely be caused by phase separation, where excess water comes out from the PSIM giving a liquid in which the nanoparticle suspension could canalize through. When PSIM is collected it is scraped from a washed small intestine. This normally causes some water to be scraped out together with the PSIM.

In its natural environment and place of origin, the mucus is in constant renewal and the turnover time can be quite short, as in the eyes where the tear film is replaced approximately every ten seconds (Boegh and Nielsen, 2014, Cone, 2005). When the PSIM is collected from the small intestine it is removed from its environment and the cells that are needed to renew it. Because of this it will begin to degrade as soon as it is collected and it loses some of its stability. To slow down the degradation it is kept cold, and frozen when not in use.

To avoid the phase separation of the PSIM and perhaps make it more stable, the PSIM was "washed". This is a process described in section 2.2.3.3 and includes agitating the PSIM with physiological saline before centrifugation. The washing of the PSIM was done following the protocol from Friedl et al. (Friedl et al., 2013), and the result was what seemed to be a much more stable PSIM. After centrifugation and removing the supernatant containing the excess water from the scraping of the small intestines, the PSIM pellet was much more compact. The washed PSIM generally seemed more homogeneous and less particular than it did before the washing. When introducing the washed PSIM to the canal it became clear that it was much easier to work with and seemed to be more stable. It could be pushed into the canal by a syringe and would stop when pressure was removed, to create a stable front. When inserting nanoparticle suspension from the other side the PSIM stayed in place and there was no evidence of phase separation.

This method seemed to be functional, and experiments using 40 nm yellow-green FluoSpheres® in some canals and SNEDDS in others was planned. To see if the presence of G-block would have any effect on the diffusion through the PSIM, samples were made both without and with G-block in the nanoparticle suspension. The different tests and diffusions were to be observed on the confocal microscope. Figure 3.17 shows the µ-slide after insertion of PSIM and FluoSpheres®.

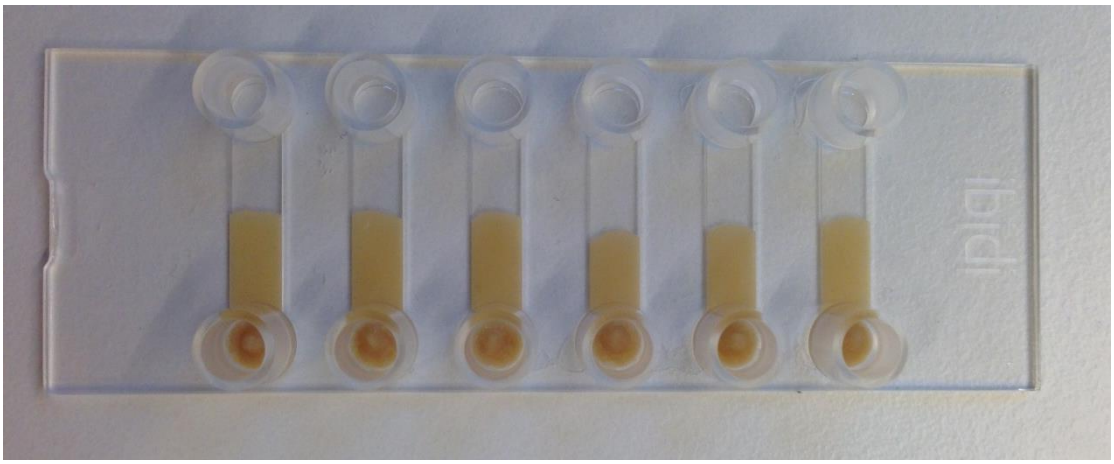

Figure 3.17: *Photo of the µ-slide after insertion of PSIM (brown) and FluoSpheres® suspension.*

3.3.1 Results from the diffusion study on the confocal microscope

The different µ-slides were photographed using a confocal microscope. This gave the possibility to take photos of the fluorescence in the samples, and study how the particles moved in the different samples by watching the fluorescence. Photos from the diffusion of FluoSpheres® into PSIM are shown in figure 3.18 under section 3.3.1.1 and photos from diffusion of SNEDDS into PSIM are shown under section 3.3.1.2. The rest of the corresponding photos are found in appendix D.

Plot profiles from the samples were made using the ImageJ program and by adding several plots together it was possible to study differences in the samples. The µ-slides containing FluoSpheres® and SNEDDS with and without G-block was studied after 24 hours, 48 hours and 72 hours. This is initially a very long time span when compared to drug delivery and physiological relevance. However, when establishing a method it is desirable to know what is possible, practically speaking. It is interesting to see how long it will take to see significant results.

3.3.1.1 Diffusion studies of FluoSpheres® with PSIM in the µ-slide

Figure 3.18 shows two photos of the diffusion of yellow-green carboxylate 40 nm FluoSpheres® into PSIM after 24 hours. Figure 3.18a is a photo of FluoSpheres® without G-block while figure 3.18b is of FluoSpheres® with G-block. The left side of the photos contains the FluoSpheres® suspension and the right side of the photos is the PSIM. These images are somewhat overexposed as the FluoSpheres® are very bright. All the settings are found in table 2.5 under section 2.2.3.2, but the most likely explanation for this is that the gain, which was set to 800 V, was too high and thus overexposing the image. The amount of fluorescent particles will also affect the image, and too many particles will make the image overexposed. Since these settings were made using a control sample, the same settings were used in the rest of the samples as all the replicates need the same settings to make the results credible.

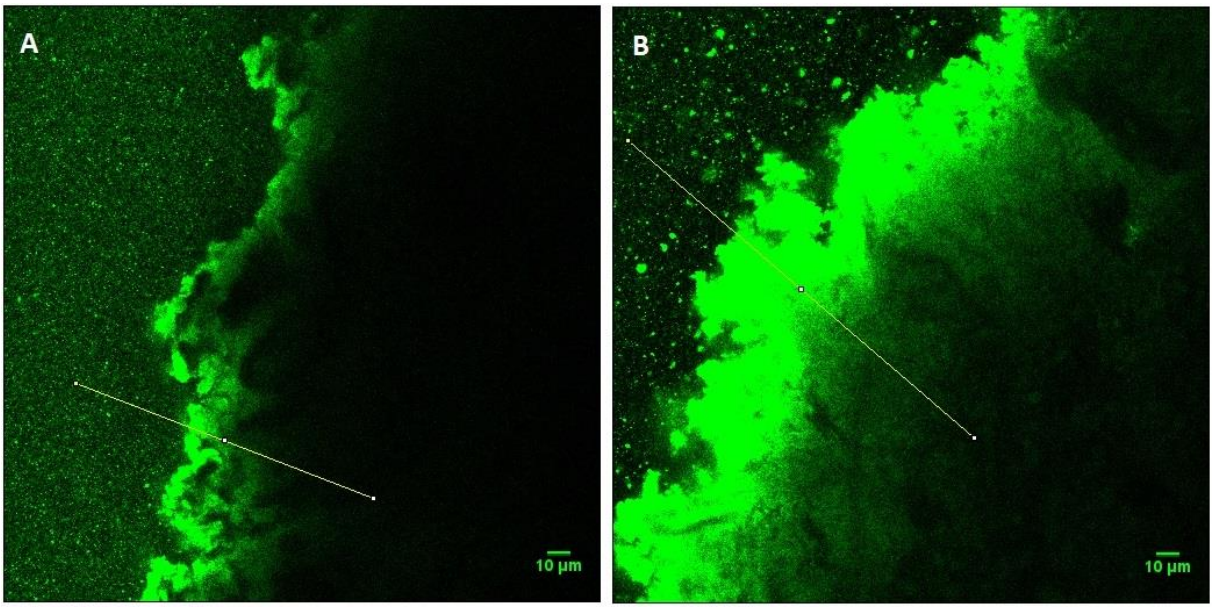

Figure 3.18: *Photo from the confocal microscope showing yellow-green 40 nm FluoSpheres® without G-block (A) and FluoSpheres® with G-block (B). The left side of the photos is the FluoSpheres® suspension and the right side of the photos is the PSIM. Taken after 24 hours. The yellow line show where the profile plot is collected from, and there is a scale bar in the lover right corner.*

Figure 3.19 show the plot for the 40 nm yellow-green carboxylate FluoSpheres® with and without G-block, measured on the confocal microscope after 24 hours. The x-axis in the distance measured in µm, and the y-axis is the intensity of fluorescence. The corresponding photos can be found in appendix D1.

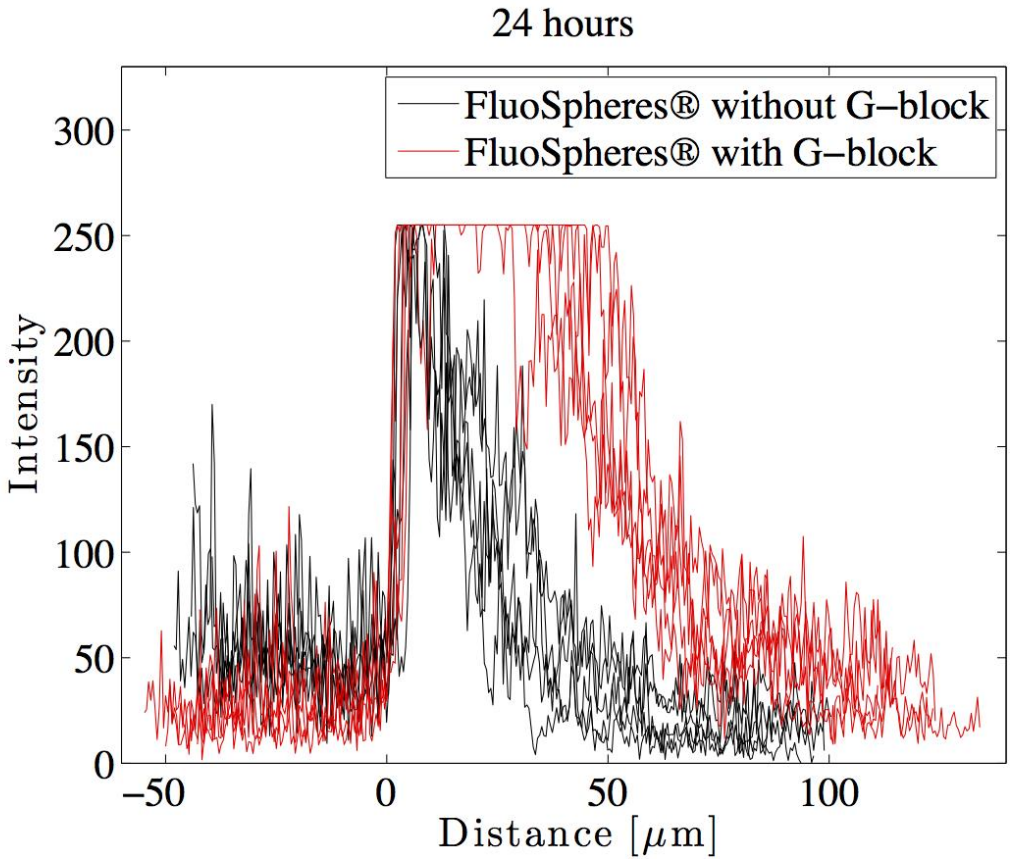

Figure 3.19: *Show the differences in plot profiles for several samples of FluoSpheres® diffusing into PSIM after a time of 24 hours. The black samples are FluoSpheres® without G-block and the red samples are FluoSpheres® with G-block. Intensity is plotted over distance measured in µm.*

In figure 3.19 the left side of the x-axis up to zero is from the FluoSpheres® suspension. At zero there is a high increase in fluorescence where the nanoparticle suspension meets the PSIM and the FluoSpheres® accumulate. The nanoparticles will naturally be drawn towards the PSIM because of the concentration gradient. When reaching the PSIM they meet a hindrance in the mucin network and diffusion into the PSIM takes some time. This is probably the causes of the accumulation of FluoSpheres® at the edge of the PSIM. From there it diffuses into the PSIM as seen on the right side of the plot. From this plot it seems that the samples containing G-block (red) have a higher intensity in the PSIM than the samples without the G-block (black). The peak is wider and the descending of the peak is further to the right, both indicating a larger penetration of FluoSpheres® due to G-block. Further out into the PSIM the intensity is clearly higher for the samples containing G-block. As mentioned before the presence of G-block is thought to disrupt the network in the mucus, making larger pores and thus ease the diffusion for the nanoparticles into and through mucus. G-block can

also inhibit of the interactions between the matrix mucins and the mobile components, which in this case would make the diffusion less difficult for the nanoparticles (Nordgård et al., 2014, Taylor Nordgård and Draget, 2011).

The x-axis in all these profile plots made from the confocal images, both of FluoSpheres® and SNEDDS show the distance of diffusion measured in µm. At the accumulation of nanoparticles at the PSIM front, the distance is set to be zero as this is the point where the diffusion into PSIM begins. From this the diffusion is measured up to slightly over 100 µm. These distances are regarded as very relevant compared to the *in vivo* situation of diffusion through mucus. When considering drug delivery over the epithelial cells in the intestines, the drugs must penetrate the mucus barrier before reaching the cells. This layer will be varying in thickness, but it is considered to stay in the µm scale. By measuring the diffusion in such a manner, it giver more of an insight as to the length the nanoparticles are capable of diffusing.

The trend with higher intensity in the PSIM for the samples containing G-block is not as clear after 48 hours or 72 hours as seen in figure 3.20 and figure 3.21, although it is still a difference to indicate the G-block increases the penetration over time. The fact that the differences between samples containing G-block and samples without G-block is less obvious might be caused by the diffused FluoSpheres® migrating further into the PSIM and spreading more out. If the G-block in fact does help the FluoSpheres® diffuse through the PSIM, it is likely that this will make them diffuse further than the FluoSpheres® which are not aided by G-block. If the FluoSpheres® in the sample containing G-block spread out in such a manner, they will make the fluorescent intensity in the PSIM look the same as for the samples without G-block, but over a larger area. To study this further it would be possible to repeat these measurements with a greater area imaged, or by moving the slide to take pictures further out in the PSIM.

Looking at the FluoSpheres® suspension on the left side of the x-axis of figure 3.19 it seems that the fluorescence is lower for the samples containing G-block than for the samples without G-block. This might indicate that more of the FluoSpheres® have diffused into the PSIM and that they have moved further that they have for the once without G-block. Figure 3.20 and 3.21 illustrates the same trend after 48 hours and 72 hours, and it does appear to be so that the intensity in the FluoSpheres® side is lower over time. This would be natural as the FluoSpheres® diffuse into the PSIM and lowers the fluorescence in the FluoSpheres®

suspension while increasing the intensity of the fluorescence in the PSIM. Since the fluorescence in the PSIM is not increasing over time, this could be data to further back up the theory that the FluoSpheres® are migrating further in the PSIM when G-block is present. The photos for figure 3.20 and 3.21 can be found in appendix D2 and D3.

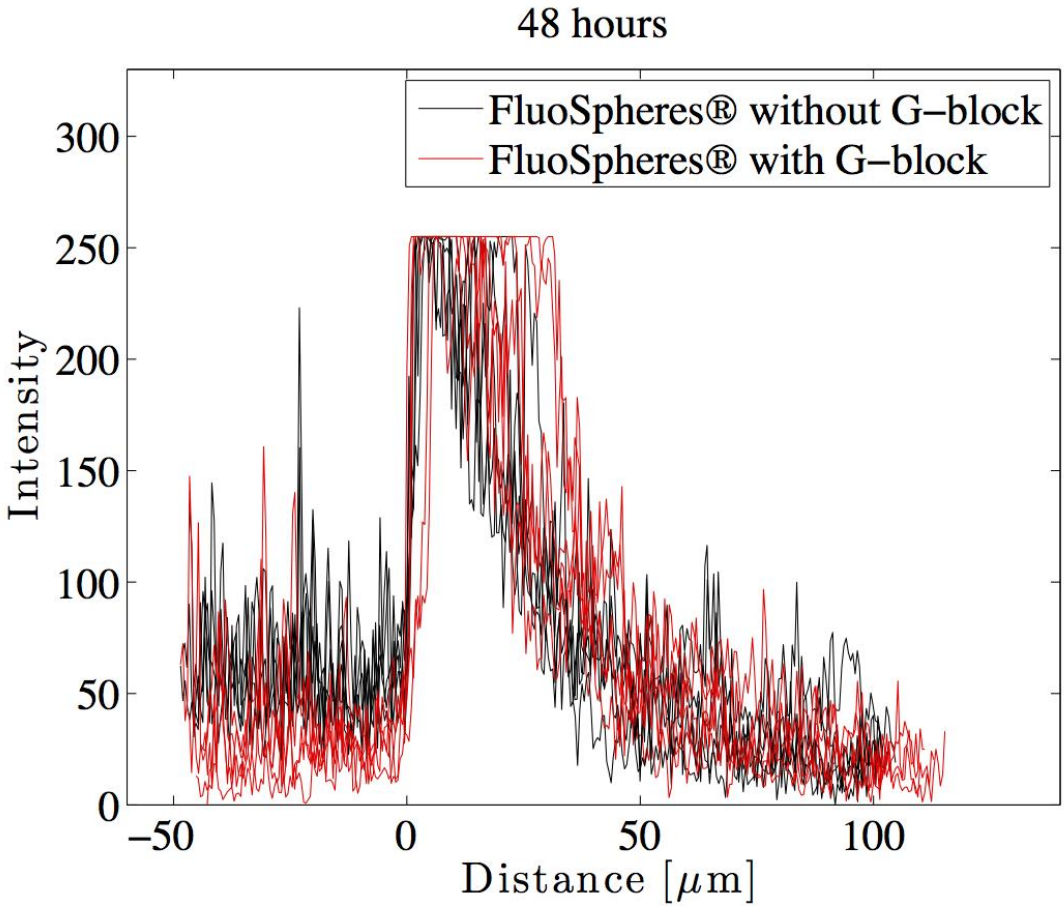

Figure 3.20: *Show the differences in plot profiles for several samples of FluoSpheres® diffusing into PSIM after a time of 48 hours. The black samples are FluoSpheres® without G-block and the red samples are FluoSpheres® with G-block. Intensity is plotted over distance measured in µm.*

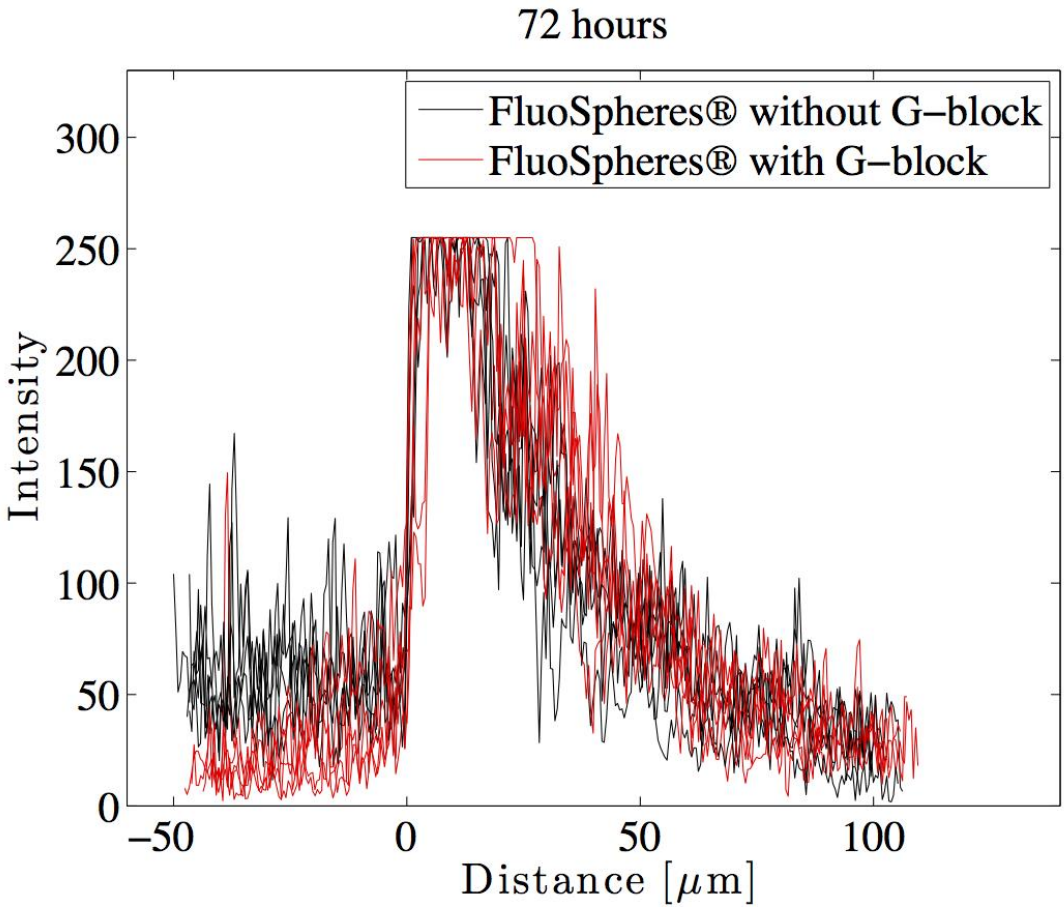

Figure 3.21: *Show the differences in plot profiles for several samples of FluoSpheres® diffusing into PSIM after a time of 72 hours. The black samples are FluoSpheres® without G-block and the red samples are FluoSpheres® with G-block. Intensity is plotted over distance measured in µm.*

The tests was also plotted to show development over time. In figure 3.22 and 3.23 plots for FluoSpheres® without and with G-block are presented. Figure 3.22 shows the FluoSpheres® without G-block after 24 hours, 48 hours and 72 hours. Figure 3.23 on the other hand shows the FluoSpheres® with G-block after 24 hours, 48 hours and 72 hours.

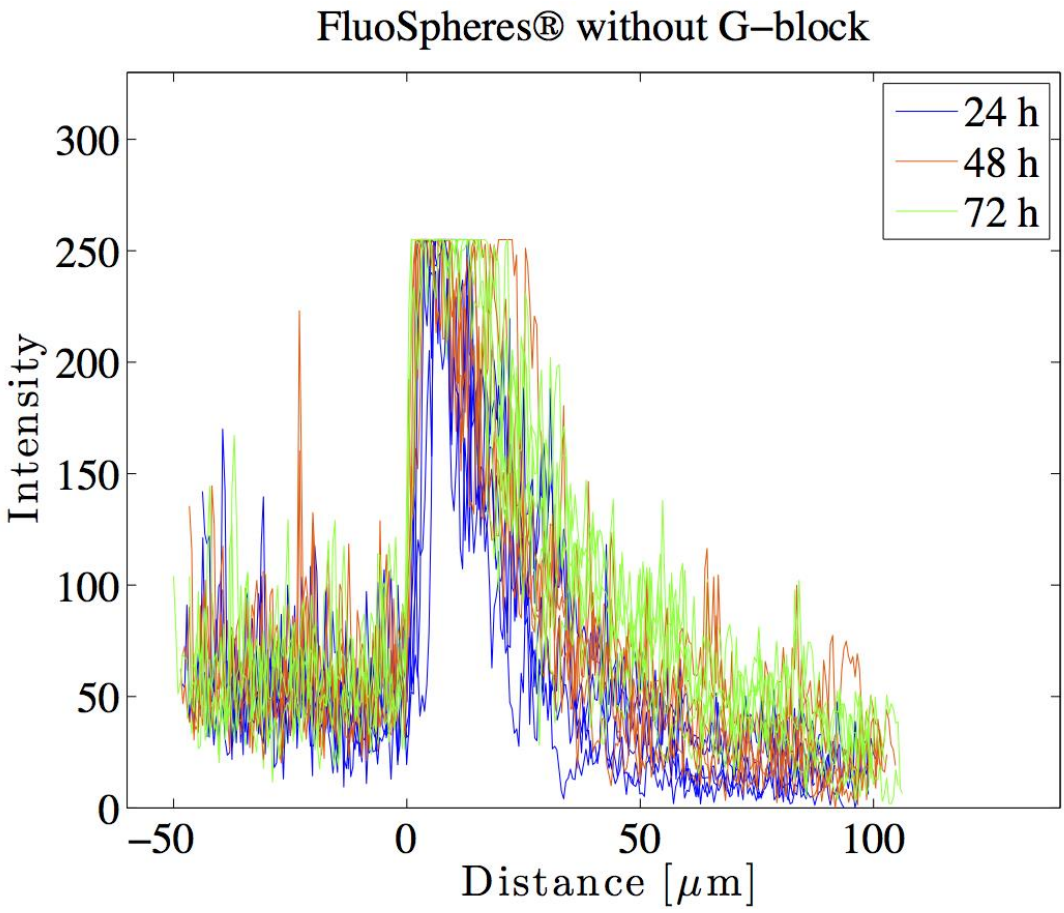

Figure 3.22: *Show the differences in plot profiles for several samples of FluoSpheres® without G-block diffusing into PSIM after different time intervals. The blue plots are after 24 hours, the orange plots are after 48 hours and the green plots are after 72 hours. Intensity is plotted over distance measured in µm.*

From figure 3.22 it seems that the fluorescence in the FluoSpheres® suspension is more or less the same for all three times when G-block is not present. In the right side of the plot however, which is in the PSIM part of the sample, there is a difference in the three. It seems that the intensity is increasing over time. The green plots which are all made from the 72 hour samples, have higher fluorescence in the PSIM than the red and the blue plots. It would also seem that the red plots representing 48 hours, have higher intensity than the blue 24 hours plots.

These results from figure 3.22 most likely indicate that the particles are moving in to the PSIM but that they don't migrate very far. This gives an increase in fluorescence near the front in the PSIM side as more FluoSpheres® diffuse into the PSIM. As time goes more FluoSpheres® diffuse into the PSIM but they are hindered by the PSIM and its barrier

functions, and thus the FluoSpheres® are not able to diffuse very far into the PSIM. This gives a larger intensity at the beginning of the PSIM. Had they diffused further into the PSIM there would probably not be a large increase in fluorescence, since the FluoSpheres® would be spread more throughout the PSIM.

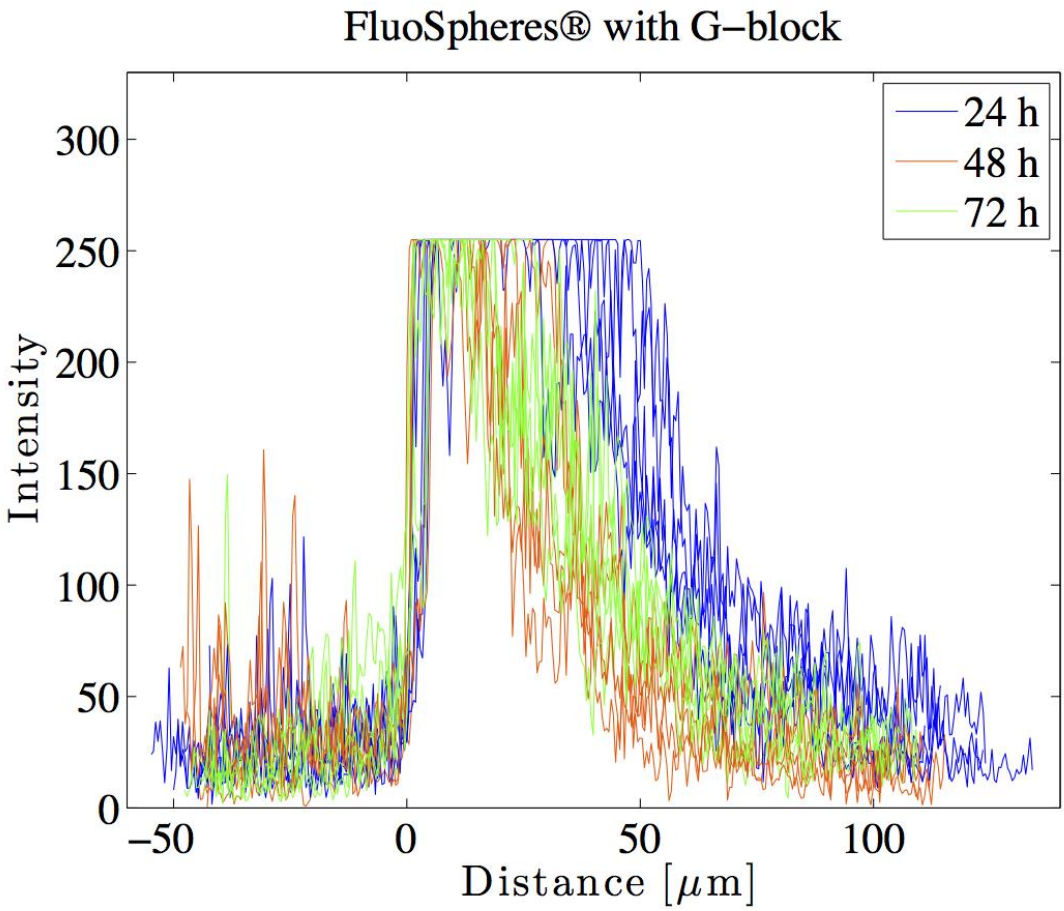

Figure 3.23: *Show the differences in plot profiles for several samples of FluoSpheres® with G-block diffusing into PSIM after different time intervals. The blue plots are after 24 hours, the orange plots are after 48 hours and the green plots are after 72 hours. Intensity is plotted over distance measured in µm.*

For the samples containing G-block we get a different picture than for the samples without G-block. In figure 3.23 the left side of the plot up to zero is the FluoSpheres® side of the sample. There is not much that separates the three times in this part of the sample, but there is a difference to be observed. The 72 hours plots are lower in fluorescence intensity than the plots for 24 hours and 48 hours, with the exception from single peaks. This indicates that the fluorescence in the FluoSpheres® suspension decreases over time. Knowing that the lack of

fluorescence most likely comes from the lack of particles it is only natural to think that these particles might have diffused into the PSIM.

Studying the PSIM side of the plot in figure 3.23 gives an image of how the diffusion into the PSIM changes over time when G-block is present. Unlike the plots in figure 3.22 where the intensity in the PSIM was increasing over time, the plots in figure 3.23 gives a different story for the samples containing G-block. After 24 hours there is a relatively large fluorescence intensity indicating a large diffusion of FluoSpheres®. This intensity decreases very much after 48 hours, before increasing again after 72 hours. The data after 48 hours and 72 hours does appear to have some differences as the 72 hours data seem to have a higher intensity than the 48 hours data, but when looking more closely they might not be that different. There is a large overlap of the results, and this makes it difficult to say that one of them have more intensity than the other, as they in fact are relatively similar to each other. The data that does stand out is the 24 hours, as their intensity clearly is higher than after 48 hours and 72 hours. Again the large intensity after 24 hours may be a result of the G-block making the pores of the PSIM larger, helping the FluoSpheres® to diffuse more easily into the PSIM. The FluoSpheres® seem to be rushing to the PSIM due to the concentration gradient. The decreasing fluorescence intensity after 48 hours could be a result of the FluoSpheres® spreading out through the PSIM thus making the fluorescence at the front less intense.

After 72 hours the intensity in the FluoSpheres® suspension is lower than before. There are two likely explanations for this. The first is that the FluoSpheres® diffuse into the PSIM and because of that the fluorescence is lowered in the FluoSpheres® suspension. This is the most likely explanation, but it is also important to consider the possibility that the fluorescence of the FluoSpheres® are under degradation. This would give a lower fluorescence without it meaning that the particles are actually migrating. Looking at the PSIM side of the plot in figure 3.23 however, the degradation theory is dismissed to some degree. The intensity is actually increasing somewhat after 72 hours, which does not indicate degradation of fluorescence, but that will be dependent on the distribution. However, these FluoSpheres® are supposed to be very photostable and not degrade that easily, which makes it less likely that there is degradation. What is worth noticing is that all the plots for FluoSpheres® and G-block are truncated and the data in the peaks of the plot is unknown. It is not certain what is hidden there, and it is important to be aware that there might be many particles not visible

which are distributed differently over time. Because of this it is even more difficult to draw any conclusion from these plots.

It is also worth noting that after 72 hours, the distribution of the FluoSpheres® in the sample is less even, and where the plot line is placed in the photo will affect the profile. As can be seen by the photos in appendix D1-D3.This gives that the data from the earlier measurements taken after 24 hours and 48 hours may be more reliable since the distribution is less spread and the front is more even, giving a more similar distribution for the different replicates. When making such a profile plot there is a question as to how reliable the results are. Where the line to the plot is drawn in the picture, will affect the plot, and there is important to get as correct and representative results as possible. A low spread in the data is desirable as it gives an indication that the data from the different replicates are similar to each other and therefor the results are more reliable. To make the results even more reliable several independent replicates should be performed and compared to each other.

The results obtained from the study of yellow-green 40 nm carboxylate FluoSpheres® diffusion into PSIM were interesting, and seemed to indicate proof of the principle of G-block increasing the diffusion of nanoparticles through PSIM. To test these results further SNEDDS labelled with rhodamine were tested in the µ-slide in the same way as the FluoSpheres®. Samples with and without G-block was made to investigate if the G-block would affect the diffusion of SNEDDS through the PSIM. The µ-slide was studied on the confocal microscope.

3.3.1.2 Diffusion studies of rhodamine labelled SNEDDS with PSIM in the µ-slide

As for the yellow-green 40 nm carboxylate FluoSpheres® in the previous section, this experiment was conducted using rhodamine labelled SNEDDS as mobile nanoparticles. The SNEDDS are similar in size to the yellow-green 40 nm carboxylate FluoSpheres®, but the fluorescence in the SNEDDS is much lower. Figure 3.24 shows two photos of the diffusion of SNEDDS into PSIM after 24 hours. Figure 3.24a is a photo of SNEDDS without G-block while figure 3.24b is of SNEDDS with G-block. The left side of the photos contains the SNEDDS suspension and the right side of the photos is the PSIM. All the settings for the confocal microscope are found in table 2.5 under section 2.2.3.2.

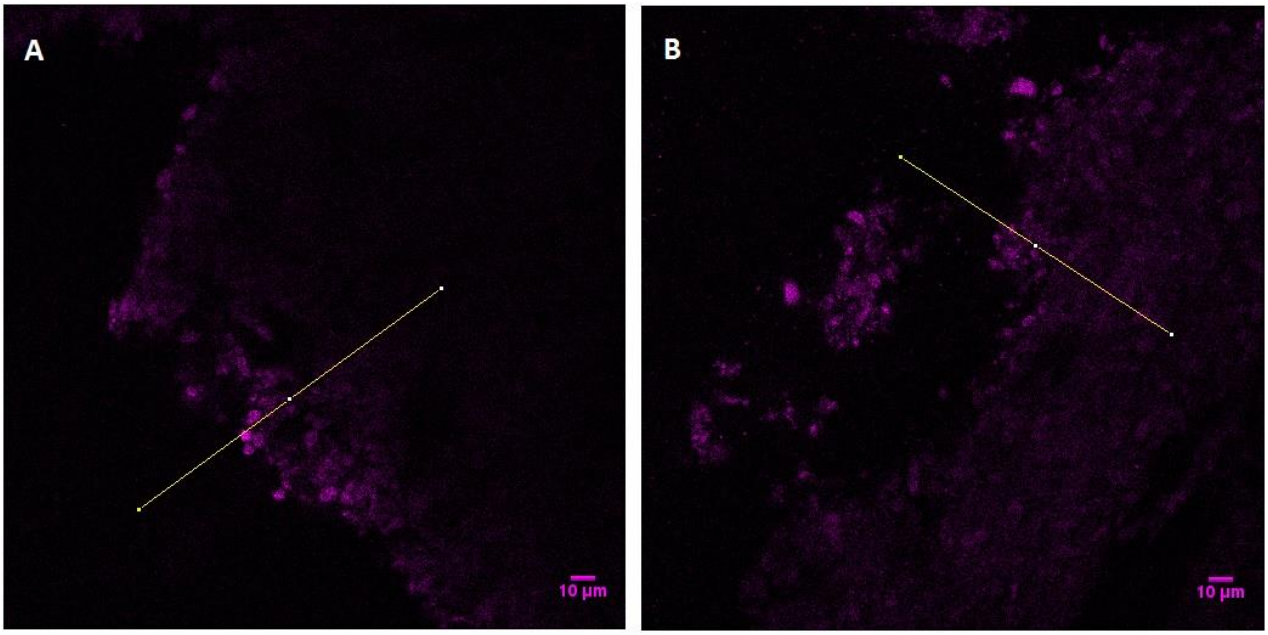

Figure 3.24: *Photo from the confocal microscope showing SNEDDS without G-block (A) and SNEDDS with G-block (B). The left side of the photos is the SNEDDS suspension and the right side of the photos is the PSIM. Taken after 24 hours. The yellow line show where the profile plot is collected from, and there is a scale bar in the lover right corner.*

Figure 3.25 show plots from the results after 24 hours with and without G-block included in the samples. The photos from which the plots are made are found in appendix D4 (for the 24 hour samples), D5 (48 hours) and D6 (72 hours).

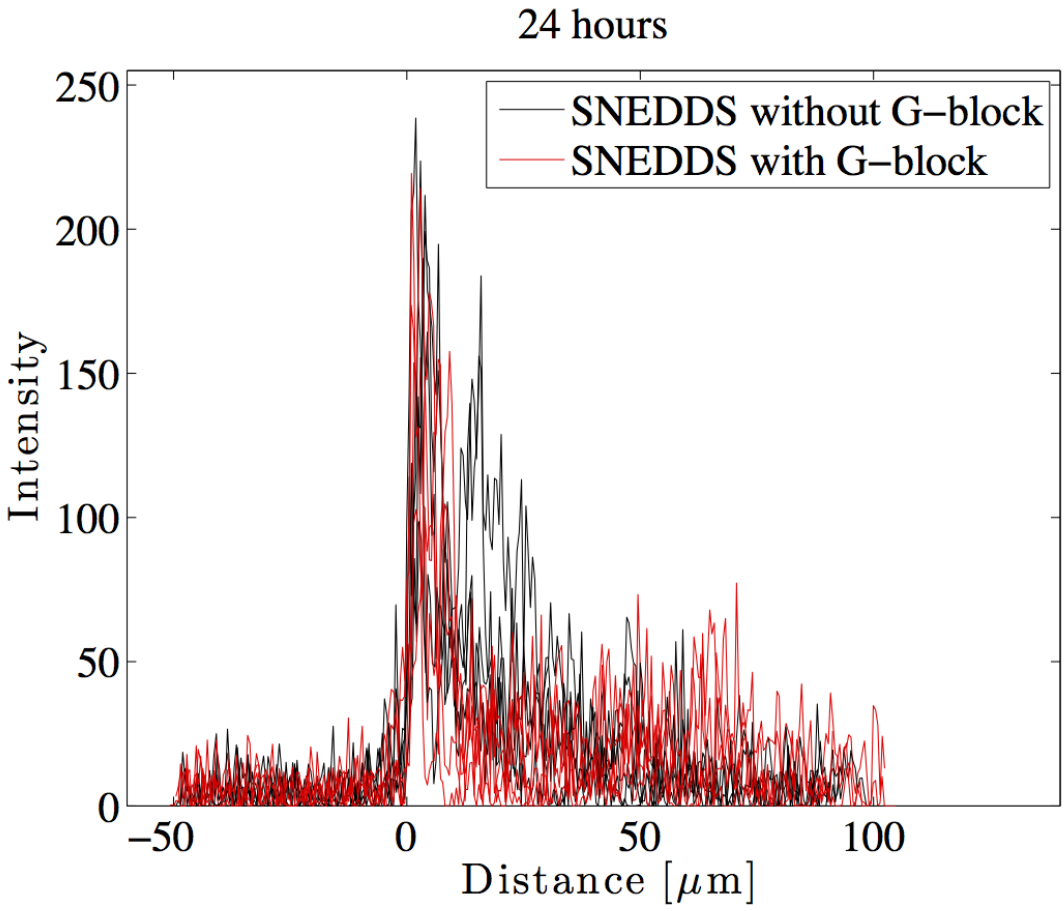

Figure 3.25: *Show the differences in plot profiles for several samples of SNEDDS diffusing into PSIM after a time of 24 hours. The black samples are SNEDDS without G-block and the red samples are SNEDDS with G-block. Intensity is plotted over distance measured in µm.*

After 24 hours there is not much difference in the plots for SNEDDS with and SNEDDS without G-block (figure 3.25). The shape of the plots is similar but the one thing that stands out is the high intensity in the PSIM for the samples containing G-block, when further away from the SNEDDS suspension. This intensity is higher than for the samples without G-block which again could indicate that G-block increases the pore size in PSIM, or inhibit interactions between the mucus and the mobile particles. Both the samples containing G-block and the once without G-block have a relatively high diffusion of SNEDDS into the PSIM as can be seen in figure 3.25. The intensity in the PSIM is actually higher than the intensity in the SNEDDS solution. The high fluorescence in the PSIM is probably due to the SNEDDS diffusing rapidly into the PSIM. The reason for this high diffusion might be that the concentration gradient is driving the SNEDDS into the PSIM, but it could also be because of the different charges in the two, as the SNEDDS have a neutral charge it is possible this affects the transport through PSIM. Lai et al, stated that such a neutral charge could give a

higher diffusion than a negative charge, due to less interactions with the mucus (Lai et al., 2007). It is worth noting that this only show a small sample of the PSIM, and that it is most likely not this large an intensity throughout the PSIM. From figure 3.26 and 3.27 which show the SNEDDS after 48 hours and 72 hours, it would seem the intensity in the samples with G-block is considerably higher than the once without G-block, this is especially clear after 72 hours (figure 3.27). This high intensity would seem to indicate that the SNEDDS with G-block have a higher diffusion into PSIM than the samples without G-block.

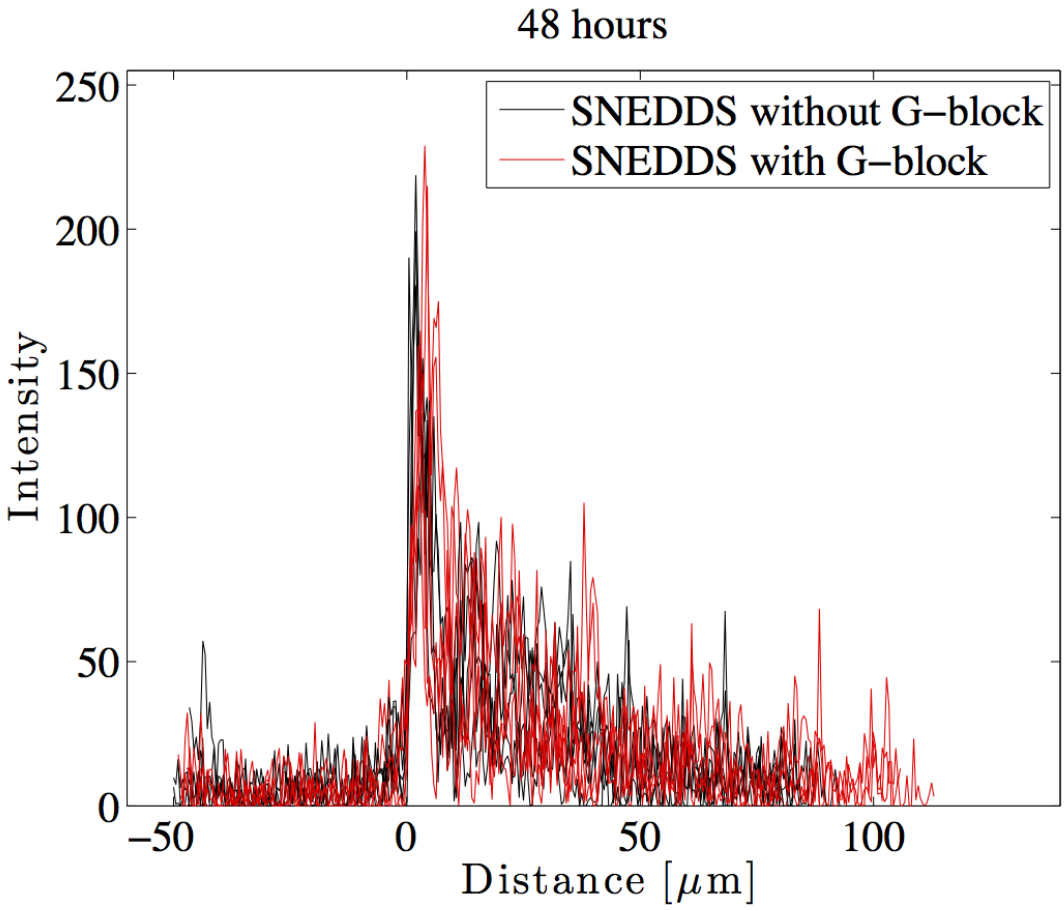

Figure 3.26: *Show the differences in plot profiles for several samples of SNEDDS diffusing into PSIM after a time of 48 hours. The black samples are SNEDDS without G-block and the red samples are SNEDDS with G-block. Intensity is plotted over distance measured in µm.*

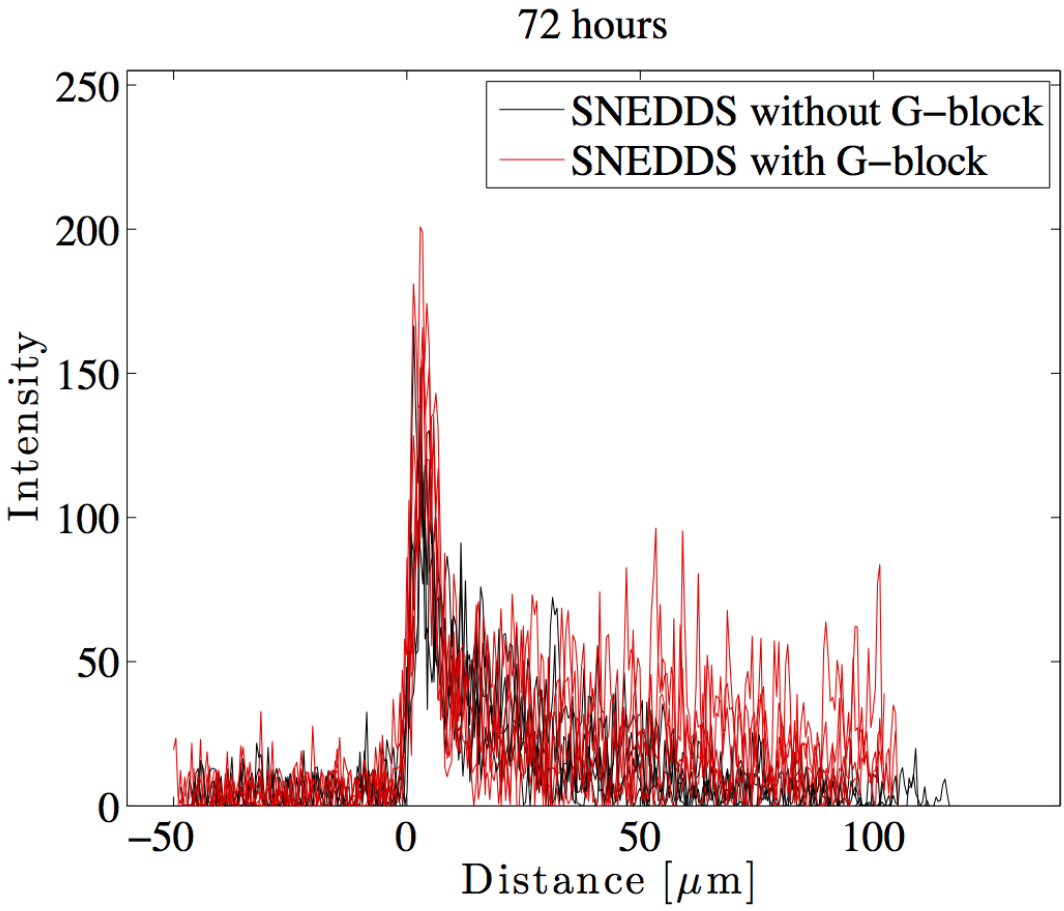

Figure 3.27: *Show the differences in plot profiles for several samples of SNEDDS diffusing into PSIM after a time of 72 hours. The black samples are SNEDDS without G-block and the red samples are SNEDDS with G-block. Intensity is plotted over distance measured in µm.*

As with the FluoSpheres® the SNEDDS was also plotted to show development over time. In figure 3.28 and 3.29 plots for SNEDDS without and with G-block are presented. Figure 3.28 shows the SNEDDS that does not contain G-block after 24 hours, 48 hours and 72 hours. Figure 3.29 on the other hand shows the SNEDDS with G-block after 24 hours, 48 hours and 72 hours.

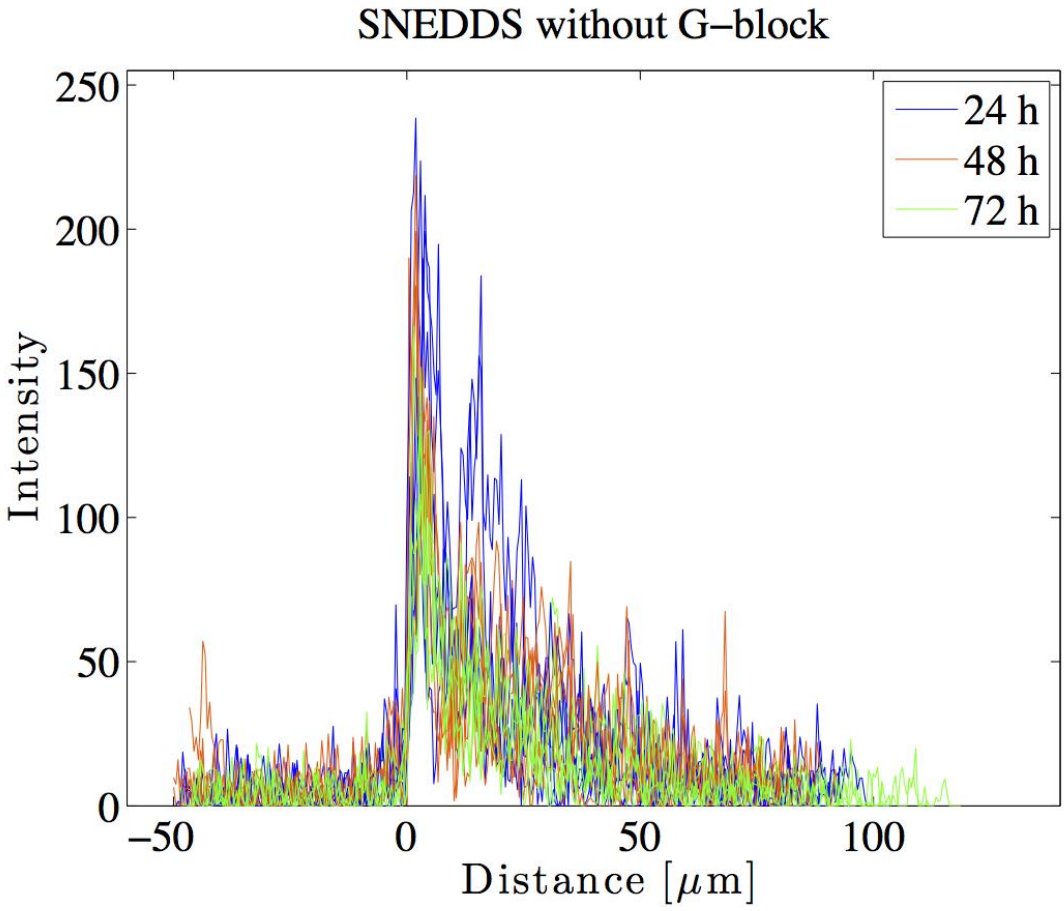

Figure 3.28: *Show the differences in plot profiles for several samples of SNEDDS without G-block diffusing into PSIM after different time intervals. The blue plots are after 24 hours, the orange plots are after 48 hours and the green plots are after 72 hours. Intensity is plotted over distance measured in µm.*

In the samples without G-block present it looks like the intensity from the SNEDDS are decreasing over time (figure 3.28). The intensity after 72 hours are lower than at 24 and 48 hours probably indicating that the diffused SNEDDS have moved further into the PSIM, spreading out and so lowering the intensity. Another possible explanation for the decreasing intensity might be degradation of fluorescence in the SNEDDS. Looking at the SNEDDS containing G-block on the other hand gives a different image (figure 3.29). Here the amount of intensity in the PSIM is generally lager than for the samples without G-block. Looking at the times, it also seems that the intensity is increasing over time. The samples from 72 hours seems to be somewhat larger than the ones at 24 hours and 48 hours when looking further into the PSIM, indicating the SNEDDS migrates further into the PSIM after some time. This

would also support the claims that G-block helps the nanoparticles, in this case SNEDDS, penetrate the PSIM barrier.

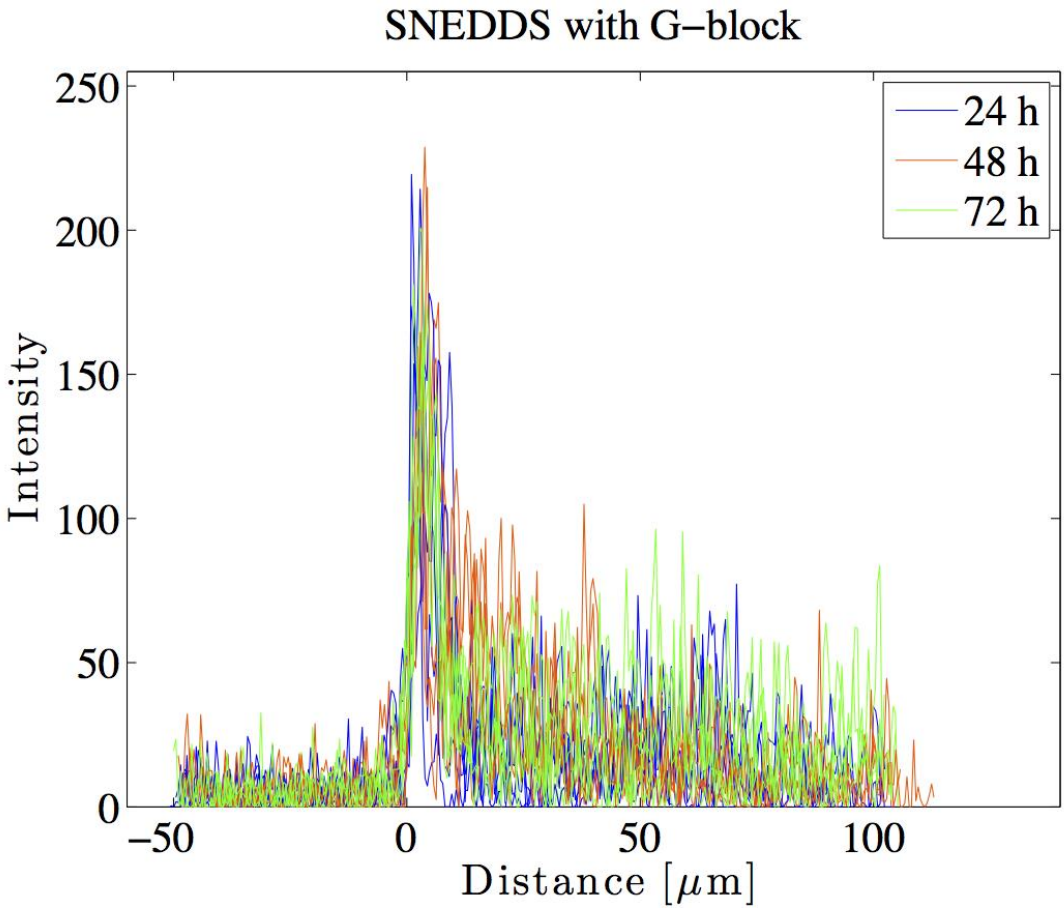

Figure 3.29: *Show the differences in plot profiles for several samples of SNEDDS with G-block diffusing into PSIM after different time intervals. The blue plots are after 24 hours, the orange plots are after 48 hours and the green plots are after 72 hours. Intensity is plotted over distance measured in µm.*

After analyzing these photos from the diffusion of SNEDDS into PSIM in the µ-slide, it becomes clearer that this might not be the best method for studying the diffusion of SNEDDS. SNEDDS distribute itself in a more bulky manner than does the FluoSpheres®. This makes it increasingly difficult to get representative measurements using the "line" method where a line is drawn on the picture to create a profile plot. It makes more sense to draw a line over a clear front as is the case with the FluoSpheres®, than with the SNEDDS, where the front is much more diffuse. Due to the differences in the distribution of SNEDDS in the samples, it is

difficult to extrapolate these results further. However, this method gives a possibility to see large differences in the distribution of nanoparticles of relatively similar size.

Another method for presenting the results of SNEDDS diffusion through PSIM would be to present 3D plots of the images taken by the confocal microscope. The plots may give images where there is easier to see the different distributions of the SNEDDS in the PSIM. Figure 3.31 and 3.32 show the 3D plots of the images used to make figure 3.25. In figure 3.31 the images for SNEDDS without G-block after 24 hours are presented as 3D plots, and in figure 3.32 the images for SNEDDS with G-block after 24 hours are presented as 3D plots. The corresponding pictures are in appendix D4. Since 24 hours are the timespan closest to any physiological state, these images are the most interesting, and are shown as 3D plots in figure 3.31 and figure 3.32. The settings used to make the 3D plot are the same for all the pictures and are presented in table 3.3. The settings are also visible in the pictures in the figures (3.31 and 3.32). The right side of the plots is in the PSIM side of the sample and the left side is in the nanoparticle side of the sample. This is illustrated better in figure 3.30.

Table 3.3: *Table showing settings for all the 3D plots made from confocal images of SNEDDS penetrating the PSIM in µ-slides.*

Settings	
Grid size	512
Smoothing	5.0
Perspective	0.0
Lighting	0.11
Scale	1.1
z-Scale	0.75
Max	75 %
Min	0 %

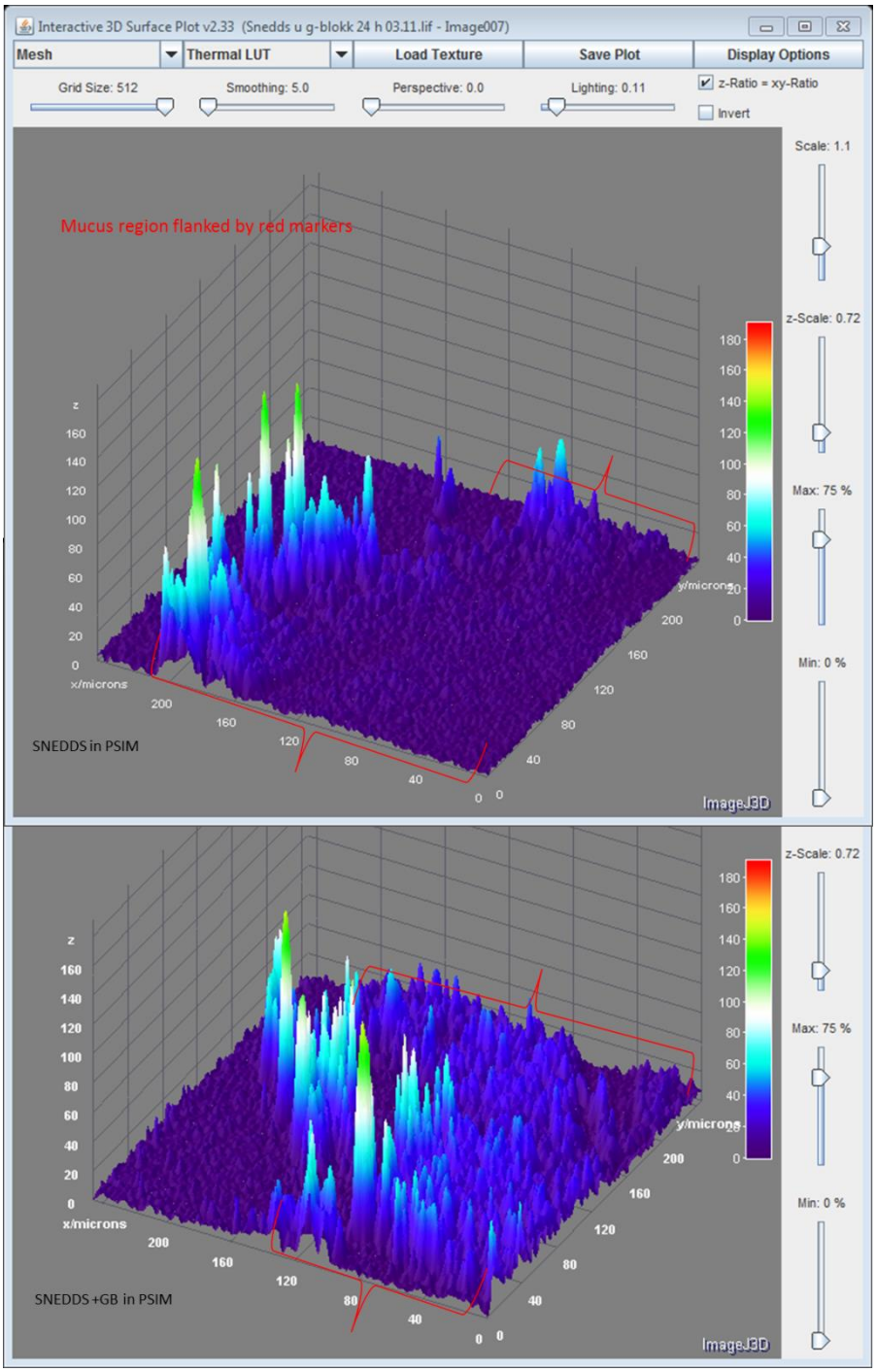

Figure 3.30: *3D plot of SNEDDS penetrating the PSIM after 24 hours. The upper plot is without G-block added and the lower plot is with G-block. The PSIM region is flanked by red markers.*

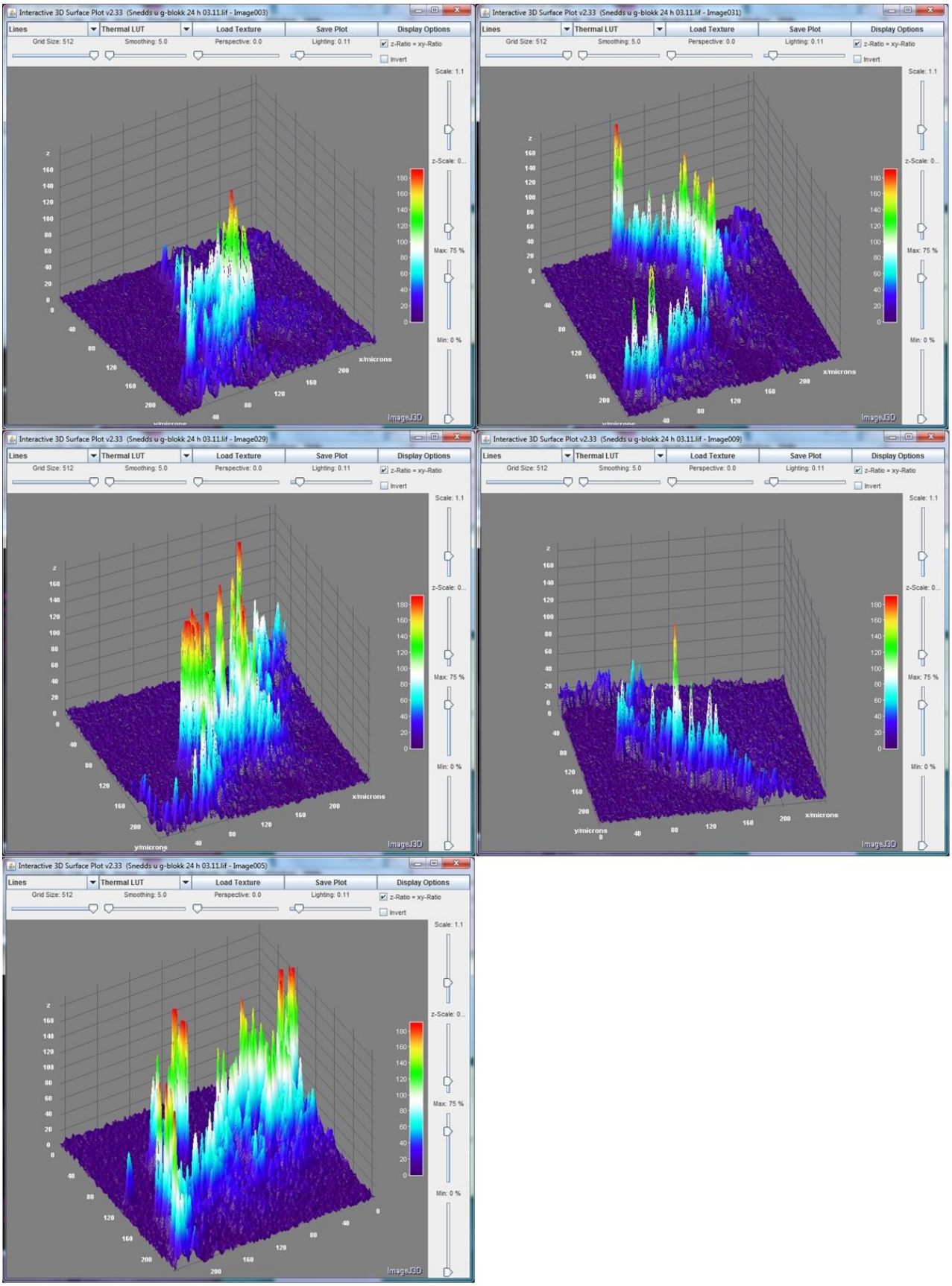

Figure 3.31: *3D plot of photos taken by the confocal microscope when studying diffusion of SNEDDS without G-block into PSIM after 24 hours.*

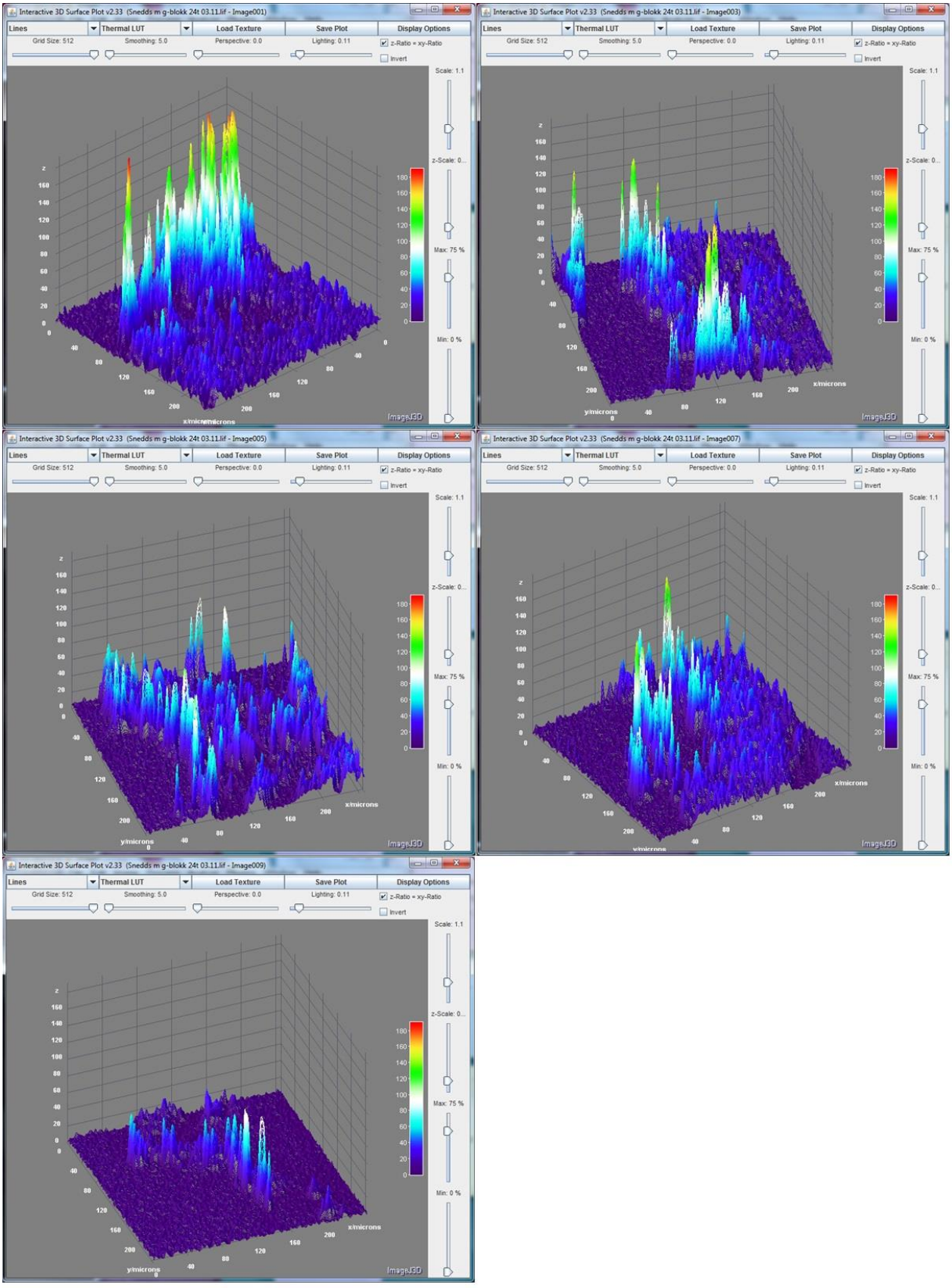

Figure 3.32: *3D plot of photos taken by the confocal microscope when studying diffusion of SNEDDS with G-block into PSIM after 24 hours.*

From the 3D plots of the diffusion of SNEDDS into PSIM after 24 hours, in figure 3.27 and 3.28, there is possible to study the diffusion in a new way. The 3D plots give an indication that there in fact is more diffusion further into the PSIM in the samples containing G-block (figure 3.28) than it is in the samples without G-block (figure 3.27). Although the distribution differs a great deal between the different pictures, it seems to be so that there is on a general basis more fluorescence in the PSIM when the G-block is present. This is perhaps more easy to observe when the pictures are presented as 3D plots instead of plot profiles for the SNEDDS, due to the variating distribution of SNEDDS through the sample.

3.4 General discussion

Throughout the thesis different methods for studying diffusion of nanoparticles in PSIM have been tested and optimization of them has begun. The two methods that were most successful were the Transwell method and the µ-slide method using washed PSIM and studying the slide on the confocal microscope. Both yellow-green carboxylate 40 nm FluoSpheres® and SNEDDS were used in these methods, with and without G-block. The two methods give indications of the same results when comparing them. Both state that there is an increase in diffusion when G-block is present probably due to G-block increasing the pore size in the PSIM network, and there is generally a higher diffusion of SNEDDS in the PSIM than it is with FluoSpheres®. It would appear that the SNEDDS are more mobile in the PSIM than the FluoSpheres® are. The 40 nm FluoSpheres® and the SNEDDS have similar size which makes it possible to compare them. The SNEDDS however have much lower fluorescence intensity than the FluoSpheres®, which makes it less detectable. This is important to remember when studying the data from the confocal microscope.

In the plot profiles from the FluoSpheres® it would appear that the diffusion is very large, and it is easy to look at the high intensity found in the peak. But the FluoSpheres® are very fluorescent and the peak is over the maximum measured by the confocal. This is due to the settings used for the FluoSpheres®, and the peak does not say anything of the distribution of nanoparticles out in the PSIM. Looking at the distance of diffusion it would seem the SNEDDS are more mobile than the FluoSpheres®. The SNEDDS have a more neutral charge than the negatively charged FluoSpheres® which could affect the interactions between the nanoparticles and the PSIM in some way. Lai et al. states that viruses capable of rapid transport in mucus have a net neutral shell which minimizes hydrophobic and electrostatic interactions. In their article it is claimed that neutral particles are less hindered than negatively charged particles (Lai et al., 2007). This could be an explanation for the larger diffusion of the SNEDDS, compared to the FluoSpheres®. Another explanation could be that the particle concentration plays a role in the diffusion. The concentration for the SNEDDS is 0.45%, while it is 0.025% for the FluoSpheres®. The reason for this higher concentration of SNEDDS was the low fluorescence, which was difficult to detect at low concentrations.

It is however a question of how comparable these two methods are. The µ-slide method lets the nanoparticle suspension meet the PSIM in a canal and then diffusing into the PSIM. In the Transwell the nanoparticles are already mixed into the PSIM to avoid large differences in the replicates. This means that the nanoparticles only diffuse out of the PSIM and not into it. Also remember that the µ-slide method uses washed PSIM while the Transwell does not. Washed PSIM will in many cases be more similar to the PSIM found *in vivo* as it displays more stability than the PSIM which is not washed and therefor contains excess water. This however should not give much of a difference, since there is not a problem with the phase separation in the Transwell, because of the particles being mixed into the PSIM on a filter. As a general there are differences between the two methods, but they seem to be comparable and to give similar results, which increases the credibility of both the methods and the results. Never the less, there is still a need to optimize these methods further, and to preform several independent replicates of the tests.

From the µ-slide method it was observed that the distribution of the FluoSpheres® and the SNEDDS were very different. The FluoSpheres® distributed themselves more evenly through the PSIM with a clear front of accumulated FluoSpheres® at the PSIM. The SNEDDS had a very different distribution with much more bulky and not that even a distribution. These differences in the distribution give some problems when analyzing the samples. Initially the photos taken by the confocal microscope was analyzed by drawing a line across the front between the nanoparticle suspension and the PSIM. This was done for several replicates and the profiles provided by this line were plotted to see similarities and differences between them. For the FluoSpheres® this was a method which gave good and readable results, due to the fact that the front was relatively even and the distribution of FluoSpheres® in the PSIM was even. For the SNEDDS this was however not a very good method, since the distribution was so uneven. There was not a clear front between the SNEDDS suspension and the PSIM, and because of that the method of drawing a line was not representative for the sample as a whole. A better way of displaying the results for the SNEDDS was to make a 3D plot of the photo; this gave a plot of the entire photo, which showed a more complete image. Due to the differences in the distribution for the samples containing FluoSpheres® and the samples containing SNEDDS, this method of drawing a line and plotting a profile was not the best way of comparing the two. It is however important to remember that results very often are dependable of the method. Therefor it is desirable to have multiple methods giving the same results before making conclusions about the results gained from a single method.

Although the methods of Transwell and µ-slides seem to be somewhat comparable over a similar time scale, it is difficult to conclude on the basis of such few replicates. The methods also need further optimization as they are not completely comparable to *in vivo* situations. Both methods are relevant to the *in vivo* situation due to the use of *ex vivo* PSIM which is more similar to *in vivo* than biosimilar mucus or many other mucus models. In Transwell the nanoparticles are mixed into the PSIM and then the diffusion out through a filter is studied. This process is further from the *in vivo* situation as the particles are already in the PSIM. In an *in vivo* situation the nanoparticles must meet the mucus and penetrate it before they diffuse through it and reach the epithelium cells. When considering this, the µ-slide method seems to be more comparable to an *in vivo* state. In the µ-slide method the nanoparticles meet the PSIM in the canal and diffuse into it much like the situation in the small intestine. The distance of diffusion can then be studied using a confocal microscope. In the µ-slide method however, the time scale need optimization. The diffusions were studied after 24 hours, 48 hours and 72 hours, to get an image of how the method worked and to be able to optimize the time scale and the method from there. In a medical situation this time scale is not very relevant as it is too large for most physiological situations. The µ-slide method therefor needs more optimization and study after shorter time intervals to be closer to the *in vivo* situation.

At the end of this discussion I feel it is important to make a point of the fact that these results are not conclusive data as to the effect of G-block on the penetration of nanoparticles through mucus. When studying these images from the confocal microscope it is important to not draw conclusions from them. They are regarded as representative selections, but may still not show all the details regarding distribution of the nanoparticles in the PSIM. With this in mind, these data is not meant to give generalized conclusions but rather illustrates that the Transwell method and the µ-slide method appears to be good methods to measure an effect of G-block on the diffusion of nanoparticles through mucus.

4. Conclusion

The process of optimizing the methods used for studying diffusion of nanoparticles through PSIM was considered successful as it proved some of the methods and materials to be less suitable for these diffusion studies, while others were more successful. From the results it can for example be stated that the use of agar in such diffusion studies are not efficient. The agar was meant to provide a clear front to the PSIM by holding it in place, but proved to be very difficult for the nanoparticles to diffuse through. Both the Transwell method and the µ-slide seemed to be good methods, which provided similar results, and can be regarded as comparable to each other. They both need some more optimization and it is possible to claim that the use of the profile plot method was not as efficient to study diffusion for the SNEDDS as for the FluoSpheres®, because of the large differences in distribution of SNEDDS in the samples. The optimized methods gave indications that the presence of G-block in the nanoparticle suspension, whether FluoSpheres® or SNEDDS, seems to have a positive effect on the diffusion of the nanoparticles through the PSIM. The samples containing G-block did on average have a higher diffusion than similar samples without G-block, supporting previous studies indicating that G-block may alter the mucin network in mucus by increasing the pore size, thus allowing for more transport of particles over the mucus. It is however difficult to make conclusive statements since the process should be further optimized and several replicates should be performed.

5. Future work

As previously emphasized, this thesis does not provide any conclusive data as to the effect of G-block on nanoparticle diffusion over PSIM, nor does it provide any other conclusive data. This thesis gives an indication on what might be the case, but more work needs to be done. By further optimizing the methods used in the studies of diffusion, better diffusion studies could be obtained. In the future optimization, the time scale of the studies should be optimized, especially for the µ-slides studied on the confocal microscope, where a shorter time scale would give a situation which resembled the *in vivo* situation more. It should also be performed several independent replicates to test if these results are representative. By testing several independent replicates the data will be more reliable, and the methods could be further developed. In the future it could also be possible to investigate new methods to observe the diffusion of nanoparticles through PSIM. The µ-slide chemotaxis which was not suitable for this study due to the problems caused by the agar gel, could still be suitable for diffusion studies if a different agent was to hold the PSIM in place. By finding such an agent, this method could be optimized into a good method for diffusion studies. It would also be interesting to study the effect of G-block on diffusion through PSIM further. One interesting line of inquiry would for instance be to see what effect different concentrations of G-block would give.

References

ACKERS, G. & STEERE, R. 1962. Restricted diffusion of macromolecules through agar-gel membranes. *Biochimica et biophysica acta,* 59**,** 137-149.

AULTON, M. E. & TAYLOR, K. M. 2007. *Aulton's Pharmaceutics: the design and manufacture of medicines*.

BALAKUMAR, K., RAGHAVAN, C. V., SELVAN, N. T., PRASAD, R. H. & ABDU, S. 2013. Self nanoemulsifying drug delivery system (SNEDDS) of Rosuvastatin calcium: Design, formulation, bioavailability and pharmacokinetic evaluation. *Colloids and Surfaces B: Biointerfaces,* 112**,** 337-343.

BOEGH, M. & NIELSEN, H. M. 2014. Mucus as a Barrier to Drug Delivery–Understanding and Mimicking the Barrier Properties. *Basic & clinical pharmacology & toxicology*.

COMPACT. 2015. *Compact objectives* [Online]. Available: http://www.compact-research.org/project/objectives.php [Accessed 10.03 2015].

CONE, R. A. 2005. *Mucus,* Elsevier academic press.

CONE, R. A. 2009. Barrier properties of mucus. *Advanced drug delivery reviews,* 61**,** 75-85.

CRATER, J. S. & CARRIER, R. L. 2010. Barrier properties of gastrointestinal mucus to nanoparticle transport. *Macromolecular bioscience,* 10**,** 1473-1483.

CROMMELIN, D. J., STORM, G., VERRIJK, R., DE LEEDE, L., JISKOOT, W. & HENNINK, W. E. 2003. Shifting paradigms: biopharmaceuticals versus low molecular weight drugs. *International journal of pharmaceutics,* 266**,** 3-16.

D'HAENS, G. 2007. Risks and benefits of biologic therapy for inflammatory bowel diseases. *Gut,* 56**,** 725-732.

DAMGÉ, C., MICHEL, C., APRAHAMIAN, M., COUVREUR, P. & DEVISSAGUET, J. P. 1990. Nanocapsules as carriers for oral peptide delivery. *Journal of Controlled Release,* 13**,** 233-239.

DATE, A. A., DESAI, N., DIXIT, R. & NAGARSENKER, M. 2010. Self-nanoemulsifying drug delivery systems: formulation insights, applications and advances. *Nanomedicine,* 5**,** 1595-616.

DATE, A. A. & NAGARSENKER, M. S. 2007. Design and evaluation of self-nanoemulsifying drug delivery systems (SNEDDS) for cefpodoxime proxetil. *International Journal of Pharmaceutics,* 329**,** 166-172.

DAWSON, M., KRAULAND, E., WIRTZ, D. & HANES, J. 2004. Transport of Polymeric Nanoparticle Gene Carriers in Gastric Mucus. *Biotechnology Progress,* 20**,** 851-857.

DRAGET, K. I. 2011. Oligomers: Just background noise or as functional elements in structured biopolymer systems? *Food Hydrocolloids,* 25**,** 1963-1965.

DRAGET, K. I., SKJÅK-BRÆK, G. & SMIDSRØD, O. 1997. Alginate based new materials. *International Journal of Biological Macromolecules,* 21**,** 47-55.

DRAGET, K. I. & TAYLOR, C. 2011. Chemical, physical and biological properties of alginates and their biomedical implications. *Food Hydrocolloids,* 25**,** 251-256.

DRAZBA, J. 2006. Introduction to confocal microscopy. *Microscopy and Microanalysis,* 12**,** 1756-1757.

ENSIGN, L. M., CONE, R. & HANES, J. 2012. Oral drug delivery with polymeric nanoparticles: the gastrointestinal mucus barriers. *Advanced drug delivery reviews,* 64**,** 557-570.

FRIEDL, H., DÜNNHAUPT, S., HINTZEN, F., WALDNER, C., PARIKH, S., PEARSON, J. P., WILCOX, M. D. & BERNKOP-SCHNÜRCH, A. 2013. Development and Evaluation of a Novel Mucus Diffusion Test System Approved by Self-

Nanoemulsifying Drug Delivery Systems. *Journal of pharmaceutical sciences,* 102**,** 4406-4413.
GRANT, G. T., MORRIS, E. R., REES, D. A., SMITH, P. J. C. & THOM, D. 1973. Biological interactions between polysaccharides and divalent cations: The egg-box model. *FEBS Letters,* 32**,** 195-198.
GROO, A.-C. & LAGARCE, F. 2014. Mucus models to evaluate nanomedicines for diffusion. *Drug discovery today,* 19**,** 1097-1108.
GUILBAULT, G. G. 1990. *Practical fluorescence*, CRC Press.
GUIOCHON, G. & BEAVER, L. A. 2011. Separation science is the key to successful biopharmaceuticals. *Journal of Chromatography A,* 1218**,** 8836-8858.
HOFFMAN, A. S. 2008. The origins and evolution of "controlled" drug delivery systems. *Journal of Controlled Release,* 132**,** 153-163.
JOHNSON, E. M., BERK, D. A., JAIN, R. K. & DEEN, W. M. 1996. Hindered diffusion in agarose gels: test of effective medium model. *Biophysical journal,* 70**,** 1017-1023.
JYOTHI, B. J. & SREELAKSHMI, K. 2011. Design and evaluation of self-nanoemulsifying drug delivery system of flutamide. *Journal of young pharmacists,* 3**,** 4-8.
KASHIMA, K. & IMAI, M. 2012. *Advanced membrane material from marine biological polymer and sensitive molecular-size recognition for promising separation technology*, INTECH Open Access Publisher.
KHANVILKAR, K., DONOVAN, M. D. & FLANAGAN, D. R. 2001. Drug transfer through mucus. *Advanced drug delivery reviews,* 48**,** 173-193.
KWON, K.-C., VERMA, D., SINGH, N. D., HERZOG, R. & DANIELL, H. 2013. Oral delivery of human biopharmaceuticals, autoantigens and vaccine antigens bioencapsulated in plant cells. *Advanced Drug Delivery Reviews,* 65**,** 782-799.
LAI, S. K., O'HANLON, D. E., HARROLD, S., MAN, S. T., WANG, Y.-Y., CONE, R. & HANES, J. 2007. Rapid transport of large polymeric nanoparticles in fresh undiluted human mucus. *Proceedings of the National Academy of Sciences,* 104**,** 1482-1487.
LAKOWICZ, J. R. 2013. *Principles of fluorescence spectroscopy,* Springer Science & Business Media.
MCGILL, S. L. & SMYTH, H. D. 2010. Disruption of the mucus barrier by topically applied exogenous particles. *Molecular pharmaceutics,* 7**,** 2280-2288.
MEYVIS, T. K., DE SMEDT, S. C., VAN OOSTVELDT, P. & DEMEESTER, J. 1999. Fluorescence recovery after photobleaching: a versatile tool for mobility and interaction measurements in pharmaceutical research. *Pharmaceutical research,* 16**,** 1153-1162.
NIELSEN, F. S., GIBAULT, E., LJUSBERG-WAHREN, H., ARLETH, L., PEDERSEN, J. S. & MÜLLERTZ, A. 2007. Characterization of prototype self-nanoemulsifying formulations of lipophilic compounds. *Journal of Pharmaceutical Sciences,* 96**,** 876-892.
NORDGÅRD, C. T., NONSTAD, U., OLDERØY, M. Ø., ESPEVIK, T. & DRAGET, K. I. 2014. Alterations in mucus barrier function and matrix structure induced by guluronate oligomers. *Biomacromolecules,* 15**,** 2294-2300.
ORIVE, G., GASCÓN, A. R., HERNÁNDEZ, R. M., DOMíNGUEZ-GIL, A. & PEDRAZ, J. L. 2004. Techniques: New approaches to the delivery of biopharmaceuticals. *Trends in Pharmacological Sciences,* 25**,** 382-387.
PADDOCK, S. W. 1999. Confocal laser scanning microscopy. *Biotechniques,* 27**,** 992-1007.
REHM, B. & VALLA, S. 1997. Bacterial alginates: biosynthesis and applications. *Applied microbiology and biotechnology,* 48**,** 281-288.
ROSEN, H. & ABRIBAT, T. 2005. The rise and rise of drug delivery. *Nature Reviews Drug Discovery,* 4**,** 381-385.

SAKLOETSAKUN, D., DÜNNHAUPT, S., BARTHELMES, J., PERERA, G. & BERNKOP-SCHNÜRCH, A. 2013. Combining two technologies: Multifunctional polymers and self-nanoemulsifying drug delivery system (SNEDDS) for oral insulin administration. *International Journal of Biological Macromolecules,* 61**,** 363-372.
SALTZMAN, W. M., RADOMSKY, M. L., WHALEY, K. J. & CONE, R. A. 1994. Antibody diffusion in human cervical mucus. *Biophysical journal,* 66**,** 508.
SEKHON, B. S. 2010. Biopharmaceuticals: an overview. *Thai J. Pharm. Sci,* 34**,** 1-19.
SMART, J. D. 2005. The basics and underlying mechanisms of mucoadhesion. *Advanced Drug Delivery Reviews,* 57**,** 1556-1568.
SMIDSRØD, O. 1973. Some physical properties of alginates in solution and in the gel state.
SMIDSRØD, O. & MOE, S. T. 2008. *Biopolymer Chemistry,* Trondheim, Tapir Academic Press.
SO, P. T. & DONG, C. Y. 2002. Fluorescence spectrophotometry. *eLS.*
STAUB, A., GUILLARME, D., SCHAPPLER, J., VEUTHEY, J.-L. & RUDAZ, S. 2011. Intact protein analysis in the biopharmaceutical field. *Journal of pharmaceutical and biomedical analysis,* 55**,** 810-822.
STROHL, W. R. & KNIGHT, D. M. 2009. Discovery and development of biopharmaceuticals: current issues. *Current opinion in biotechnology,* 20**,** 668-672.
SUH, J., DAWSON, M. & HANES, J. 2005. Real-time multiple-particle tracking: applications to drug and gene delivery. *Advanced Drug Delivery Reviews,* 57**,** 63-78.
TAYLOR NORDGÅRD, C. & DRAGET, K. I. 2011. Oligosaccharides as modulators of rheology in complex mucous systems. *Biomacromolecules,* 12**,** 3084-3090.
TRAN, T. H., GUO, Y., SONG, D., BRUNO, R. S. & LU, X. 2014. Quercetin-Containing Self-Nanoemulsifying Drug Delivery System for Improving Oral Bioavailability. *Journal of pharmaceutical sciences,* 103**,** 840-852.
VARUM, F. J. O., VEIGA, F., SOUSA, J. S. & BASIT, A. W. 2012. Mucus thickness in the gastrointestinal tract of laboratory animals. *Journal of Pharmacy and Pharmacology,* 64**,** 218-227.
WANG, L., DONG, J., CHEN, J., EASTOE, J. & LI, X. 2009. Design and optimization of a new self-nanoemulsifying drug delivery system. *Journal of Colloid and Interface Science,* 330**,** 443-448.
WANG, Y.-Y., LAI, S. K., SO, C., SCHNEIDER, C., CONE, R. & HANES, J. 2011. Mucoadhesive nanoparticles may disrupt the protective human mucus barrier by altering its microstructure. *PLoS One,* 6**,** e21547.
WRIGHT, S. J. & WRIGHT, D. J. 2002. Introduction to confocal microscopy. *Cell Biological Applications of Confocal Microscopy, in Methods in Cell Biology,* 70**,** 1-85.
ZHANG, L., GU, F. X., CHAN, J. M., WANG, A. Z., LANGER, R. S. & FAROKHZAD, O. C. 2008. Nanoparticles in Medicine: Therapeutic Applications and Developments. *Clinical Pharmacology & Therapeutics,* 83**,** 761-769.

List of Appendices

Appendix A: Standard curves

A1: Data and standard curve for red carboxylate 100 nm FluoSpheres®

Cons. %	Intensity
0.0004	out of range
0.0002	608.319
0.0001	307.201
0.00005	153.949
0.000025	77.159
0.0000125	38.521
0.00000625	19.105

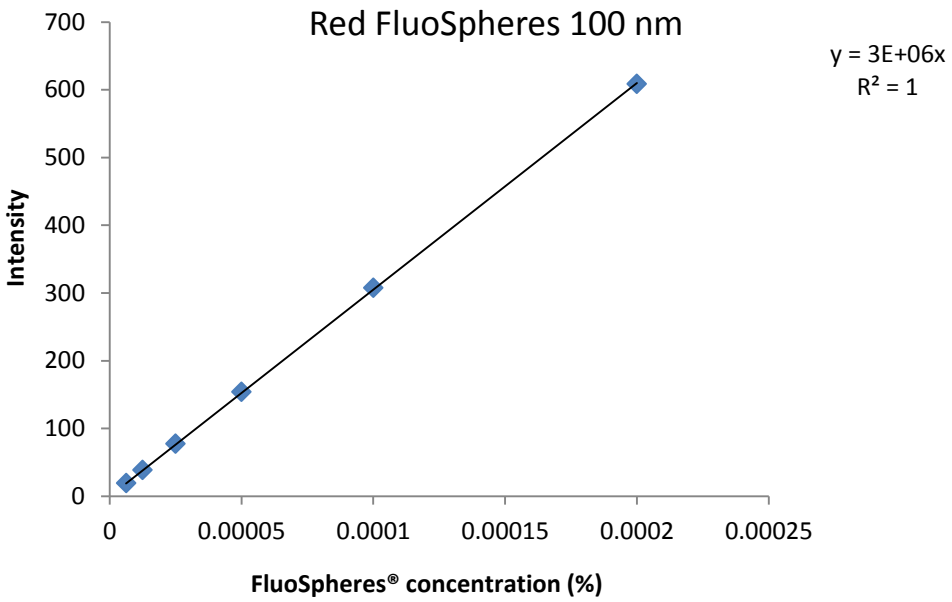

A2: Data and standard curve for yellow-green carboxylate 40 nm FluoSpheres®

Cons. %	Intensity
0.0004	out of range
0.0002	607.068
0.0001	306.6
0.00005	156.899
0.000025	80.957
0.0000125	44.237
0.00000625	30.028

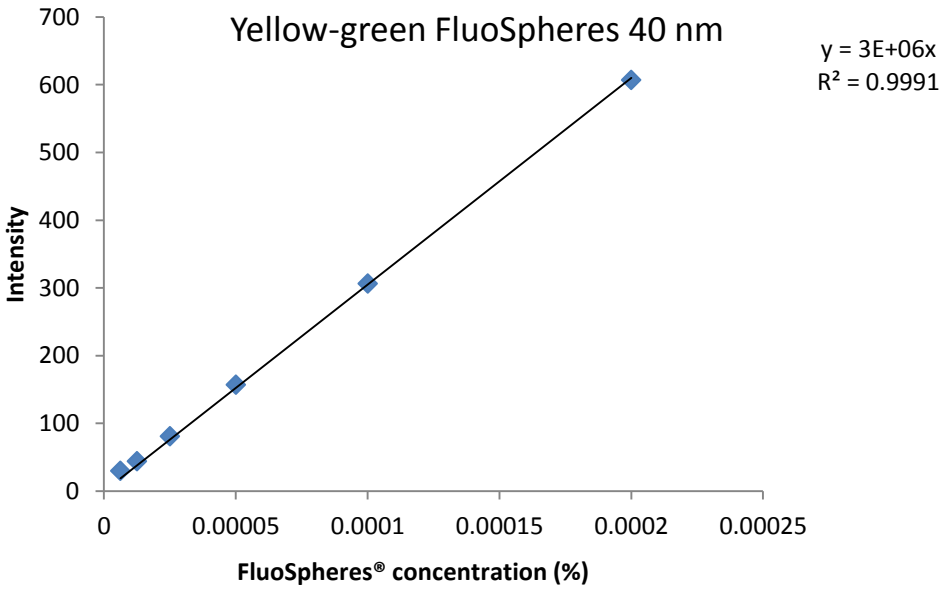

A3: Data and standard curve for SNEDDS

Cons. %	Intensity
0.9	out of range
0.45	884.234
0.225	460.278
0.112	242.732
0.056	129.554
0.028	67.737
0.014	34.381
0.007	17.129
0.0035	8.167
0.0018	3.974

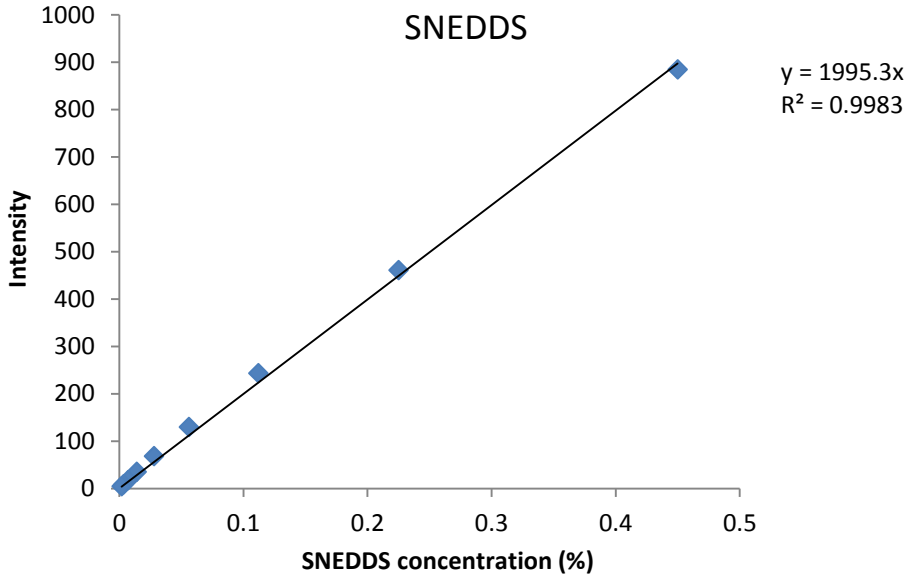

Appendix B: Raw data and calculations from Transwell diffusion study

B1: Diffusion of red carboxylate 100 nm FluoSpheres® through PSIM on 24-well Transwell

In table B1.1 the raw data from the first measurement with FluoSpheres® in PSIM is presented.

Table B1.1: *Raw data from the fluorometer*

	Intensity											
Time (h)	**1**	**2**	**3**	**4**	**5**	**6**	**7**	**8**	**9**	**10**	**11**	**12**
0	0.188	0.04	0.446	0.263	0.086	0.094	0.629	0.181	0.148	0.333	0.167	0.336
1	0.662	0.203	0.727	1.861	0.549	1.615	1.973	1.927	0.135	0.94	0.724	0.957
2	0.858	0.191	0.66	1.862	0.387	1.264	1.595	0.956	0.183	0.838	0.815	0.7
4	1.026	0.246	0.615	1.287	0.404	0.927	1.14	0.9	0.135	0.793	0.845	0.662
24	1.736	0.58	1.299	2.09	1.125	1.581	1.798	1.4	0.311	1.223	1.901	1.246

The raw data was then calculated to account for dilutions caused by taking samples from the acceptor chamber and adding physiological saline. This was done by multiplying the data from the sample by the amount of physiological saline added to the cuvette, and then dividing this by the amount in the sample. In this case it means the samples are multiplied by 1700 (µl) and divided by 300 (µl). This gives the results in table B1.2.

Table B1.2: *Data from table B1.1 after calculating for the dilution.*

	Intensity											
Time (h)	**1**	**2**	**3**	**4**	**5**	**6**	**7**	**8**	**9**	**10**	**11**	**12**
0	1.065	0.227	2.527	1.490	0.487	0.533	3.564	1.026	0.839	1.887	0.946	1.904
1	3.751	1.150	4.120	10.546	3.111	9.152	11.180	10.920	0.765	5.327	4.103	5.423
2	4.862	1.082	3.740	10.551	2.193	7.163	9.038	5.417	1.037	4.749	4.618	3.967
4	5.814	1.394	3.485	7.293	2.289	5.253	6.460	5.100	0.765	4.494	4.788	3.751
24	9.837	3.287	7.361	11.843	6.375	8.959	10.189	7.933	1.762	6.930	10.772	7.061

Half of the value from the previous measurement is then subtracted to account for the amount of that sample still left in the acceptor chamber (table B1.3). Then the measurements are added together to give the diffusion development over time (table B1.4).

Table B1.3: *Data after subtracting the previous measurement.*

	Intensity											
Time (h)	**1**	**2**	**3**	**4**	**5**	**6**	**7**	**8**	**9**	**10**	**11**	**12**
0	1.065	0.227	2.527	1.490	0.487	0.533	3.564	1.026	0.839	1.887	0.946	1.904
1	3.219	1.037	2.856	9.801	2.867	8.885	9.398	10.407	0.346	4.383	3.630	4.471
2	2.986	0.507	1.680	5.279	0.638	2.587	3.448	-0.042	0.655	2.085	2.567	1.255
4	3.383	0.853	1.615	2.017	1.193	1.672	1.941	2.391	0.247	2.119	2.479	1.768
24	6.930	2.590	5.619	8.197	5.230	6.333	6.959	5.383	1.380	4.684	8.378	5.185

Table B1.4: *Data after adding the value of the samples.*

	Intensity											
Time (h)	**1**	**2**	**3**	**4**	**5**	**6**	**7**	**8**	**9**	**10**	**11**	**12**
0	1.065	0.227	2.527	1.490	0.487	0.533	3.564	1.026	0.839	1.887	0.946	1.904
1	4.284	1.264	5.383	11.291	3.355	9.418	12.963	11.433	1.184	6.270	4.576	6.375
2	7.270	1.771	7.064	16.569	3.992	12.005	16.411	11.390	1.839	8.356	7.143	7.630
4	10.653	2.624	8.679	18.587	5.185	13.677	18.352	13.781	2.085	10.475	9.622	9.398
24	17.584	5.213	14.297	26.784	10.415	20.009	25.310	19.165	3.465	15.158	18.000	14.583

This procedure for calculating the raw data was used for all the diffusion experiments on Transwell, but the volumes used when diluting and collecting samples was not the same, and so the numbers are not the same for all the experiments.

B2: Control experiment with PSIM and physiological saline on 24-well Transwell

A control experiment was conducted using PSIM with physiological saline instead of fluorescent particles. Table B2.1 shows the raw data from the fluorometer. As mentioned earlier the method of calculation is the same as under section B1.

Table B2.1: *Raw data from the fluorometer*

	Intensity				
Time (h)	**1**	**2**	**3**	**4**	**5**
0	0.006	0.000	0.013	0.013	0.006
1	0.040	0.020	0.020	0.020	0.027
2	0.027	0.027	0.034	0.034	0.040
4	0.034	0.034	0.027	0.041	0.027
24	0.034	0.020	0.027	0.013	0.020

Table B2.2: *Data after calculating for dilutions done at sample collection*

	Intensity				
Time (h)	**1**	**2**	**3**	**4**	**5**
0	0.034	0.000	0.074	0.074	0.034
1	0.227	0.113	0.113	0.113	0.153
2	0.153	0.153	0.193	0.193	0.227
4	0.193	0.193	0.153	0.232	0.153
24	0.193	0.113	0.153	0.074	0.113

Table B2.3: *Data after subtraction of half of the previous measurement*

	Intensity				
Time (h)	**1**	**2**	**3**	**4**	**5**
0	0.034	0.000	0.074	0.074	0.034
1	0.210	0.113	0.077	0.077	0.136
2	0.040	0.096	0.136	0.136	0.150
4	0.116	0.116	0.057	0.136	0.040
24	0.096	0.017	0.077	-0.043	0.037

Table B2.4: *Data after adding the values of the samples*

	Intensity				
Time (h)	**1**	**2**	**3**	**4**	**5**
0	0.034	0.000	0.074	0.074	0.034
1	0.244	0.113	0.150	0.150	0.170
2	0.283	0.210	0.286	0.286	0.320
4	0.400	0.326	0.343	0.422	0.360
24	0.496	0.343	0.419	0.380	0.397

B3: Control experiment with red carboxylate 100 nm FluoSpheres® and physiological saline on 24-well Transwell

A control experiment was conducted using red FluoSpheres® with physiological saline instead of PSIM.

Table B3.1: *Raw data from the fluorometer*

	Intensity											
Time (h)	**1**	**2**	**3**	**4**	**5**	**6**	**7**	**8**	**9**	**10**	**11**	**12**
0	0,177	0,419	4,259	2,823	2,777	4,363	1,000	2,493	0,067	1,397	2,532	0,174
0,5	8,047	6,949	5,281	5,904	5,890	5,042	12,608	10,547	7,562	9,980	9,503	3,508
1	3,655	9,511	3,622	2,667	3,294	7,847	5,549	4,777	3,309	16,427	4,549	2,565
1,5	2,610	4,886	2,534	4,338	2,125	8,911	2,824	2,627	3,145	9,068	1,607	2,437
2	1,380	6,743	7,874	1,990	6,744	6,717	1,261	1,255	1,617	4,443	1,105	0,851
2,5	1,028	3,019	3,581	0,926	3,258	3,071	0,746	0,821	5,788	2,155	0,831	0,462
3	0,569	1,697	5,962	6,878	1,672	1,649	6,649	0,573	3,056	3,980	0,531	0,211
3,5	6,160	1,069	4,264	7,287	1,089	1,448	2,053	4,304	4,741	1,991	0,658	0,896
4	2,711	0,513	4,008	3,381	0,912	1,019	1,178	2,177	5,846	2,062	6,110	0,266

Table B3.2: *Data after calculating for dilutions done at sample collection*

	Intensity											
Time (h)	**1**	**2**	**3**	**4**	**5**	**6**	**7**	**8**	**9**	**10**	**11**	**12**
0	1,003	2,374	24,134	15,997	15,736	24,724	5,667	14,127	0,380	7,916	14,348	0,986
0,5	45,600	39,378	29,926	33,456	33,377	28,571	71,445	59,766	42,851	56,553	53,850	19,879
1	20,712	53,896	20,525	15,113	18,666	44,466	31,444	27,070	18,751	93,086	25,778	14,535
1,5	14,790	27,687	14,359	24,582	12,042	50,496	16,003	14,886	17,822	51,385	9,106	13,810
2	7,820	38,210	44,619	11,277	38,216	38,063	7,146	7,112	9,163	25,177	6,262	4,822
2,5	5,825	17,108	20,292	5,247	18,462	17,402	4,227	4,652	32,799	12,212	4,709	2,618
3	3,224	9,616	33,785	38,975	9,475	9,344	37,678	3,247	17,317	22,553	3,009	1,196
3,5	34,907	6,058	24,163	41,293	6,171	8,205	11,634	24,389	26,866	11,282	3,729	5,077
4	15,362	2,907	22,712	19,159	5,168	5,774	6,675	12,336	33,127	11,685	34,623	1,507

Table B3.3: *Data after subtraction of half of the previous measurement*

	Intensity											
Time (h)	**1**	**2**	**3**	**4**	**5**	**6**	**7**	**8**	**9**	**10**	**11**	**12**
0	1,003	2,374	24,134	15,997	15,736	24,724	5,667	14,127	0,380	7,916	14,348	0,986
0,5	45,098	38,191	17,859	25,458	25,509	16,210	68,612	52,703	42,662	52,595	46,676	19,386
1	-2,088	34,207	5,562	-1,615	1,978	30,181	-4,278	-2,814	-2,675	64,810	-1,147	4,596
1,5	4,434	0,740	4,097	17,026	2,709	28,263	0,280	1,352	8,446	4,842	-3,783	6,542
2	0,425	24,367	37,440	-1,014	32,195	12,815	-0,856	-0,332	0,252	-0,516	1,709	-2,083
2,5	1,915	-1,998	-2,017	-0,391	-0,646	-1,629	0,655	1,097	28,217	-0,377	1,578	0,207
3	0,312	1,063	23,639	36,352	0,244	0,643	35,564	0,921	0,918	16,448	0,655	-0,113
3,5	33,295	1,250	7,270	21,805	1,434	3,533	-7,205	22,766	18,207	0,006	2,224	4,480
4	-2,091	-0,122	10,631	-1,488	2,083	1,672	0,858	0,142	19,695	6,044	32,759	-1,031

Table B3.4: *Data after adding the values of the samples*

	Intensity											
Time (h)	**1**	**2**	**3**	**4**	**5**	**6**	**7**	**8**	**9**	**10**	**11**	**12**
0	1,003	2,374	24,134	15,997	15,736	24,724	5,667	14,127	0,380	7,916	14,348	0,986
0,5	46,101	40,565	41,993	41,455	41,245	40,933	74,279	66,830	43,041	60,512	61,024	20,372
1	44,013	74,772	47,555	39,840	43,223	71,114	70,000	64,016	40,367	125,321	59,877	24,967
1,5	48,447	75,511	51,652	56,865	45,931	99,376	70,281	65,368	48,813	130,163	56,094	31,510
2	48,872	99,878	89,091	55,851	78,126	112,192	69,425	65,036	49,065	129,648	57,803	29,427
2,5	50,788	97,880	87,074	55,460	77,480	110,562	70,080	66,133	77,282	129,271	59,381	29,634
3	51,099	98,943	110,713	91,811	77,724	111,206	105,644	67,054	78,200	145,718	60,036	29,521
3,5	84,394	100,192	117,983	113,617	79,158	114,739	98,439	89,820	96,407	145,724	62,260	34,000
4	82,303	100,071	128,614	112,129	81,240	116,410	99,297	89,961	116,102	151,768	95,019	32,969

B4: Control experiment with red carboxylate 100 nm FluoSpheres® and physiological saline on 12-well Transwell

Control to see if the results of the different parallels will be more similar if the experiment is performed on a Transwell with larger pores and larger area. The calculations are the same, but now the sample is at 750 µl and the volume added to the cuvette is 1250 µl.

Table B4.1: *Raw data from the fluorometer*

	Intensity					
Time (h)	**1**	**2**	**3**	**4**	**5**	**6**
0	87.032	144.720	131.362	154.062	130.574	141.875
0.5	118.621	94.174	106.806	108.347	104.267	130.034
1	83.662	70.573	78.775	70.142	70.331	78.298
1.5	77.331	66.321	72.346	60.854	61.509	67.292
2	57.431	52.060	54.669	47.795	49.809	40.897
2.5	42.866	37.971	39.013	35.456	32.822	28.032
3	30.718	27.564	30.354	24.816	28.545	19.918
3.5	24.875	23.193	24.179	20.033	25.638	19.507
4	20.195	19.786	17.314	17.062	19.629	15.620
24	13.126	13.893	8.340	13.027	15.148	15.440

Table B4.2: *Data after calculating for dilutions done at sample collection*

	Intensity					
Time (h)	**1**	**2**	**3**	**4**	**5**	**6**
0	203.075	337.680	306.511	359.478	304.673	331.042
0.5	276.782	219.739	249.214	252.810	243.290	303.413
1	195.211	164.670	183.808	163.665	164.106	182.695
1.5	128.885	110.535	120.577	101.423	102.515	112.153
2	95.718	86.767	91.115	79.658	83.015	68.162
2.5	71.443	63.285	65.022	59.093	54.703	46.720
3	51.197	45.940	50.590	41.360	47.575	33.197
3.5	41.458	38.655	40.298	33.388	42.730	32.512
4	33.658	32.977	28.857	28.437	32.715	26.033
24	21.877	23.155	13.900	21.712	25.247	25.733

Table B4.3: *Data after subtraction of half of the previous measurement*

	Intensity					
Time (h)	**1**	**2**	**3**	**4**	**5**	**6**
0	203.075	337.680	306.511	359.478	304.673	331.042
0.5	175.245	50.899	95.958	73.071	90.953	137.892
1	56.820	54.801	59.201	37.260	42.461	30.989
1.5	31.279	28.200	28.673	19.591	20.462	20.806
2	31.276	31.499	30.827	28.947	31.758	12.085
2.5	23.584	19.902	19.464	19.264	13.196	12.639
3	15.475	14.298	18.079	11.813	20.223	9.837
3.5	15.860	15.685	15.003	12.708	18.943	15.913
4	12.929	13.649	8.708	11.743	11.350	9.778
24	5.048	6.667	-0.528	7.493	8.889	12.717

Table B4.4: *Data after adding the values of the samples*

	Intensity					
Time (h)	**1**	**2**	**3**	**4**	**5**	**6**
0	203.075	337.680	306.511	359.478	304.673	331.042
0.5	378.320	388.579	402.470	432.549	395.626	468.934
1	435.140	443.380	461.671	469.809	438.087	499.923
1.5	466.419	471.580	490.344	489.400	458.549	520.728
2	497.695	503.079	521.170	518.346	490.307	532.813
2.5	521.279	522.981	540.634	537.610	503.502	545.452
3	536.754	537.278	558.714	549.424	523.726	555.289
3.5	552.614	552.963	573.717	562.132	542.668	571.202
4	565.543	566.612	582.424	573.875	554.018	580.980
24	570.591	573.279	581.896	581.368	562.907	593.697

Calculation of the maximum diffusion:

The maximum intensity is of approximately 580.

From the standard curve in appendix A1 this equation is presented:

$$y = (3*10^6)\ x \qquad (1)$$

By turning equation 1, the concentration x can be calculated from the intensity y

$$x = y / (3*10^6) \qquad (2)$$

$$x = 580 / (3*10^6) = 1.9*10^{-4}\ \%$$

From this it is given that the concentration in the acceptor chamber is at a maximum of $1.9*10^{-4}$ %. This can be calculated to an absolute weight of particles:

It is known that for a 1% solution there is 10 mg/ml. Thus the absolute weight is calculated by multiplying the concentration by 10. This gives:

$$1.9*10^{-4} * 10 = 0.0019 \text{ mg/ml}$$

This can be multiplied by the volume of 50 µl, which is the same as 0.05 ml to give an absolute weight of $9.5*10^{-5}$ mg. This is the amount which has diffused through the filter in the control sample containing red carboxylate 100 nm FluoSpheres® and physiological saline.

To see how much this is of the amount of FluoSpheres® originally in the donor chamber, the absolute weight of the particles in the donor chamber is calculated in the same way:

$$0.0025\% * 10 = 0.025 \text{ mg/ml}$$
$$0.025 \text{ mg/ml} * 0.05 \text{ ml} = 0.00125 \text{ mg}$$

The absolute weight of particles in the donor chamber is 0.00125 mg. Dividing this on the absolute weight of particle in the acceptor chamber gives how much of the total amount of particle which has diffused through the Transwell.

$$1.25*10^{-3} / 9.5*10^{-5} = 13$$

That is 1/13, less than 10 % have diffused through the filter of the Transwell from the donor chamber to the acceptor chamber.

B5: Diffusion experiment with red carboxylate 100 nm FluoSpheres in PSIM and PSIM control on 12-well Transwell

Table B5.1: *Raw data from the fluorometer. MP is samples containing PSIM and FluoSpheres®, while the CM is control samples containing PSIM and physiological saline.*

	Intensity				
Time (h)	**MP1**	**MP2**	**CM1**	**CM2**	**CM3**
0.5	1.354	2.259	0.251	0.156	0.161
1	0.918	1.188	0.108	0.040	0.027
2	0.790	0.718	0.103	0.020	0.034
4	0.468	0.388	0.056	0.027	0.049
6	0.324	0.238	0.062	0.049	0.056
24	0.443	0.406	0.235	0.214	0.221

Table B5.2: *Data after calculating for dilutions done at sample collection*

	Intensity				
Time (h)	**MP1**	**MP2**	**CM1**	**CM2**	**CM3**
0.5	2.257	3.765	0.418	0.260	0.268
1	1.530	1.980	0.180	0.067	0.045
2	1.317	1.197	0.172	0.033	0.057
4	0.780	0.647	0.093	0.045	0.082
6	0.540	0.397	0.103	0.082	0.093
24	0.738	0.677	0.392	0.357	0.368

Table B5.3: *Data after subtraction of half of the previous measurement*

	Intensity				
Time (h)	**MP1**	**MP2**	**CM1**	**CM2**	**CM3**
0.5	2.257	3.765	0.418	0.260	0.268
1	0.402	0.097	-0.029	-0.063	-0.089
2	0.552	0.207	0.082	0.000	0.034
4	0.122	0.048	0.008	0.028	0.053
6	0.150	0.073	0.057	0.059	0.053
24	0.468	0.478	0.340	0.316	0.322

Table B5.4: *Data after adding the values of the samples*

	Intensity				
Time (h)	**MP1**	**MP2**	**CM1**	**CM2**	**CM3**
0.5	2.257	3.765	0.418	0.260	0.268
1	2.658	3.863	0.389	0.197	0.179
2	3.210	4.069	0.471	0.197	0.213
4	3.332	4.118	0.478	0.225	0.267
6	3.482	4.191	0.535	0.284	0.319
24	3.950	4.669	0.875	0.600	0.641

Calculating the percentage FluoSpheres® that has come out to the acceptor chamber out of the maximum:

Assuming maximum is at 580 as is seen from the results of the FluoSpheres® control on the 12-well Transwell under section B4.

The average results for the tests with FluoSpheres® in PSIM on 12-well is as shown in table B5.5, and the average results from the PSIM control on 12-well is shown in table B5.6. By first removing the background intensity caused by the PSIM and then calculating using the maximum intensity from B4 of 580, the percentage that comes through the filter is known.

Table B5.5: *Average results of the diffusion of FluoSpheres® through PSIM on 12-well*

Time (h)	Intensity
0.5	3.011
1	3.260
2	3.640
4	3.725
6	3.836
24	4.310

Table B5.6: *Average results of the PSIM control on a 12-well.*

Time (h)	Intensity
0.5	0.316
1	0.255
2	0.294
4	0.323
6	0.379
24	0.705

After 24 hours the intensity of the sample from table B5.5 is at 4.310. By subtracting 0.705, which is the intensity of the PSIM after 24 hours (table B5.6) the intensity of FluoSpheres® is 3.605.

By multiplying this by 100 and dividing over the maximum intensity of 580, it is clear that the amount which comes out of the donor chamber and into the acceptor chamber is of 0.62%

B6: Diffusion of red carboxylate 100 nm FluoSpheres® on 6-well Transwell and comparison to the diffusion on 12-well Transwell

Calculations for the amount of PSIM needed in the 6-well

The equation for volume in a cylinder is: V = G*h

Where V is the volume, G is the ground area and h is the height.

For the 12-well Transwell:

G = 1.12 cm^2

V = 500 µl = 0.5 cm^3

h = V/G = 0.5 cm^3/1.12 cm^2 = 0.45 cm

This can be used to find the volume needed to fill the 6-well with a PSIM layer that is equally thick compared to the one in the 12-well.

For the 6-well Transwell:

G = 4.2 cm^2

h = 0.45 cm (the same as for the 12-well)

V = G*h = 4.2 cm^2 * 0.45 cm = 1.89 cm^3 = 1890 µl

This gives a total volume in the well of 1890 µl. That means 189 µl fluorescent particles and 1701 µl PSIM. Due to the problem of measuring out such volumes in the pipets, the volumes are rounded to 190 µl fluorescent particles and 1700 µl PSIM.

Table B6.1: *Raw data from the fluorometer*

	Intensity				
Time (h)	**1**	**2**	**3**	**4**	**5**
0.5	1.836	10.665	16.527	17.647	11.194
1	1.629	7.482	10.307	13.203	7.239
2	1.291	5.280	8.446	9.634	6.568
4	1.422	4.061	6.731	10.144	5.967
6	0.990	3.010	4.815	9.587	3.664
24	5.693	7.442	7.059	31.442	8.615

Table B6.2: *Data after calculating for dilutions done at sample collection*

	Intensity				
Time (h)	**1**	**2**	**3**	**4**	**5**
0.5	0.787	4.571	7.083	7.563	4.797
1	0.698	3.207	4.417	5.658	3.102
2	0.553	2.263	3.620	4.129	2.815
4	0.609	1.740	2.885	4.347	2.557
6	0.424	1.290	2.064	4.109	1.570
24	2.440	3.189	3.025	13.475	3.692

Table B6.3: *Data after subtraction of half of the previous measurement*

	Intensity				
Time (h)	**1**	**2**	**3**	**4**	**5**
0.5	0.787	4.571	7.083	7.563	4.797
1	0.305	0.921	0.876	1.877	0.704
2	0.204	0.660	1.411	1.300	1.264
4	0.333	0.609	1.075	2.283	1.150
6	0.120	0.420	0.621	1.935	0.292
24	2.228	2.544	1.994	11.421	2.907

Table B6.4: *Data after adding the values of the samples*

	Intensity				
Time (h)	**1**	**2**	**3**	**4**	**5**
0.5	0.787	4.571	7.083	7.563	4.797
1	1.092	5.492	7.959	9.440	5.501
2	1.296	6.152	9.370	10.740	6.765
4	1.629	6.761	10.445	13.023	7.915
6	1.748	7.180	11.066	14.958	8.206
24	3.976	9.725	13.059	26.378	11.113

Comparing the results to the results from 12-well Transwell:

The results are compared by first dividing them on the area of the well (table B6.5 and B6.7) and then finding the average (table B6.6 and B6.8). Then the maximum outcome from both is calculated as percentage of maximum from the control.

Table B6.5: *Dividing the results from the 6-well sample on the area of 4.2 cm^2*

	Intensity				
Time (h)	**1**	**2**	**3**	**4**	**5**
0.5	0.260	1.308	1.895	2.248	1.310
1	0.309	1.465	2.231	2.557	1.611
2	0.388	1.610	2.487	3.101	1.884
4	0.416	1.710	2.635	3.561	1.954
6	0.947	2.315	3.109	6.281	2.646
24	1.202	3.522	3.415	6.859	3.544

Table B6.6: *The average from the 6-well diffusion after dividing on the area.*

Time (h)	**Intensity**
0.5	1.404
1	1.634
2	1.894
4	2.055
6	3.060
24	3.708

Table B6.7: *Dividing the results from the 12-well samples (table B5.4) on the area of 1.12 cm^2*

	Intensity	
Time (h)	**1**	**2**
0.5	2.257	3.765
1	2.658	3.863
2	3.210	4.069
4	3.332	4.118
6	3.482	4.191
24	3.950	4.669

Table B6.8: *The average from the 12-well diffusion after dividing on the area.*

Time (h)	**Intensity**
0.5	2.688
1	2.911
2	3.250
4	3.326
6	3.425
24	3.848

The maximum outcome from the 6-well Transwell after 24 hours is 3.708 (table B6.6). The maximum outcome from the 12-well Transwell after 24 hours is 3.848 (table B6.8). These values are after dividing on the respective areas, to be able to compare them. Remember this is without accounting for the background by PSIM.

Finding the percentage outcome of the maximum outcome of 580 is done by multiplying the values by 100 and dividing them on 580. This gives:

Maximum for the 12-well: 3.848*100/580 = 0.66 %

Maximum for the 6-well: 3.708*100/580 = 0.64 %

B7: Diffusion of yellow-green carboxylate 40 nm FluoSpheres® on 6-well Transwell together with controls, with and without G-block.

Explanation to the abbreviations in table B7.1 – B7.5

WoG: Samples of FluoSpheres® without G-block

WG: Samples of FluoSpheres® with G-block

C: FluoSpheres® control without G-block

CG: FluoSpheres® control with G-block

CM: PSIM control

Table B7.1: *Raw data from the fluorometer*

	Intensity														
Time (h)	WoG1	WoG2	WoG3	WG1	WG2	WG3	C1	C2	C3	CG1	CG2	CG3	CM1	CM2	CM3
0,5	90,937	60,904	64,338	101,482	117,958	78,131	461,673	267,748	478,095	349,988	863,441	355,242	161,247	281,58	165,184
7	340,763	144,486	219,593	247,949	197,477	146,746	980,097	954,2	971,467	830,935	830,651	597,251	280,996	209,106	246,994
24	332,767	236,77	199,773	380,875	359,872	211,133	1099,06	1081,796	1124,78	830,359	740,759	676,751	437,654	357,933	348,085
48	354,36	233,09	231,978	401,515	342,075	230,479	871,544	862,368	900,958	763,282	644,396	686,123	600,646	589,133	628,357

Table B7.2: *Data after calculating for dilutions done at sample collection*

	Intensity														
Time (h)	WoG1	WoG2	WoG3	WG1	WG2	WG3	C1	C2	C3	CG1	CG2	CG3	CM1	CM2	CM3
0,5	38,973	26,102	27,573	43,492	50,553	33,485	197,860	114,749	204,898	149,995	370,046	152,247	69,106	120,677	70,793
7	146,041	61,923	94,111	106,264	84,633	62,891	420,042	408,943	416,343	356,115	355,993	255,965	120,427	89,617	105,855
24	142,614	101,473	85,617	163,232	154,231	90,486	471,026	463,627	482,049	355,868	317,468	290,036	187,566	153,400	149,179
48	151,869	99,896	99,419	172,078	146,604	98,777	373,519	369,586	386,125	327,121	276,170	294,053	257,420	252,486	269,296

Table B7.3: *Data after subtraction of half of the previous measurement*

	Intensity														
Time (h)	WoG1	WoG2	WoG3	WG1	WG2	WG3	C1	C2	C3	CG1	CG2	CG3	CM1	CM2	CM3
0,5	38,973	26,102	27,573	43,492	50,553	33,485	197,860	114,749	204,898	149,995	370,046	152,247	69,106	120,677	70,793
7	126,555	48,872	80,325	84,518	59,356	46,149	321,112	351,568	313,894	281,118	170,970	179,841	85,874	29,278	70,458
24	69,594	70,512	38,561	110,100	111,914	59,040	261,005	259,155	273,877	177,811	139,472	162,054	127,353	108,591	96,252
48	80,561	49,159	56,611	90,462	69,488	53,534	138,006	137,773	145,101	149,187	117,436	149,035	163,637	175,786	194,706

Table B7.4: *Data after adding the values of the samples*

	Intensity														
Time (h)	WoG1	WoG2	WoG3	WG1	WG2	WG3	C1	C2	C3	CG1	CG2	CG3	CM1	CM2	CM3
0,5	38,973	26,102	27,573	43,492	50,553	33,485	197,860	114,749	204,898	149,995	370,046	152,247	69,106	120,677	70,793
7	165,528	74,973	107,898	128,010	109,910	79,634	518,972	466,317	518,792	431,112	541,016	332,088	154,980	149,955	141,251
24	235,122	145,485	146,459	238,110	221,824	138,674	779,976	725,473	792,669	608,923	680,488	494,142	282,332	258,547	237,503
48	315,683	194,644	203,070	328,572	291,312	192,207	917,982	863,246	937,770	758,110	797,924	643,176	445,969	434,333	432,209

Table B7.5: *Data after calculating the average*

	Intensity				
Time (h)	WoG	WG	C	CG	CM
0,5	30,883	42,510	172,502	224,096	86,859
7	116,133	105,851	501,360	434,739	148,729
24	175,689	199,536	766,039	594,518	259,461
48	237,799	270,697	906,333	733,070	437,504

B7: Diffusion of yellow-green carboxylate 40 nm FluoSpheres® on 6-well Transwell together with controls, with and without G-block.

Explanation to the abbreviations in table B7.1 – B7.5

WoG: Samples of SNEDDS without G-block

WG: Samples of SNEDDS with G-block

C: SNEDDS control without G-block

CG: SNEDDS control with G-block

CM: PSIM control

Table B8.1: *Raw data from the fluorometer*

	Intensity														
Time (h)	WoG1	WoG2	WoG3	WG1	WG2	WG3	C1	C2	C3	CG1	CG2	CG3	CM1	CM2	CM3
0,5	0,367	0,288	0,205	0,395	0,332	0,271	7,577	7,362	8,155	23,918	8,352	23,909	0,431	0,674	0,404
7	0,960	0,805	0,672	1,035	0,790	0,772	21,335	21,851	22,371	16,530	11,361	16,345	0,924	0,773	0,804
24	1,490	1,416	0,979	1,577	1,245	1,718	24,618	26,400	27,309	12,518	10,976	12,710	1,375	1,381	1,365
48	1,477	1,510	1,263	1,669	1,558	1,579	21,785	24,283	24,621	11,132	11,192	11,708	1,814	2,109	2,142

Table B8.2: *Data after calculating for dilutions done at sample collection*

	Intensity														
Time (h)	WoG1	WoG2	WoG3	WG1	WG2	WG3	C1	C2	C3	CG1	CG2	CG3	CM1	CM2	CM3
0,5	0,157	0,123	0,088	0,169	0,142	0,116	3,247	3,155	3,495	10,251	3,579	10,247	0,185	0,289	0,173
7	0,411	0,345	0,288	0,444	0,339	0,331	9,144	9,365	9,588	7,084	4,869	7,005	0,396	0,331	0,345
24	0,639	0,607	0,420	0,676	0,534	0,736	10,551	11,314	11,704	5,365	4,704	5,447	0,589	0,592	0,585
48	0,633	0,647	0,541	0,715	0,668	0,677	9,336	10,407	10,552	4,771	4,797	5,018	0,777	0,904	0,918

Table B8.3: *Data after subtraction of half of the previous measurement*

	Intensity														
Time (h)	WoG1	WoG2	WoG3	WG1	WG2	WG3	C1	C2	C3	CG1	CG2	CG3	CM1	CM2	CM3
0,5	0,157	0,123	0,088	0,169	0,142	0,116	3,247	3,155	3,495	10,251	3,579	10,247	0,185	0,289	0,173
7	0,333	0,283	0,244	0,359	0,267	0,273	7,520	7,787	7,840	1,959	3,079	1,882	0,304	0,187	0,258
24	0,433	0,434	0,276	0,454	0,364	0,571	5,979	6,632	6,910	1,823	2,270	1,945	0,391	0,426	0,413
48	0,314	0,344	0,332	0,377	0,401	0,309	4,061	4,750	4,700	2,088	2,445	2,294	0,483	0,608	0,626

Table B8.4: *Data after adding the values of the samples*

	Intensity														
Time (h)	WoG1	WoG2	WoG3	WG1	WG2	WG3	C1	C2	C3	CG1	CG2	CG3	CM1	CM2	CM3
0,5	0,157	0,123	0,088	0,169	0,142	0,116	3,247	3,155	3,495	10,251	3,579	10,247	0,185	0,289	0,173
7	0,490	0,407	0,332	0,528	0,410	0,389	10,767	10,942	11,335	12,210	6,659	12,128	0,488	0,476	0,431
24	0,923	0,841	0,608	0,982	0,774	0,960	16,746	17,574	18,245	14,032	8,928	14,073	0,880	0,902	0,844
48	1,237	1,185	0,939	1,360	1,175	1,268	20,807	22,324	22,945	16,121	11,373	16,367	1,362	1,510	1,469

Table B8.5: *Data after calculating the average*

	Intensity				
Time (h)	WoG	WG	C	CG	CM
0,5	0,123	0,143	3,299	8,026	0,216
7	0,410	0,442	11,015	10,332	0,465
24	0,791	0,905	17,522	12,345	0,875
48	1,120	1,268	22,025	14,620	1,447

Appendix C: Raw data and calculations for diffusion through agar gel

C1: Diffusion study with yellow-green carboxylate 100 nm FluoSpheres® through agar on 12-well Transwell

Table C1.1: *Raw data from the fluorometer*

	Intensity							
Control agar (1%):	10.651	11.033	10.690					
Agar (1%) and FluoSpheres:	13.436	12.182	15.386	15.018	22.439	12.033	13.605	16.308
Control FluoSpheres:	167.63	239.051	320.761	601.053				
Agar (1%) + 200 ul physiological salin + FluoSpheres:	17.853	13.602	32.636	45.62				

Table C1.2: *Data from table C1.1 after calculation for the dilutions done at sample collection*

	Intensity							
Control agar (1%):	17.752	18.388	17.817					
Agar (1%) and FluoSpheres:	22.393	20.303	25.643	25.03	37.398	20.055	22.675	27.18
Control FluoSpheres:	279.383	398.418	534.602	1001.755				
Agar (1%) + 200 ul physiological salin + FluoSpheres:	29.755	22.67	54.393	76.033				

Table C1.3: *Average results*

	Average intensity
Control agar (1%):	17.986
Agar (1%) and FluoSpheres:	25.085
Control FluoSpheres:	553.54
Agar (1%) + 200 ul physiological salin + FluoSpheres:	45.713

C2: Diffusion study with yellow-green carboxylate 100 nm FluoSpheres® through agar without filter

Table C2.1: *Raw data from fluorometer*

	Intensity							
	1	2	3	4	5	6	7	8
Control agar (1%)	12,559	11,422	11,917	11,864	11,77	13,482	11,844	11,19
Agar (1%) and FluoSpheres (0,025%)	23,739	28,548	33,744	33,488	30,06	33,196	30,92	33,46

Table C2.2: *Data after calculation for dilution*

	Intensity							
Prøver	1	2	3	4	5	6	7	8
Control agar (1%)	20,932	19,037	19,862	19,773	19,617	22,470	19,740	18,650
Agar (1%) and FluoSpheres (0,025%)	39,565	47,580	56,240	55,813	50,100	55,327	51,533	55,767

The average intensity is presented in table C2.3 along with the percentage out of 100 %. The value for 100 % is collected from the FluoSpheres® control in table C1.3. After subtracting for the value of agar, the samples was multiplied by 100 and divided by the value for the FluoSpheres® control in table C1.3 which is 553.54.

Table C2.3: *Average intensity and calculation for percent out of 100 %. The*

	Average int.	Average after correction for the agar	Percent out of 100%
Control agar (1%)	20,01	-	-
Agar (1%) and FluoSpheres (0,025%)	51,49	31,48	5,69

Appendix D: Pictures from the confocal microscope used in profile plotting

D1: Photos of yellow-green carboxylate 40 nm FluoSpheres® without and with G-block and PSIM at 24 hours

FluoSpheres® without G-block after 24 hours:

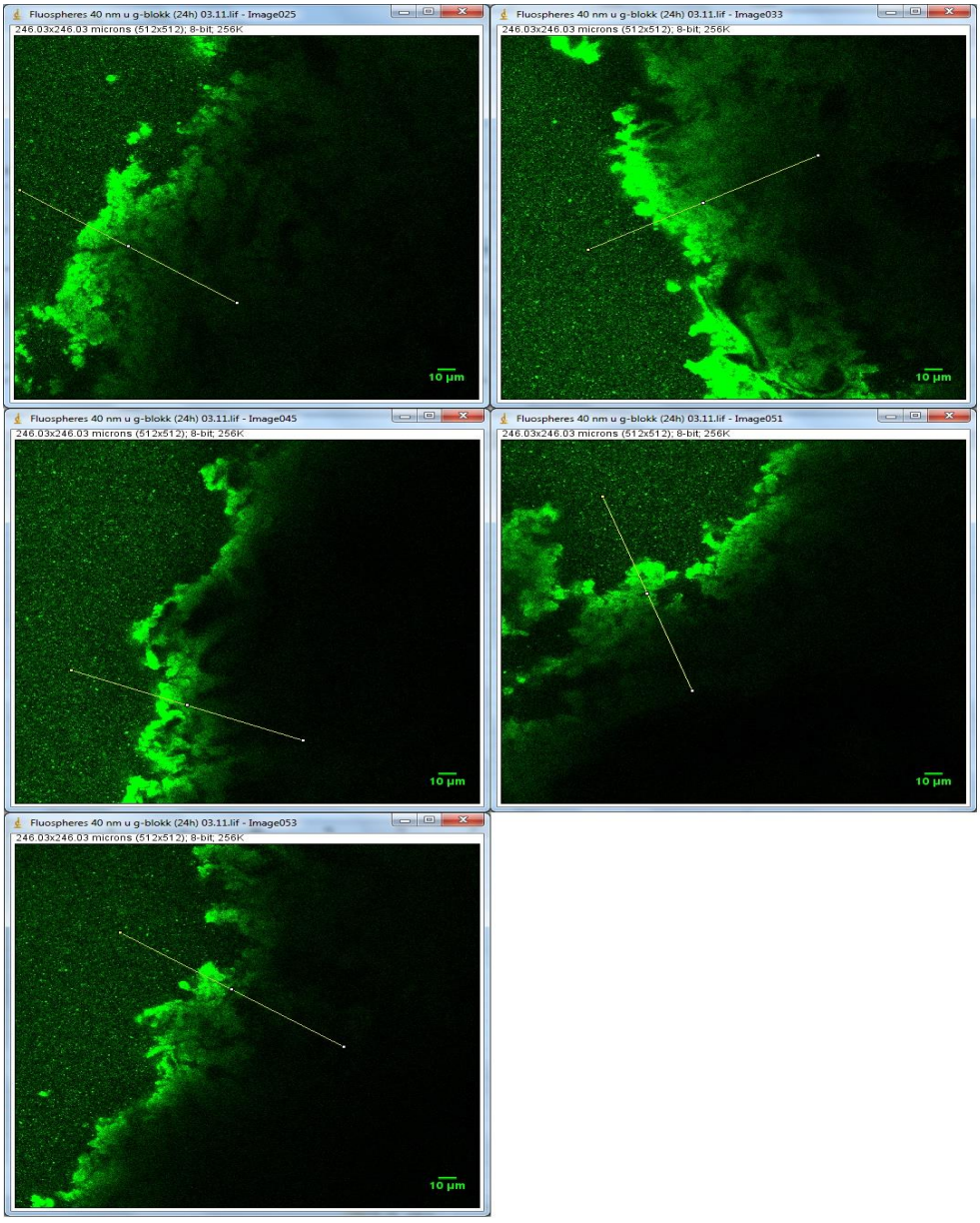

Figure D1.1: *Photos from the confocal microscope showing yellow-green 40 nm FluoSpheres® without G-block, with PSIM at the right side of the photos. Taken after 24 hours. The yellow line show where the profile plot is collected from, and there is a scale bar in the lover right corner of each photo.*

FluoSpheres® with G-block after 24 hours:

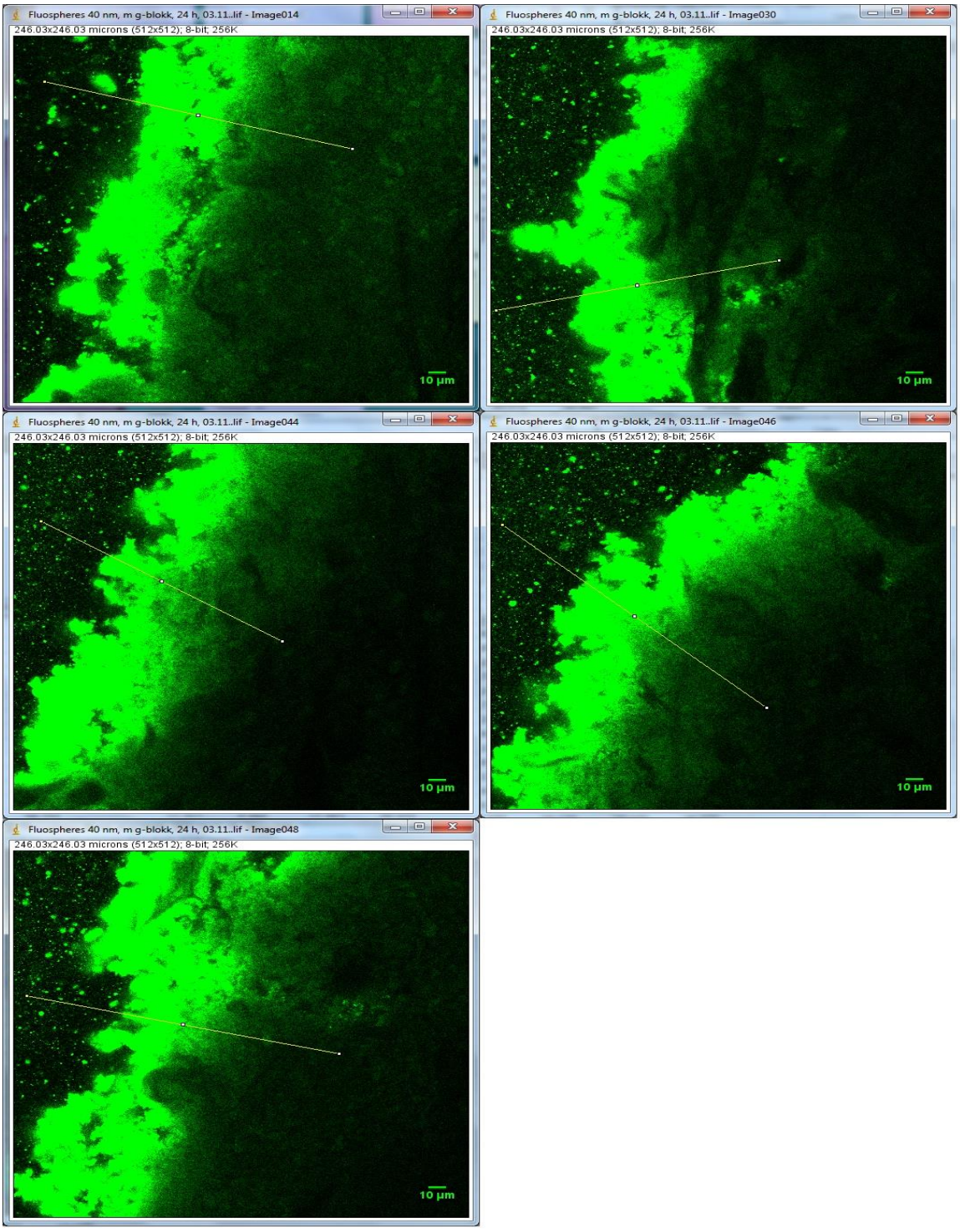

Figure D1.2: *Photos from the confocal microscope showing yellow-green 40 nm FluoSpheres® with G-block, with PSIM at the right side of the photos. Taken after 24 hours. The yellow line show where the profile plot is collected from, and there is a scale bar in the lover right corner.*

D2: Photos of yellow-green carboxylate 40 nm FluoSpheres® without and with G-block and PSIM at 48 hours

FluoSpheres® without G-block:

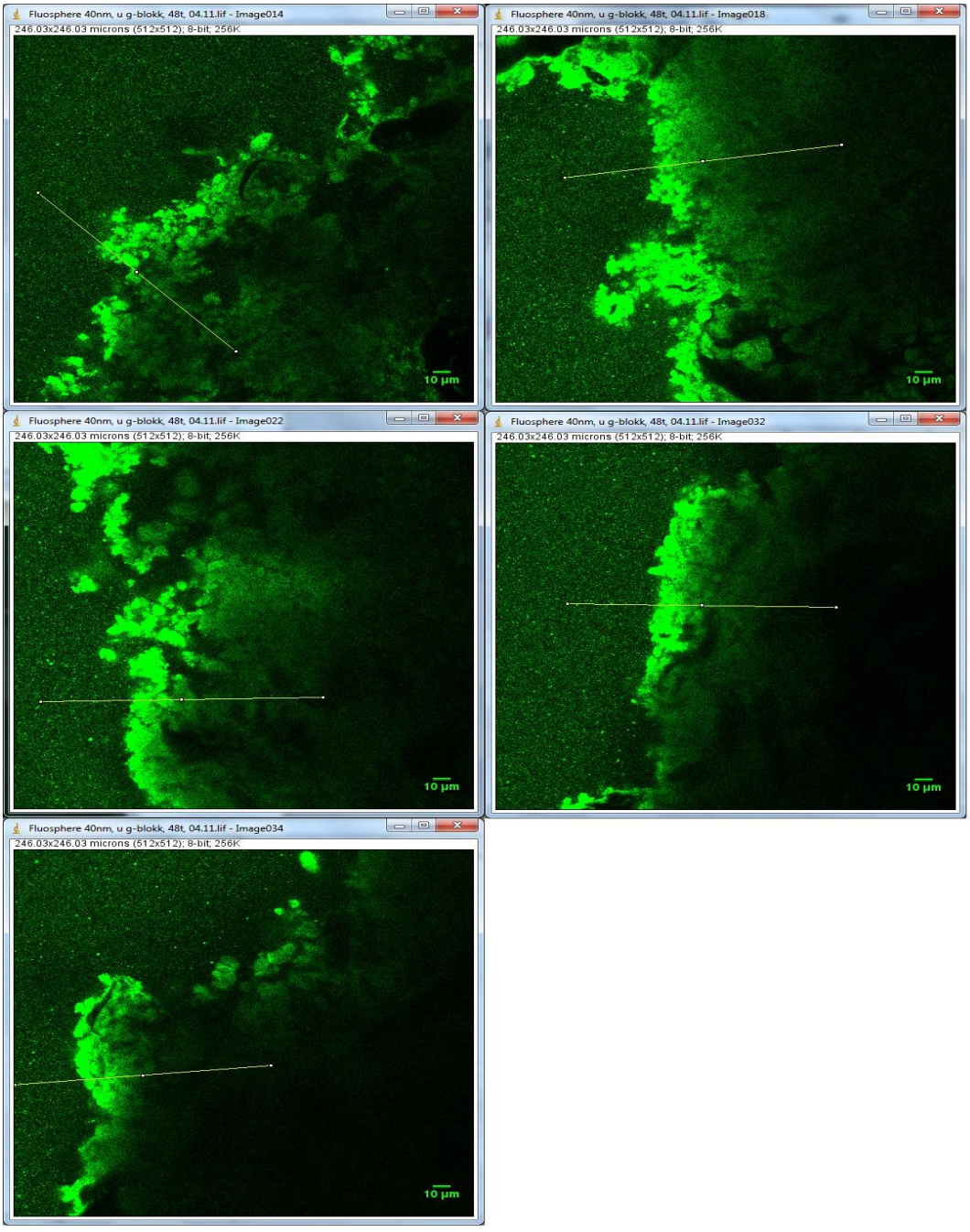

Figure D2.1: *Photos from the confocal microscope showing yellow-green 40 nm FluoSpheres® without G-block, with PSIM at the right side of the photos. Taken after 48 hours. The yellow line show where the profile plot is collected from, and there is a scale bar in the lover right corner.*

FluoSpheres® with G-block:

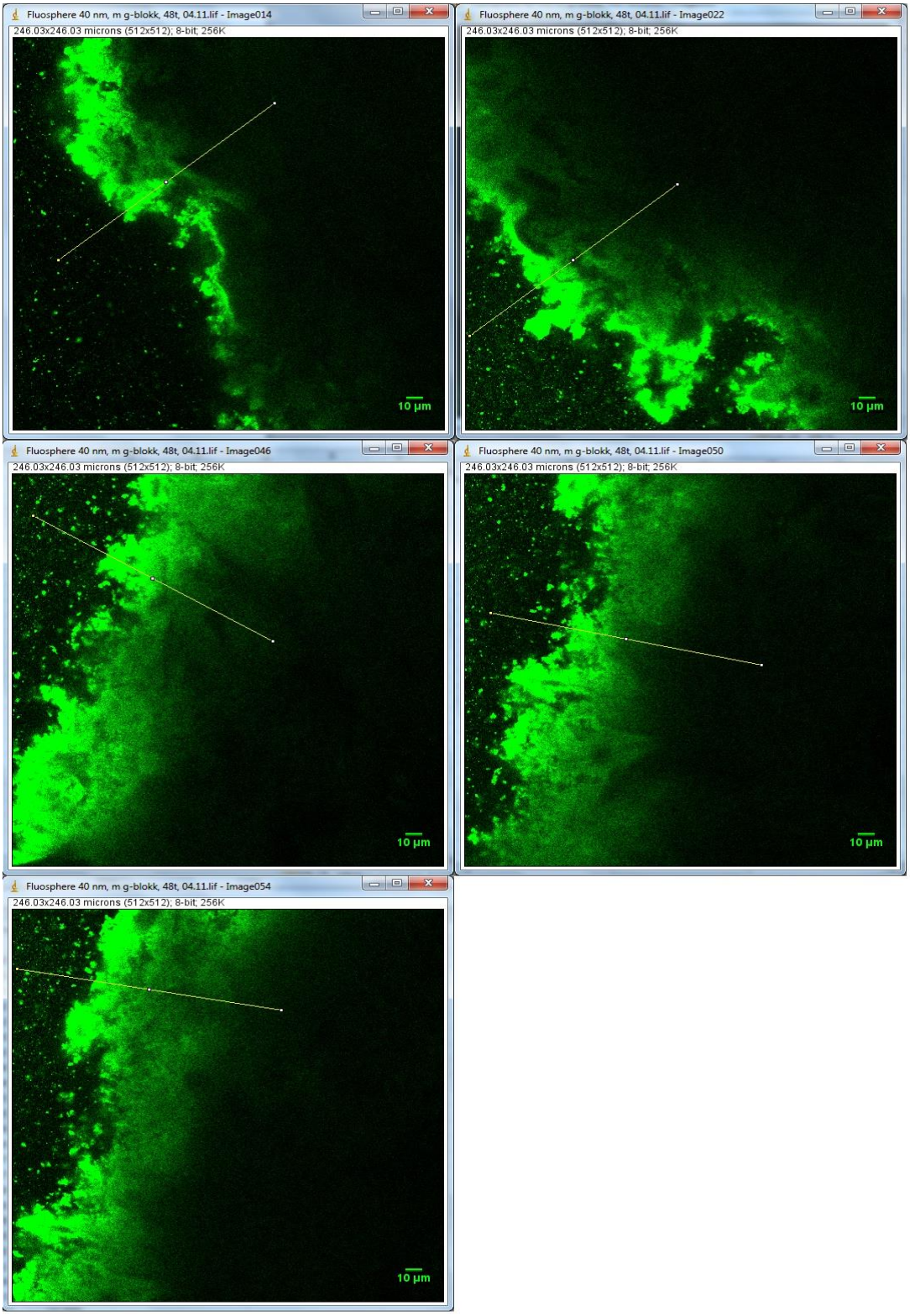

Figure D2.2: *Photos from the confocal microscope showing yellow-green 40 nm FluoSpheres® with G-block, with PSIM at the right side of the photos. Taken after 48 hours. The yellow line show where the profile plot is collected from, and there is a scale bar in the lover right corner.*

D3: Photos of yellow-green carboxylate 40 nm FluoSpheres® without and with G-block and PSIM at 72 hours

FluoSpheres® without G-block:

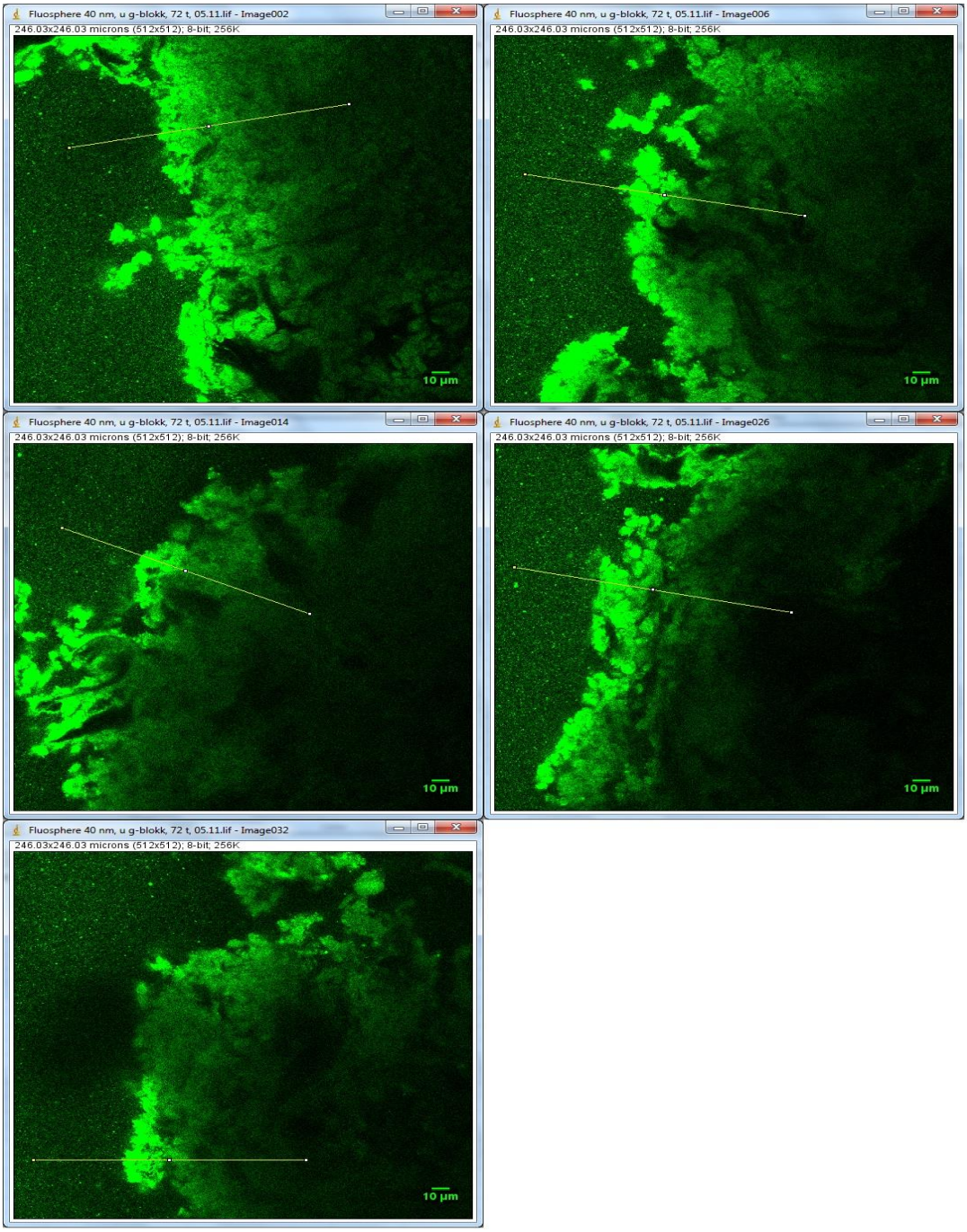

Figure D3.1: *Photos from the confocal microscope showing yellow-green 40 nm FluoSpheres® without G-block, with PSIM at the right side of the photos. Taken after 72 hours. The yellow line show where the profile plot is collected from, and there is a scale bar in the lover right corner.*

FluoSpheres with G-block:

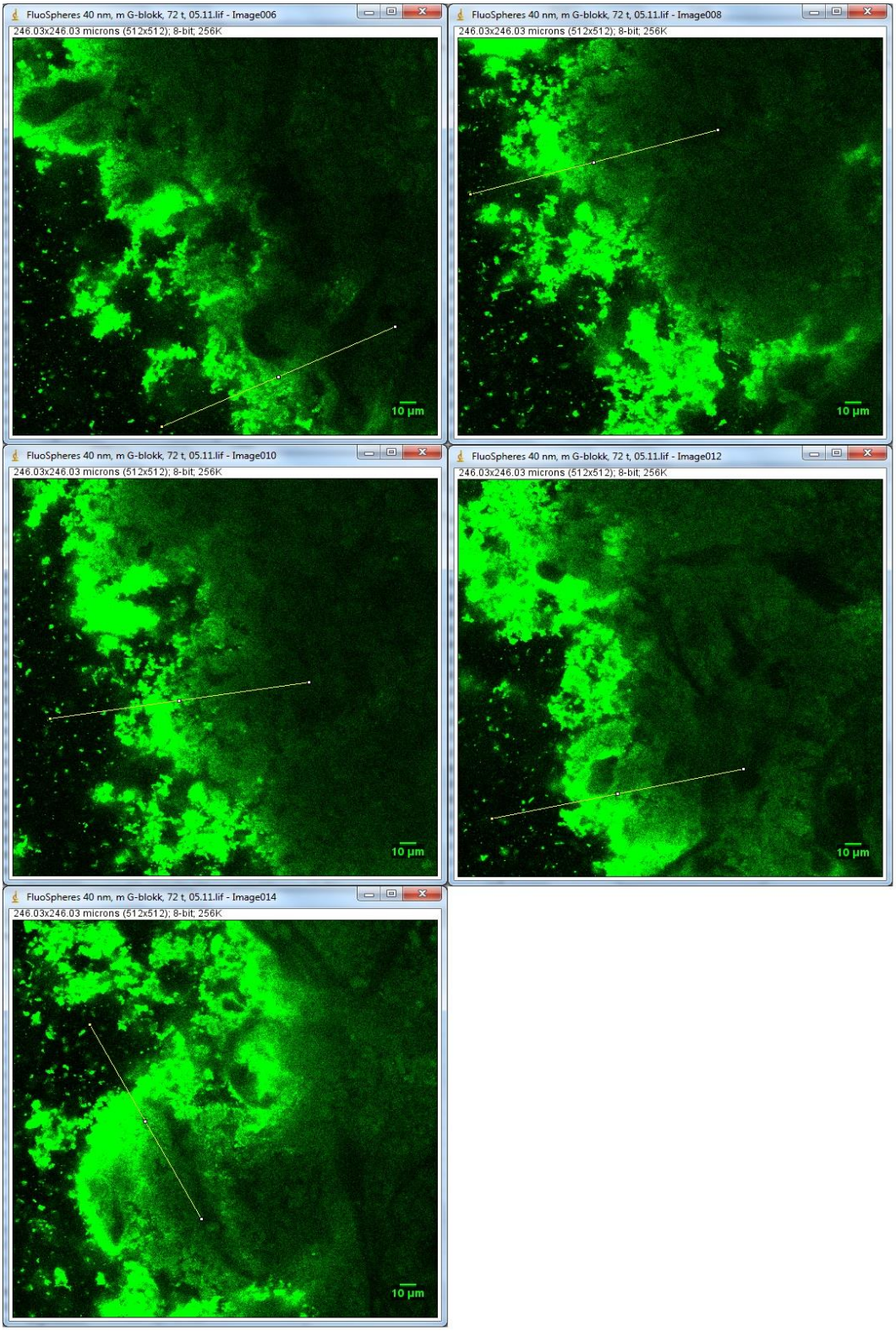

Figure D3.2: *Photos from the confocal microscope showing yellow-green 40 nm FluoSpheres® with G-block, with PSIM at the right side of the photos. Taken after 72 hours. The yellow line show where the profile plot is collected from, and there is a scale bar in the lover right corner.*

D4: Photos of SNEDDS without and with G-block and PSIM at 24 hours

SNEDDS without G-block:

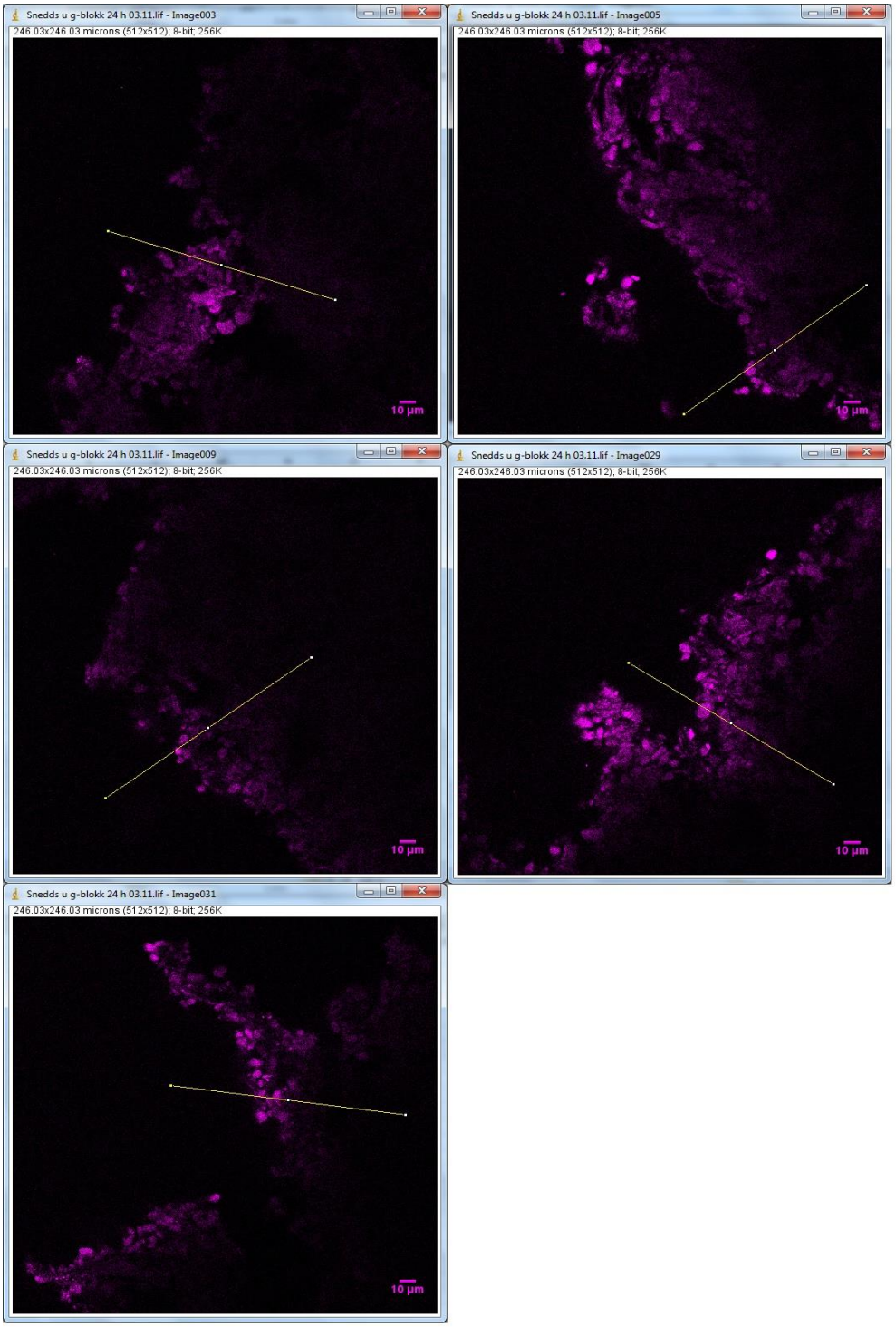

Figure D4.1: *Photos from the confocal microscope showing SNEDDS without G-block, with PSIM at the right side of the photos. Taken after 24 hours. The yellow line show where the profile plot is collected from, and there is a scale bar in the lover right corner.*

SNEDDS with G-block:

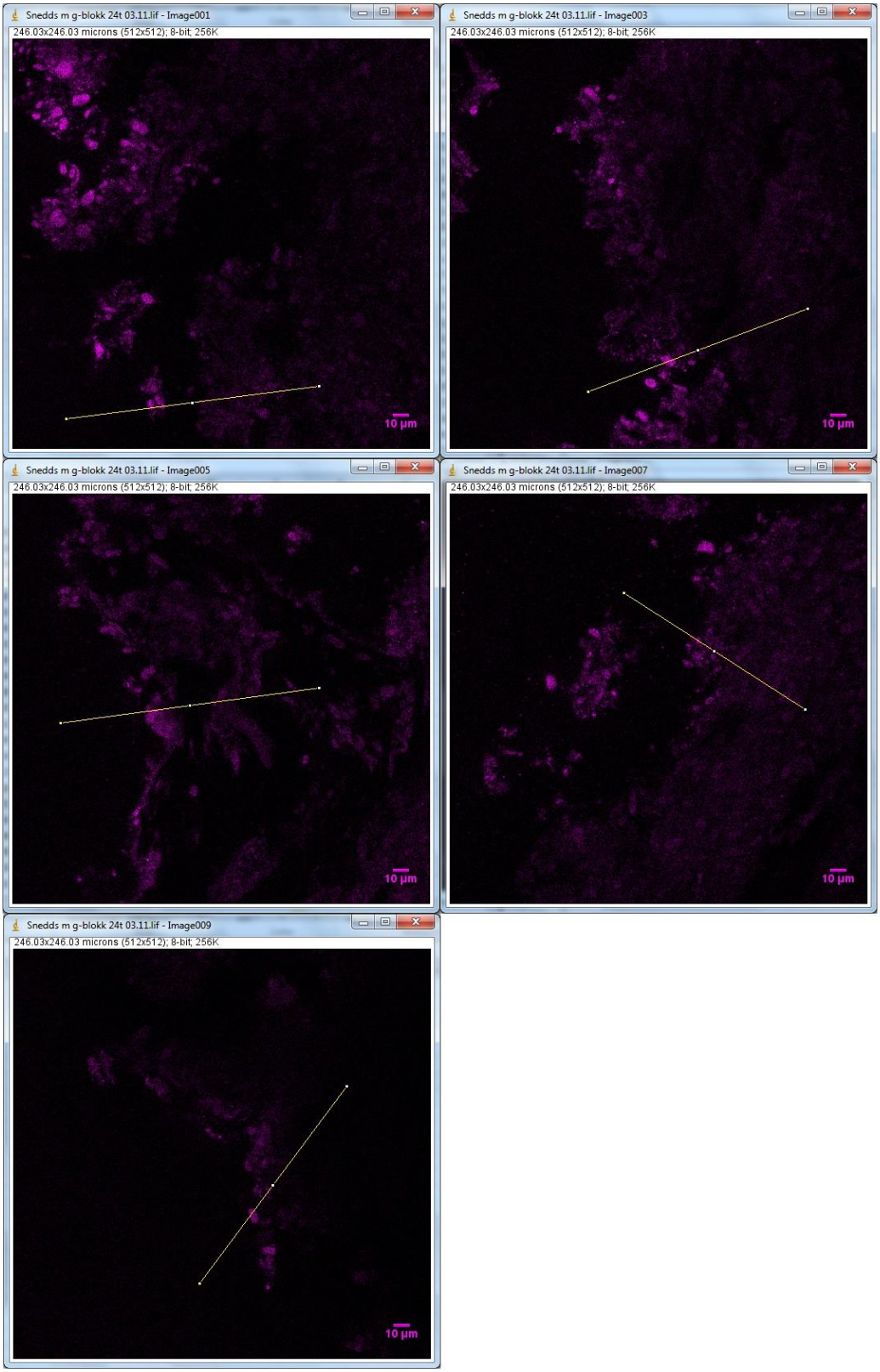

Figure D4.2: *Photos from the confocal microscope showing SNEDDS with G-block, with PSIM at the right side of the photos. Taken after 24 hours. The yellow line show where the profile plot is collected from, and there is a scale bar in the lover right corner.*

D5: Photos of SNEDDS without and with G-block and PSIM at 48 hours

SNEDDS without G-block:

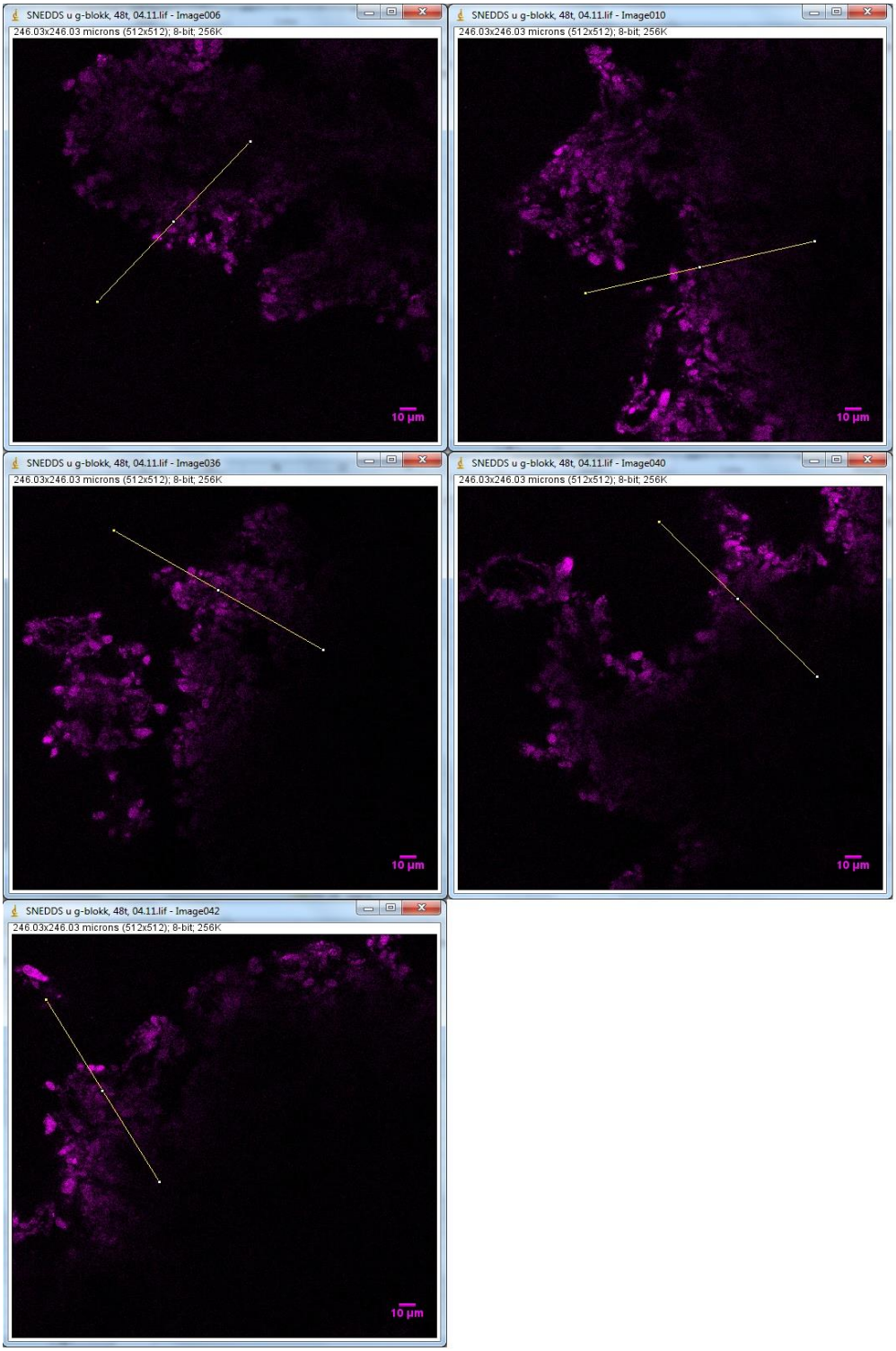

Figure D5.1: *Photos from the confocal microscope showing SNEDDS without G-block, with PSIM at the right side of the photos. Taken after 48 hours. The yellow line show where the profile plot is collected from, and there is a scale bar in the lover right corner.*

SNEDDS with G-block:

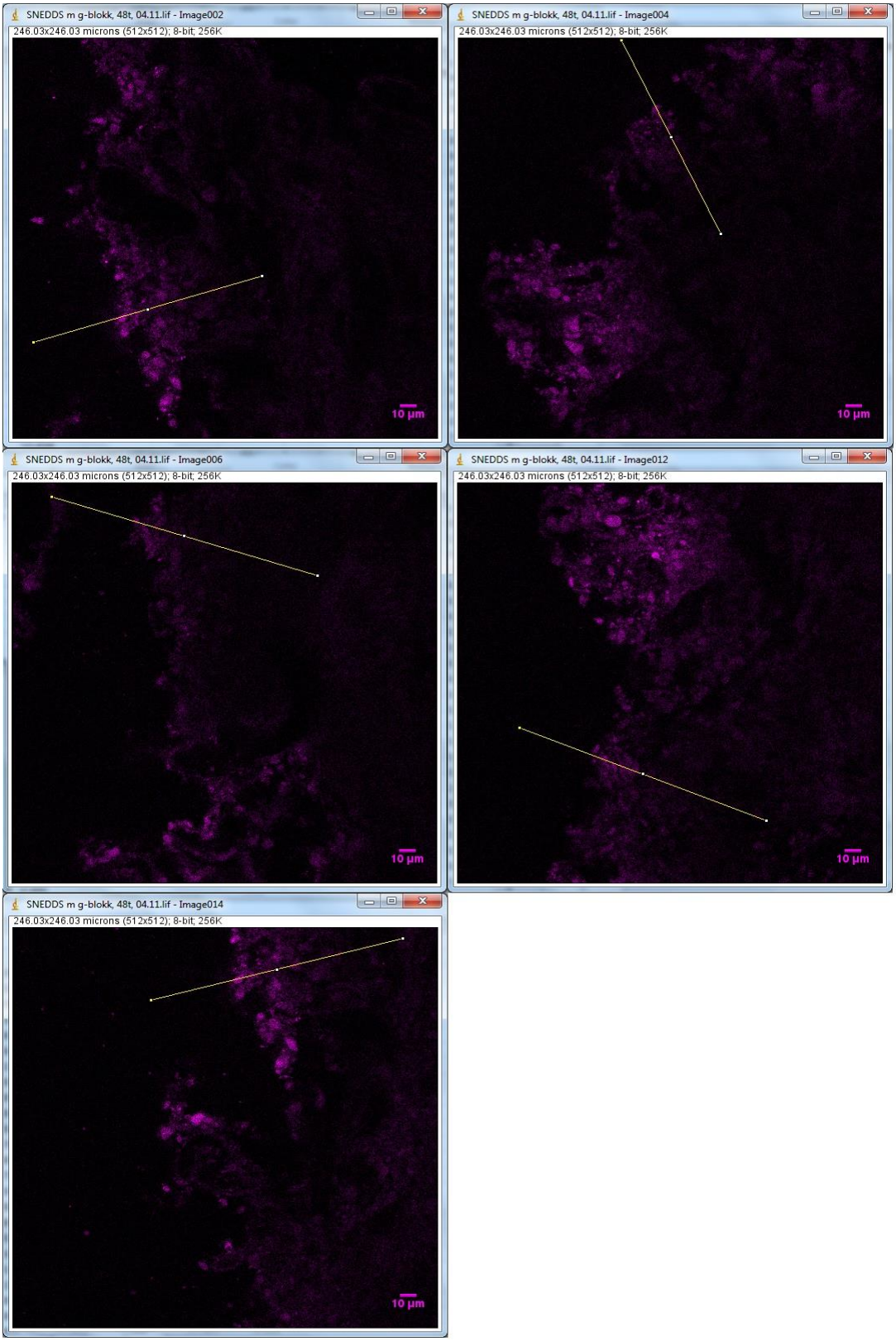

Figure D5.2: *Photos from the confocal microscope showing SNEDDS with G-block, with PSIM at the right side of the photos. Taken after 48 hours. The yellow line show where the profile plot is collected from, and there is a scale bar in the lover right corner.*

D6: Photos of SNEDDS without and with G-block and PSIM at 72 hours

SNEDDS without G-block:

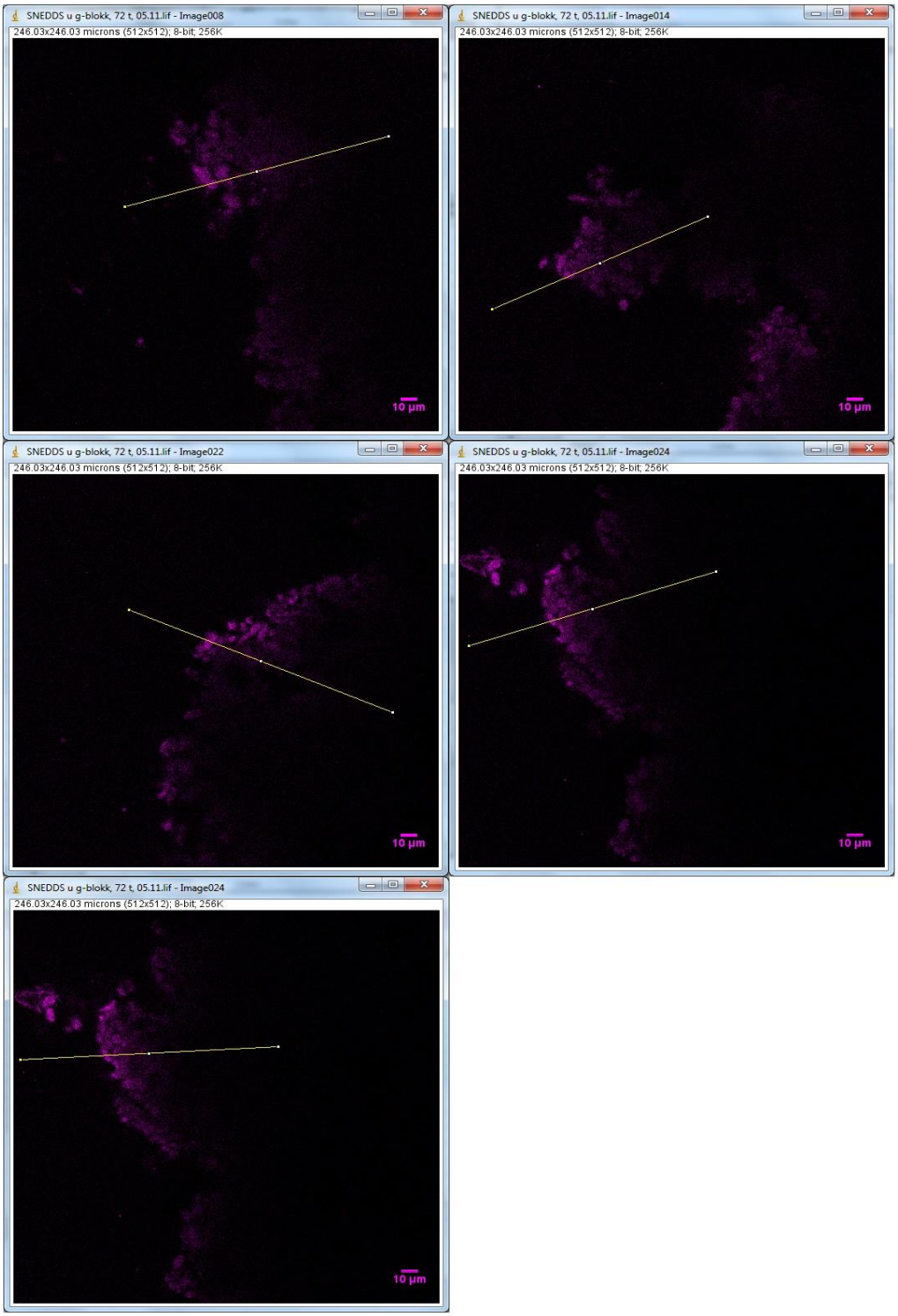

Figure D6.1: *Photos from the confocal microscope showing SNEDDS without G-block, with PSIM at the right side of the photos. Taken after 72 hours. The yellow line show where the profile plot is collected from, and there is a scale bar in the lover right corner.*

SNEDDS with G-block:

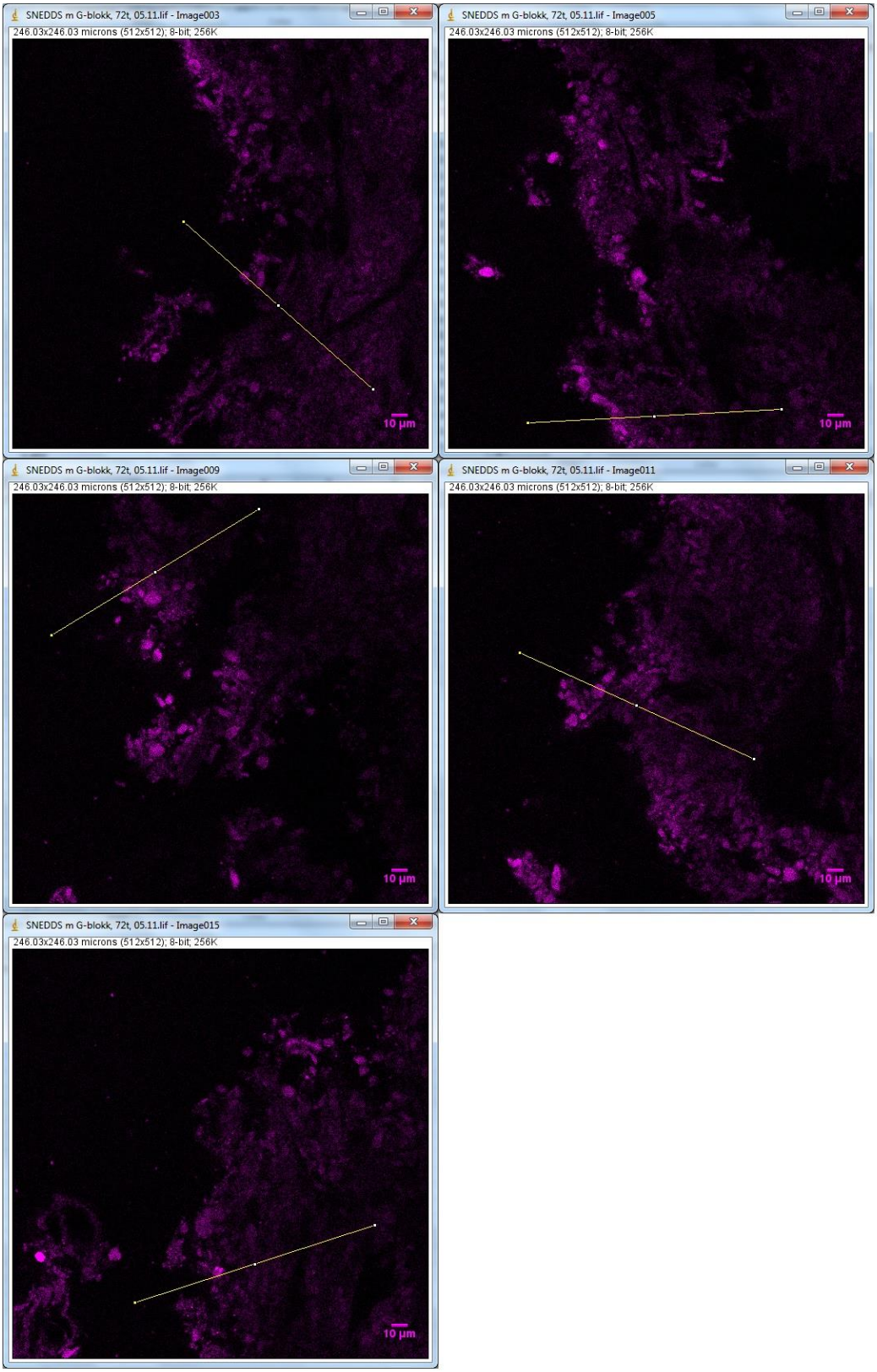

Figure D6.2: *Photos from the confocal microscope showing SNEDDS with G-block, with PSIM at the right side of the photos. Taken after 72 hours. The yellow line show where the profile plot is collected from, and there is a scale bar in the lover right corner.*

Appendix E: Procedure biosimilar mucus

Method for production of biosimilar mucus (10 mL)

This protocol was adapted from Boegh *et al.* 2013.

1. 100 mL 10 mM isotonic HEPES buffer was produced containing 1.3 mM $CaCl_2$. 1 mM $MgSO_4$ and 137 mM NaCl. 0.2383 g HEPES. 0.01911 g $CaCl_2 \times 2H_2O$. 0.02465 g $MgSO_4 \times 7H_2O$ and 0.80063 g NaCl was weighed out and mixed with 100 mL MQ water.
2. 100 mL 10 mM non-isotonic HEPES buffer was produced containing 1.3 mM $CaCl_2$ and 1 mM $MgSO_4$. 0.2383 g HEPES. 0.01911 g $CaCl_2 \times 2H_2O$ and 0.02465 g $MgSO_4 \times 7H_2O$ was weighed out and mixed with 100 mL MQ water.
3. Lipid solution: 0.0121 g linoleic acid. 0.0396 g cholesterol and 0.033 g phosphatidylcholine was weighed out and mixed in an Eppendorf tube. 0.03586 g polysorbate tween 80 was weighed out and added to the tube, along with two small magnets. 750 µL of isotonic HEPES buffer (10 mM) was added. The tube was left on vigorous magnetic stirring until the solution was visually homogenous.
4. Polymer solution: 0.09 g polyacrylic acid was added to 9.168 mL of non-isotonic HEPES buffer (10 mM) and stirred until dissolved. 0.5 g sigma mucin type II was added and stirred until dissolved. 150 µL 5 mM NaOH was added and the mixture was stirred until homogenous.
5. 0.682 mL of the homogenous lipid solution was added, and the mixture was stirred. 0.31 g bovine albumin was added and the mixture was stirred until homogenous.
6. The pH was adjusted from 4.1 to 7.4 with 1 M NaOH and a pH-meter.
7. The biosimilar mucus was stored cold (ca 3.5 °C) or frozen (ca -20 °C).

Appendix F: Procedure SNEDDS

Background information on SNEDDS prototype formulation with fluorophores

Author: Mathias Fanø (P13. Bioneer:FARMA)
E-mail: mathias.fano@sund.ku.dk
22/1-2014

Background:

Our prototype SNEDDS formulation consists of:

Soybean oil: 30 % (w/w)

Maisine™ 35-1: 30 %

Cremophor RH 40: 30 %

Ethanol: 10 %

When dispersed in MilliQ (dilution factor 1:100). a Z-average of about 60 nm is obtained. In this specific, preliminary experiment, we want to examine if the interactions with and penetration through mucus can be monitored using single particle tracking. In order to do this, we need to incorporate a fluorophore into the lipid phase of the SNEDDS, in the present study coumarin 6 and rhodamine 6G.

Samples:

We have sent the following vials:

- COM13000101: Preconcentrate without ethanol. 3 grams
- Rhodamine-6G: Sigma-Aldrich #R4127
- Coumarin-6: Sigma-Aldrich #442631

Experimentals:

Control of prototype formulation:

At room temperature, the viscosity of the preconcentrate without ethanol is very high. Therefore, place it in a heating cabinet for 10-15 minutes and transfer a small volume to an Eppendorf tube placed on a weight. Then, add 10% absolute (100%) ethanol and mix/stir with the pipette tip. Dilute the resulting preconcentrate 100x in MilliQ water and measure the size using the Malvern Zetasizer. A file has been attached for comparison, which can also be consulted for experimental details. The dispersed SNEDDS should appear transparent but with a slight blue tint. We expect the resulting SNEDDS to be rather stable kinetically but recommend doing a size measurement after a relevant period

Test of prototype formulation with coumarin-6 or rhodamine-6G:

First, stock solutions of the two fluorophores are prepared in absolute ethanol. For our preliminary experiments, we dissolved 1 mg coumarin-6 and 1.4 mg rhodamine-6G in 2 and 4 ml ethanol. Respectively, resulting in concentration of about 1 mM of each. By adding fluorophore in ethanol solutions to the preconcentrate without ethanol and then diluting 100x when dispersing in water, the approximate, final concentration of the fluorophores were 1 µM. The final concentrations can be lowered, if necessary, by diluting the fluorophore stock solutions with absolute ethanol. We expect the resulting SNEDDS to be rather stable kinetically but recommend doing a size measurement after a relevant period.